

DTIC FILE COPY

WRDC-TR-90-2079
Volume II

AD-A229 693



ADVANCED THERMALLY STABLE JET FUELS DEVELOPMENT PROGRAM ANNUAL
REPORT

VOL II - Compositional Factors Affecting Thermal Degradation of
Jet Fuels

Semih Eser
Chunshan Song
Harold Schobert
Patrick Hatcher
Ronald Copenhaver
Hong Jiang
Rongbao Li
Michael Parzynski
Ying Peng

DTIC
ELECTE
DEC 05 1990
S B D

Fuel Science Program
Department of Materials Science and Engineering
The Pennsylvania State University
University Park, PA 16802

SEPTEMBER 1990

INTERIM REPORT FOR THE PERIOD JULY 1989 - JUNE 1990

APPROVED FOR PUBLIC RELEASE; DISTRIBUTION IS UNLIMITED

AERO PROPULSION AND POWER LABORATORY
WRIGHT RESEARCH AND DEVELOPMENT CENTER
AIR FORCE SYSTEMS COMMAND
WRIGHT-PATTERSON AFB OH 45433-6563

NOTICE

WHEN GOVERNMENT DRAWINGS, SPECIFICATIONS, OR OTHER DATA ARE USED FOR ANY PURPOSE OTHER THAN IN CONNECTION WITH A DEFINITELY GOVERNMENT-RELATED PROCUREMENT, THE UNITED STATES GOVERNMENT INCURS NO RESPONSIBILITY OR ANY OBLIGATION WHATSOEVER. THE FACT THAT THE GOVERNMENT MAY HAVE FORMULATED OR IN ANY WAY SUPPLIED THE SAID DRAWINGS, SPECIFICATIONS, OR OTHER DATA, IS NOT TO BE REGARDED BY IMPLICATION, OR OTHERWISE IN ANY MANNER CONSTRUED, AS LICENSING THE HOLDER, OR ANY OTHER PERSON OR CORPORATION; OR AS CONVEYING ANY RIGHTS OR PERMISSION TO MANUFACTURE, USE, OR SELL ANY PATENTED INVENTION THAT MAY IN ANY WAY BE RELATED THERETO.

THIS REPORT HAS BEEN REVIEWED BY THE OFFICE OF PUBLIC AFFAIRS (ASD/PA) AND IS RELEASABLE TO THE NATIONAL TECHNICAL INFORMATION SERVICE (NTIS). AT NTIS IT WILL BE AVAILABLE TO THE GENERAL PUBLIC INCLUDING FOREIGN NATIONS.

THIS TECHNICAL REPORT HAS BEEN REVIEWED AND IS APPROVED FOR PUBLICATION.

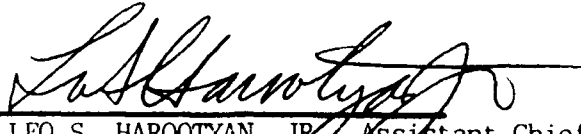


WILLIAM E. HARRISON III
Fuels Branch
Fuels and Lubrication Division



CHARLES L. DELANEY, Chief
Fuels Branch
Fuels and Lubrication Division
Aero Propulsion and Power Laboratory

FOR THE COMMANDER



LEO S. HAROOTYAN, JR., Assistant Chief
Fuels and Lubrication Division
Aero Propulsion and Power Laboratory

IF YOUR ADDRESS HAS CHANGED, IF YOU WISH TO BE REMOVED FROM OUR MAILING LIST, OR IF THE ADDRESSEE IS NO LONGER EMPLOYED BY YOUR ORGANIZATION PLEASE NOTIFY WRDC/POSF, WRIGHT-PATTERSON AFB, OH 45433-6563 TO HELP MAINTAIN A CURRENT MAILING LIST.

COPIES OF THIS REPORT SHOULD NOT BE RETURNED UNLESS RETURN IS REQUIRED BY SECURITY CONSIDERATIONS, CONTRACTUAL OBLIGATIONS, OR NOTICE ON A SPECIFIC DOCUMENT.

UNCLASSIFIED

SECURITY CLASSIFICATION OF THIS PAGE

REPORT DOCUMENTATION PAGE				Form Approved OMB No. 0704 0188	
1a REPORT SECURITY CLASSIFICATION Unclassified			1b RESTRICTIVE MARKINGS None		
2a SECURITY CLASSIFICATION AUTHORITY N/A			3 DISTRIBUTION/AVAILABILITY OF REPORT Approved for public release; Distribution is unlimited		
2b DECLASSIFICATION/DOWNGRADING SCHEDULE N/A					
4 PERFORMING ORGANIZATION REPORT NUMBER(S) N/A			5 MONITORING ORGANIZATION REPORT NUMBER(S) WRDC-TR-90-2079, Vol II		
6a NAME OF PERFORMING ORGANIZATION Dept of Materials Science and Engineering		6b OFFICE SYMBOL (If applicable)	7a NAME OF MONITORING ORGANIZATION Wright Research and Dev Cntr Aero Propulsion and Power Lab		
6c ADDRESS (City, State, and ZIP Code) Penn State University University Park, PA 16802			7b ADDRESS (City, State, and ZIP Code) Wright-Patterson AFB OH 45433-6563		
8a NAME OF FUNDING/SPONSORING ORGANIZATION N/A		8b OFFICE SYMBOL (If applicable) N/A	9 PROCUREMENT INSTRUMENT IDENTIFICATION NUMBER FY1455-89-NO635		
8c ADDRESS (City, State, and ZIP Code) N/A			10 SOURCE OF FUNDING NUMBERS		
			PROGRAM ELEMENT NO 62209F	PROJECT NO 3048	TASK NO 05
			WORK UNIT ACCESSION NO 81		
11 TITLE (Include Security Classification) Advanced Thermally Stable Jet Fuels Development Program Annual Report Vol II - Compositional Factors Affecting Thermal Degradation of Jet Fuels					
12 PERSONAL AUTHOR(S) S. Eser, C. Song, H. Schobert, P. Hatcher, R. Copenhaver, H. Jiang, R. Li					
13a TYPE OF REPORT Interim		13b TIME COVERED FROM 7/89 TO 6/90		14. DATE OF REPORT (Year, Month, Day) September 1990	
15 PAGE COUNT 97					
16 SUPPLEMENTARY NOTATION None					
17 COSATI CODES			18 SUBJECT TERMS (Continue on reverse if necessary and identify by block number)		
FIELD	GROUP	SUB-GROUP	Jet Fuels, Thermal Stability, Coking, Thermal Degradation, Fouling, Kinetics High Temperature Fuels, Chemical Species		
19 Model hydrocarbon compounds derived from both petroleum and coal liquids were thermally stressed in microautoclave reactors at temperatures of 350-500°C. Regardless of starting material, alkylated benzenes, alkylated naphthalenes, biphenyls, and complex polycyclic aromatics are formed by this thermal stressing. The concentration of these intermediates depends on the starting material and the experimental conditions. The formation of solids is directly related to high concentrations of alkylbenzenes and polycyclic aromatics in the liquid phase. Solid products consist primarily of large polycyclic aromatics with varying aliphatic substitution and their composition depends on the compound and the thermal conditions. Analysis of the solids showed anisotropic structures consistent with pseudo-nematic liquid crystalline mesophase. From these experiments a preliminary ordering of compound stability based on structure has been established.					
20 DISTRIBUTION/AVAILABILITY OF ABSTRACT <input type="checkbox"/> UNCLASSIFIED/UNLIMITED <input type="checkbox"/> SAME AS RPT <input type="checkbox"/> DTIC USERS			21 ABSTRACT SECURITY CLASSIFICATION Unclassified		
22a NAME OF RESPONDING INDIVIDUAL William L. Harrison III			22b TELEPHONE (Include Area Code) 513-255-6601		22c OFFICE SYMBOL WRDC/POSE

DISCLAIMER

This report was prepared as an account of work sponsored by the United States Government. Neither the United States nor any agency thereof, nor any of their employees, makes any warranty express or implied, or assumes any legal liability or responsibility for the accuracy, completeness, or usefulness of any information, apparatus, product, or process disclosed, or represents that its use would not infringe privately owned rights. Reference herein to any specific commercial product, process or service by trade name, mark manufacturer, or otherwise, does not necessarily constitute or imply its endorsement, recommendation, or favoring by the United States Government or any agency thereof. The views and opinions of authors expressed herein do not necessarily state or reflect those of the United States Government or any agency thereof.



Accession For	
NTIS GRA&I	<input checked="checked" type="checkbox"/>
DTIC TAB	<input type="checkbox"/>
Unannounced	<input type="checkbox"/>
Justification	
By	
Distribution/	
Availability Codes	
Dist	Avail and/or Special
A-1	

FOREWORD

In May 1989, the Fuels Branch of the Aero Propulsion Laboratory at Wright-Patterson Air Force Base, Ohio, commenced an investigation to develop advanced, thermally stable jet fuels as well as physical and computer models that could simulate the thermal degradation of those fuels under operational conditions. Funding was provided to the Department of Energy (DOE) Pittsburgh Energy Technology Center (PETC) to administer this effort. This report, Volume 2 of 3 volumes, details the efforts of Pennsylvania State University (PSU), under contract to Sandia National Laboratories (SNL), a prime contractor to DOE (DOE Contract Number DE-AC04-76DP00789). Investigations to identify classes of hydrocarbon compounds and mixtures which are thermally stable are described. Dr. Elmer Klavetter was the Contract Monitor. Mr. William E. Harrison III was the Air Force Program Manager, Dr. Nand Narain, Dr. Richard Hickey, and Mr. Swenam Lee were the DOE/PETC Program Managers, and Dr. Howard Stephens was the SNL Program Manager.

TABLE OF CONTENTS

	Page
LIST OF FIGURES	vii
LIST OF TABLES	x
OBJECTIVE	1
SUMMARY	2
TECHNICAL PROGRESS	3
TASK 1	4
ACTIVITY 1. LITERATURE SEARCH	4
ACTIVITY 2. MODEL COMPOUND REACTIONS	5
GENERAL PROCEDURES	6
n-BUTYLBENZENE	8
n-BUTYLCYCLOHEXANE	15
n-DECANE	19
DECALIN	27
TETRALIN AND NAPHTHALENE	33
t-BUTYLBENZENE	33
TETRADECANE	34
KINETICS OF SOLID FORMATION	35
OPTICAL MICROSCOPIC CHARACTERIZATION OF SOLID DEPOSITS	42
TASK 2	42
ACTIVITY 1. FRACTIONATION OF FUEL SAMPLES	42

TABLE OF CONTENTS (Concluded)

	Page
BACKGROUND	42
SEPARATION METHOD	43
EXPERIMENTAL.....	44
RESULTS	45
ACTIVITY 2. THERMAL STABILITY TESTING OF FUEL FRACTIONS.	76
ACTIVITY 3. THERMAL STABILITY TESTING OF UNSEPARATED FUELS	76
REFERENCES	85

LIST OF FIGURES

		Page
Figure 1.	A schematic diagram of the 15 ml capacity tubing bomb reactor.....	5
Figure 2.	GC/MS total ion chromatogram of the liquid product from n-butylbenzene treated at 450°C for 4 hours.	7
Figure 3.	DRIFT spectrum of the solids produced from n-butylbenzene at 450°C for 4 h.	10
Figure 4.	DRIFT spectrum of the solids produced from 2,4,6-tri-t-butylphenol at 450°C for 4 h.....	11
Figure 5.	DRIFT spectrum of the solids produced from JP-8/JFA-5 treated at 450°C for 4 h	12
Figure 6.	Solid State CPMAS ¹³ C NMR spectrum of n-butylbenzene solids produced at 450°C for 4 hours	14
Figure 7.	Total ion chromatogram of the liquid product from n-butylcyclo-hexane treated at 450°C for 1 h	15
Figure 8.	Specific ion (m/z=83) chromatogram of the liquid product from n-butylcyclohexane treated at 450°C for 1 h.	16
Figure 9.	Total ion chromatogram of the liquid product from n-butylcyclo-hexane treated at 450°C for 4 h.	18
Figure 10.	DRIFT spectrum of the solids produced from n-butylcyclohexane at 450°C for 4 h.	19
Figure 11.	Formation of solids from n-decane at 400, 425, and 450°C	20
Figure 12.	Total ion chromatogram of the liquid product from decane treated at 450°C for 6 (a) and 24 (b) hours.	21
Figure 13.	Solid State CPMAS ¹³ C NMR spectrum of the solids produced from decane at 450°C for 6 hours.	24
Figure 14.	Solid formation from decane and decalin at 425 °C (a) and 450°C (b)	26
Figure 15.	GC/MS total ion chromatogram of the liquid products from decalin treated at 450°C for 6 (a) and 24 (b) hours.	27
Figure 16.	Solid State CPMAS ¹³ C NMR spectrum of decalin solids produced at 450°C for 73 hours.	30

LIST OF FIGURES (Continued)

	Page
Figure 17. Solid formation from t-butylbenzene at 450°C.....	32
Figure 18. Solid formation from tetradecane at 425°C.	33
Figure 19. Formation of solids from model compounds as a function of treatment severity.	35
Figure 20. Formation of solids from decane, tetradecane and decalin as a function of treatment severity	35
Figure 21. Depletion of liquid products as a function of time in thermal	36
Figure 22. Arrhenius plots for the formation of solids and depletion of liquids during thermal treatment of decane.treatment of decane	38
Figure 23. Arrhenius plots for the depletion of liquids during thermal treatment of decane and decalin.	38
Figure 24. Arrhenius plots for the darkening of liquids during thermal treatment of decalin.	39
Figure 25. Preliminary procedure for chromatographic separation of jet fuel.	43
Figure 26. GC/MS total ion chromatogram of n-pentane eluted saturated Fraction (Fr.1) of coal-derived jet fuel JP8-C.....	47
Figure 27. GC/MS total ion chromatogram of 5% benzene-n-pentane eluted Fraction (Fr.2) of coal-derived jet fuel JP8-C.....	49
Figure 28. GC/MS total ion chromatogram of benzene eluted fraction (Fr.3) of coal-derived jet fuel JP8-C.....	52
Figure 29. GC/MS total ion chromatogram of n-pentane eluted saturated Fraction (Fr.1) of petroleum-derived jet fuel JP8-P.	55
Figure 30. GC/MS total ion chromatogram of 5% benzene-n-pentane eluted Fraction (Fr.2) of petroleum-derived jet fuel JP8-P.	58
Figure 31. GC/MS total ion chromatogram of benzene eluted Fraction (Fr.3) of petroleum-derived jet fuel JP8-P.	61

LIST OF FIGURES (Concluded)

	Page
Figure 32. GC/MS total ion chromatogram of petroleum-derived jet fuel JP8-P.	63
Figure 33. GC/MS total ion chromatogram of coal-derived jet fuel JP8-C..... petroleum-derived jet fuel JP8-P.	65
Figure 34. GC/MS total ion chromatogram of 185-215°C fraction of the coal- derived jet fuel JP8-C.	68
Figure 35. GC/MS total ion chromatogram of 215-240°C fraction of the coal- derived jet fuel JP8-C.	69
Figure 36. GC/MS total ion chromatogram of 185-215°C fraction of the coal- derived jet fuels JP8-P.	70
Figure 37. GC/MS total ion chromatogram of 215-240°C fraction of the coal- derived jet fuels JP8-P.	71
Figure 38. Transmittance of 520 nm light through the liquid products obtained from JP-8-Neat and JP-8/JFA-5 at 300°C-24 h and 350°C-4 h with or without deoxygenation before thermal treatment.	78
Figure 39. Transmittance of the products obtained from JP-8/JFA-5 at 350°C-5 h in air and in helium after deoxygenation by a helium	79
Figure 40. Transmittance of the products obtained from JP-8-Neat under different conditions in a helium atmosphere after deoxygenation by helium flush.	80
Figure 41. First-order plots for the thermal treatment of JP-8-Neat at four different temperatures.	81
Figure 42. The Arrhenius plot for the rate constants calculated from the transmittance data shown in Figure 41.	81

LIST OF TABLES

	Page
Table 1. Identified products in thermally treated n-butylbenzene at 450°C for 4 h under He atmosphere.	8
Table 2. Identified products in thermally treated n-butylcyclohexane at 450°C for 4 h under He atmosphere.	18
Table 3. Identified products in thermally treated decane at 450°C for 6 h under N ₂ atmosphere.	22
Table 4. Identified products in thermally treated decane at 450°C for 24 h under N ₂ atmosphere.	23
Table 5. Identified products in thermally treated decalin at 450°C for 6 h under N ₂ atmosphere.	28
Table 6. Identified products in thermally treated decalin at 450°C for 24 h under N ₂ atmosphere.	29
Table 7. Chromatographic separation of coal-derived jet fuel JP8-C on neutral alumina column.	44
Table 8. Chromatographic separation of petroleum-derived jet fuel JP8-P on neutral alumina column.	44
Table 9. Identified compounds in n-pentane eluted saturated Fraction (Fr.1) of coal-derived jet fuel JP8-C.	45
Table 10. Identified compounds in 5% benzene-pentane elute fraction (Fr.2) of coal-derived jet fuel JP8-C.	50
Table 11. Identified compounds in benzene elute fraction (Fr.3) of coal-derived jet fuel JP8-C.	53
Table 12. Identified compounds in n-Pentane eluted saturate fraction (Fr. 1) of petroleum-derived jet fuel JP8-P.	56
Table 13. Identified compounds in 5% benzene-pentane elute (Fr.2) of petroleum-derived jet fuel JP8-P.	59
Table 14. Identified compounds in benzene elute (Fr.3) of petroleum-derived jet fuel JP8-P.	62
Table 15. Identified compounds in petroleum-derived jet fuel JP8-P.	64
Table 16. Identified compounds in coal-derived jet fuel JP8-C.	66

LIST OF TABLES (Concluded)

	Page
Table 17. Components of the 185-215°C fraction of the coal-derived jet fuel JP8-C.	72
Table 18. Components of the 215-240°C fraction of the coal-derived jet fuel JP8-C.	72
Table 19. Components of the 185-215°C fraction of the petroleum-derived jet fuel JP8-P.	73
Table 20. Components of the 215-240°C fraction of the petroleum-derived jet fuel JP8-P.	74
Table 21. Comparative thermal testing of JP-8 Neat and JP-8/JFA-5.	75

OBJECTIVE

There are two broad objectives of this project. The first is to identify classes of hydrocarbon compounds which are thermally stable. Thermal stability of hydrocarbons refers to their resistance to chemical decomposition at high temperatures to form materials which can be deposited on metal surfaces. The second objective, which is essentially an extension of the first, is to identify stable hydrocarbon mixtures as would be obtained from distillate cuts typical of jet fuels.

SUMMARY

A set of model compounds including n-butylbenzene, n-butylcyclohexane, decane, decalin, tetralin, and naphthalene and two samples of jet fuel, JP-8 Neat, and JP8-JFA5 which contains an additive, were subjected to heat treatment in microautoclave reactors within a temperature range from 350°C to 500°C. Preliminary data were also obtained from the initial heat treatment experiments on t-butylbenzene and tetradecane. Among the model compounds, n-butylbenzene and n-decane were found to be reactive in forming solid deposits, while n-butylcyclohexane and decalin displayed a high thermal stability. The thermal treatment of tetralin and naphthalene under a selected set of conditions did not produce any apparent solids; however, an extensive thermal degradation of tetralin was evident from the discoloration of the liquid products. Naphthalene was found to be the most stable compound in the selected subset of model compounds with ten carbon atoms. Compared to the n-butylbenzene, t-butylbenzene appeared to be significantly less reactive in forming solids at 450°C; and tetradecane appeared to be slightly more reactive than n-decane at 425°C.

Gas Chromatography/ Mass Spectrometry (GC/MS) analysis of the liquids produced by the thermal treatment of the model compounds has shown primarily the formation of alkylbenzenes, naphthalene, alkyl naphthalenes, biphenyls, and more complex polyaromatic and alkylated polyaromatic compounds. The concentration of these compounds in the liquid products depends upon the starting materials and the treatment conditions. The formation of solids from the model compounds (such as n-butylbenzene and decane) has been generally associated with the relatively high concentrations of heavily substituted alkylbenzenes and polyaromatics in the accompanying liquid products. Thermally stable compounds (such as decalin and n-butylcyclohexane) have produced liquids containing relatively high concentrations of naphthalene and alkylbenzenes with a low-degree of substitution. Consistent with the generally accepted free radical mechanisms, the analytical and the kinetic data obtained in this study indicate that the nature of the nascent thermal degradation products play a critical role in determining the thermal behavior of hydrocarbons.

The characterization of the solid deposits by Fourier Transform Infrared Spectroscopy (FTIR), Cross Polarization Magic Angle Spinning ^{13}C Nuclear Magnetic Resonance Spectroscopy (CPMAS ^{13}C NMR) and optical microscopy has revealed that the solids consists principally of large polynuclear aromatic compounds with a varying concentration of aliphatic groups depending on the starting materials and the treatment conditions. Notably, almost all the solids produced from model compounds displayed

anisotropic microstructures indicating the formation of a pseudo-liquid crystalline phase - carbonaceous mesophase- during thermal treatment.

Kinetics of thermal degradation were studied by using the mass of solid deposits, the volume of liquid products, and percent light transmittance of the liquid products as indicators for the extent of thermal degradation as a function of treatment temperature and time. The apparent activation energies and preexponential factors for thermal degradation of some model compounds and the jet fuel JP-8 Neat were calculated by assuming a pseudo first-order kinetics. An activation energy of 53 kcal/mole and a preexponential factor of $4.56 \times 10^{16} \text{ h}^{-1}$ were calculated for the change in the light transmittance of the thermal stressing products obtained from JP-8 Neat.

A procedure has been developed to fractionate a petroleum-derived and a coal-derived JP-8 jet fuel by column chromatography using a neutral alumina gel and a series of solvent systems including pentane, benzene-pentane, benzene, ethanol-chloroform, and ethanol-tetrahydrofuran (THF). A high resolution GC/MS analysis of the column chromatographic and distillate fractions has revealed significant differences in the chemical composition of the petroleum- and coal-derived jet fuels. The coal-derived jet fuel consists mainly of monocyclic and bicyclic alkanes and some hydroaromatic compounds as the major components. In contrast, the petroleum-derived jet fuel is composed mainly of long-chain paraffins mixed with low concentrations of alkylbenzenes and alkylnaphthalenes. The fractionation procedure was also used on a preparative scale to separate the petroleum- and coal-derived jet fuel samples into well-defined fractions for thermal stability testing.

A comparative study of the thermal stability of the jet fuels JP-8 Neat and JP-8/JFA-5 suggested a lower stability of JP-8/JFA-5 in the presence of dissolved oxygen in fuel. In the thermal treatment experiments where the fuels were subjected to exhaustive deoxygenation prior to heating JP-8/JFA-5 appeared to be more stable than JP-8 Neat.

TECHNICAL PROGRESS

TASK 1

The objective of Task 1 is to identify classes of hydrocarbon compounds which are thermally stable. The Task consists of three activities: a literature search, an extensive series of model compound reactions, and the development of mathematical models of thermal stability ratings of the different compounds.

Activity 1. Literature Search.

Activity 1 is essentially complete, as envisioned as a one-time major review of existing work in the area. The literature search had three main thrusts: 1) articles appearing in the last few years in relevant technical journals, such as *Fuel*, *Energy and Fuels*, and the *ACS Division of Petroleum Chemistry Preprints*; 2) an extensive accumulation of reports and journal articles kindly provided to us by Dr. Elmer Klavetter of Sandia National Laboratory and Mr. William Harrison and Lt. Jeffery Moler of Wright-Patterson Air Force Base; and 3) a computer search of the NTIS, CA SEARCH, and COMPENDEX PLUS databases, with acquisition of copies of key publications.

The three prominent references on thermal stability of jet fuels are the "CRC Literature Survey on the Thermal Oxidation Stability of Jet Fuel" [1] and the fundamental studies reported by Bolshakov [2] and Nixon [3]. The proceedings and preprints of a NASA conference [4], the 62nd Propulsion and Energetics Panel Symposium [5], and the two symposia on the structure of future jet fuels [6,7] are good collections of more recent data and information on thermal stability of jet fuels. As a background to the present study, a brief review of the relevant literature is given below by selecting only a very small fraction of the publications in this area.

The initial studies on jet fuel stability were focused on thermal oxidation stability of air-saturated fuels and pure hydrocarbons as well as their mixtures at relatively low temperatures up to 300°C. A standard equipment called the Jet Fuel Thermal Oxidation Tester (JFTOT) (ASTM D 3241) has been commonly used for studying the stability of fuels [8]. In the JFTOT, the fuel is tested in an oxidative atmosphere under nonisothermal conditions. The standard test procedure provides only a qualitative measure of the formation of solids on the heated tubes. There have been some recent efforts to quantify JFTOT heater tube deposits [9-11]. However, it appears that these efforts suffer from the lack of a measurable property of the deposits which is directly proportional to their quantity but not dependent on the nature of the solids. The mechanisms of deposit formation in air-saturated fuels have been discussed by a number of researchers including Mayo [12], Boss

and Hazlett [13], and Taylor [14]. There is a general consensus that the formation of solids results from complex free radical autoxidation reactions involving molecular oxygen. However, the detailed chemical reactions that are involved in the formation of solid deposits are not well understood.

Among other researchers, Taylor and coworkers [15-18] have extended the thermal stability studies to include deoxygenated fuels and pure hydrocarbons tested at higher temperatures and pressures up to 649°C and 69 atm, respectively. The kinetics of solid formation from air-saturated and deoxygenated fuels gave complex Arrhenius plots with activation energies ranging from negative values to 45 kcal/mole [15]. A reduction in molecular oxygen content produced a marked reduction in the rate of solid formation for the majority of fuels. However, it was shown that a hydrocarbon jet fuel can exhibit high deposit formation rates in the absence of molecular oxygen [15]. Taylor [15] suggested that reaction mechanisms leading to solids are dominated by autoxidation for low temperature regimes and by pyrolysis for high temperature stressing of deoxygenated fuels. The presence of some trace impurity sulfur [16], and nitrogen and oxygen compounds [17] was seen to increase the rate of deposit formation. This effect was, however, strongly dependent on the functionality of the heteroatom compounds. In comparing the relative stability of various hydrocarbon functionalities, it was noted that cycloalkyl compounds were, in general, less harmful than their aliphatic and aromatic counterparts [17].

In addition to the changes in deposition rate, the morphology of the deposits was also seen to change with the varying amounts of dissolved oxygen in fuels. It was reported that at high oxygen levels, spherical deposits; at low oxygen levels, plate-like deposits were observed on tube surfaces. At intermediate oxygen levels, both types of deposits were observed [18].

The efforts for modelling the thermal stability of jet fuel can be exemplified by the two recent reports by Krazinski and Vanka [19] and Deshpande et al. [20] concentrating on the prediction of thermal stability based on chemical and physical processes involved. It should be noted that the success of modelling studies depends upon a good understanding of the chemistry and kinetics of thermal degradation processes.

Activity 2. Model Compound Reactions.

This section begins with a brief discussion of the general procedures used for conducting thermal stability experiments. Data and results for the specific model compounds tested are then presented in a compound-by-compound discussion. Kinetics of solid formation and microscopic characterization of solids are discussed separately at the end of this section.

A complication of the model compound work not anticipated at the start of the project is that many compounds of interest are either not available at all from commercial vendors of organic chemicals, or are available only at exorbitant prices. For example, 2-methylnonane, which would be of interest for comparison with decane, currently costs \$165.40 per 5 ml. Since at least this amount of material is used in each microautoclave test, it was decided that the original ambitious approach to model compound testing would have to be restricted to those compounds readily available at reasonable prices. A set of model compounds chosen to initiate the model compound reactions include n-butylbenzene, n-butylcyclohexane, decane, decalin, tetralin, and naphthalene. A common aspect of all the compounds in this subset is that they contain ten carbon atoms. The differences between their carbon and hydrogen atom configurations, such as straight chain vs cyclization, ring saturation vs unsaturation, alkyl substitution vs saturated ring, are expected to be reflected in their relative thermal stability. Some preliminary results on thermal treatment of t-butylbenzene and tetradecane are also presented in this report.

General procedures

All experiments on thermal stability, whether of model compounds, fuel fractions, or unseparated fuels, are conducted in microautoclave reactors. The design of the microautoclave reactors is shown in Figure 1. From time to time, minor modifications in the selection and specification of components are made, mainly to improve ease of assembly and disassembly, longevity in service, or both. However, the fundamental design and method of operation are not changed.

A 5 or 10 ml sample is generally used for each test. The procedure employed to remove air from the microautoclave involves repetitive pressurization to 1000 psi with ultra-high purity (UHP) He and purging after the sample is loaded. Typically, the cycle is repeated five times before the microautoclave is pressurized to the operating pressure of 100 psi. After a reactor has been assembled, filled with the desired headspace gas, and leak-tested, it is immersed into a fluidized bed sand bath which has been preheated to the desired temperature. Essentially any desired temperature in the range 150° - 550° C can be selected. Experience on prior projects in this laboratory has shown that the microautoclave reaches reaction temperature in 2 - 3 minutes. Reaction times range from 30 minutes to hundreds of hours; in principle there is no upper limit to reaction time in the apparatus. At the end of the planned reaction time the microautoclave is removed from the sand bath and plunged into cold water, to provide rapid quenching of the contents. The pressure is then reduced to ambient, and the microautoclave is opened for removal of the products and their subsequent work-up for analysis.

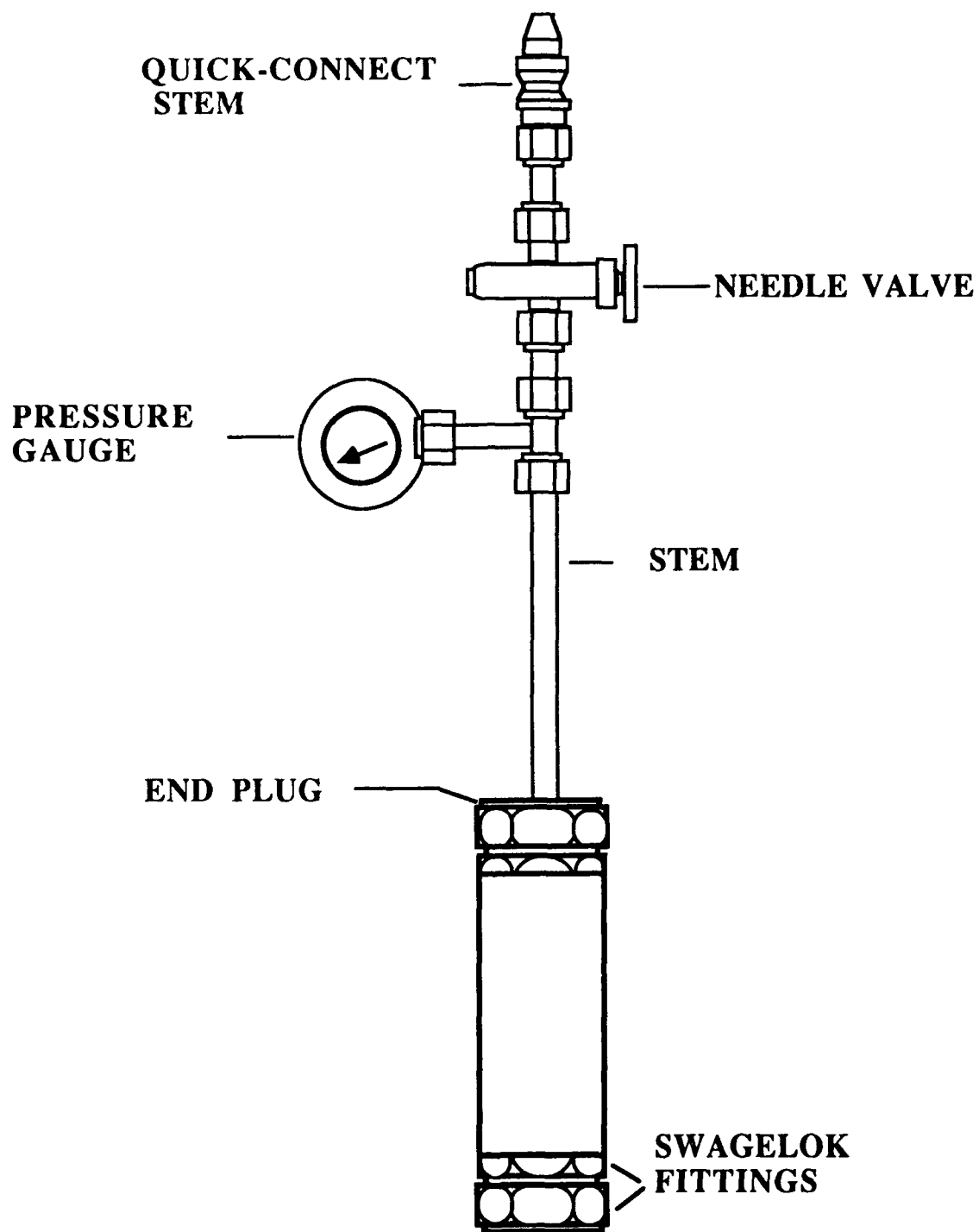


Figure 1. A schematic diagram of the 15 ml capacity tubing bomb reactor.

n-Butylbenzene

Treatment of *n*-butylbenzene formed a significant quantity of solids at 450°C for 1 h under a 100 psi (cold) He atmosphere. In comparison, *n*-butylcyclohexane (discussed below) did not produce any solids at all although the reaction products showed some signs of thermal degradation, e.g., color change. This preliminary observation shows that an aromatic ring with an alkyl substituent is much less stable than a saturated ring with the same alkyl substituent. The liquid products from the treatment of *n*-butylbenzene and *n*-butylcyclohexane were analyzed by GC/MS and the solids produced from *n*-butylbenzene by diffuse reflectance Fourier transform infrared spectroscopy (DRIFT).

A Dupont model 21-490 B gas chromatograph/mass spectrometer system with J & W DB 17 Column was used for GC/MS analysis of liquids remaining after reaction. The column was heated from 80 to 280°C at a rate of 8°C/min during the analysis. The total ion chromatogram (TIC) of the liquid product from *n*-butylbenzene showed a poor separation of the sample, most probably due to the presence of high molecular weight compounds with low volatility that either could not be introduced into, or eluted from, the capillary column. This observation shows that, in addition to the formation of solids, the liquid product from *n*-butylbenzene consists of compounds with complex molecular structures.

The liquid products from *n*-butylbenzene obtained at 450°C for 4 hours were analyzed by GC/MS using Kratos MS-80 system. Figure 2 shows a total ion chromatogram of the liquid product. The major peaks marked with the scan numbers are identified in Table 1. It can be seen in Table 1 that *n*-butylbenzene underwent substantial thermal degradation. The major components of the liquids include several types of compounds such as alkylbenzenes, naphthalene and alkyl naphthalenes, biphenyl and alkylbiphenyls and phenyl naphthalene, bibenzyl, phenanthrene and terphenyl.

The presence of toluene at a high concentration in the liquid product suggests the cleavage of the benzylic C-C bond in *n*-butylbenzene followed by hydrogen abstraction. Bibenzyl, also found in the liquid phase, can be considered to be formed by the coupling of two benzyl radicals. It is widely considered that the benzylic C-C bond in alkylbenzenes is relatively weak. The above results are consistent with the known chemistry involving the

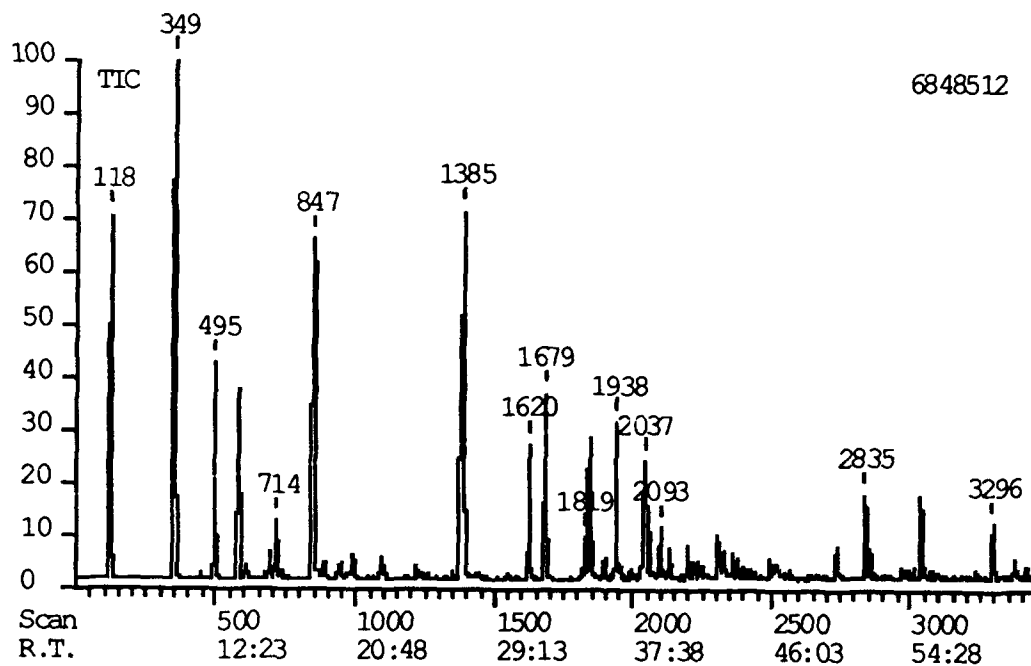


Figure 2. GC/MS total ion chromatogram of the liquid product from n-butylbenzene treated at 450°C for 4 hours.

Table 1. Identified products in thermally treated n-butylbenzene at 450°C for 4 h under He atmosphere.

Peak Scan No.	Molecular Ion	Base Peak	Identified Compounds
118	92	91	Toluene
349	106	91	Ethylbenzene
495	120	105	iso-Propylbenzene
578	120	91	n-Propylbenzene
714	134	105	C ₄ -benzene
847	134	91	n-Butylbenzene
1385	128	128	Naphthalene
1620	142	142	2-Methylnaphthalene
1679	142	142	1-Methylnaphthalene
1819	156	141	2-Ethylnaphthalene
1842	154	154	Biphenyl
1938	168	168	Methylbiphenyl
2037	168	168	Methylbiphenyl
2093	182	91	Bibenzyl
2737	178	178	Phenanthrene
2835	204	204	1-Phenylnaphthalene
3034	204	204	2-Phenylnaphthalene
3296	230	230	Terphenyl

cleavage of benzylic bond in alkylbenzenes. However, the liquids also contain high concentrations of ethylbenzene and propylbenzene, indicating the extensive cleavage of the C-C bonds in the butyl side chain in addition to the cleavage of the benzylic C-C bond. Figure 2 shows that naphthalene is one of the major components of the liquid product. Probably, naphthalene was formed by cyclization of n-butylbenzene followed by dehydrogenation. The formation of biphenyl, on the other hand, can be attributed to the formation and coupling of phenyl radicals. The presence of phenylnaphthalene and terphenyl can also be explained by the formation and subsequent reactions of phenyl radicals. The small concentration of phenanthrene can be considered to have resulted from the cyclization and dehydrogenation of bibenzyl.

The polyaromatics and especially the alkylated polyaromatic probably more complex in structure than those identified in the liquid product are most likely the precursors to solid deposits. It can be argued that the polyaromatics identified in the liquid product may actually represent thermally stable structures rather than precursors to solids. For example, unsubstituted polyaromatics such as naphthalene and biphenyl are not likely precursors to solids because of their relatively high thermal stability. The solid deposits formed in thermal treatments are operationally defined as the materials which are not soluble in the resulting liquid coproduct. Therefore, especially the initial precipitation of solids during thermal treatment will depend on the physical properties, essentially the solvent power of the liquid coproduct, as well as on the molecular structure of the actual solids. It should be stressed that the nature of solids produced from different starting materials can, thus, be different depending not only on the severity of the thermal treatment but also on the solvent properties of the liquid coproduct.

The DRIFT spectrum of the solids produced from n-butylbenzene at 450°C for 4 hours was obtained in an ANALECT-AQS-20 spectrometer with a resolution of 4 cm⁻¹. The sample was prepared by grinding KBr with 1%wt of the solid product. The DRIFT spectrum in Figure 3 shows strong absorptions in the aromatic C-H stretch (3000-3050 cm⁻¹) and out-of-plane bending (750 -900 cm⁻¹) regions, indicating that the most prominent structural feature of the solids is their high aromaticity. The substantially higher intensity of the 750 cm⁻¹ band compared to the other bending vibrations indicate a low degree of substitution on the aromatic rings. The absorptions at 2950 cm⁻¹ (methyl and methylene stretch) and 1450 cm⁻¹ (methyl and methylene bend) in conjunction with weak absorptions at 1375 cm⁻¹ (methyl bend) suggest low concentrations of methyl substitution on aromatic rings conjugated via methylene groups. These structural features are similar to those observed by GC/MS analysis of the thermal degradation products of alkylated phenols reported in a collateral DOE-funded project on jet fuels (Contract No. DE-AC-88PC88827, Second and Fourth Quarterly Reports). For comparison, the DRIFT spectrum of solids produced from 2,4,6-tri-t-butylphenol at 450°C for 4 hours is shown in Figure 4. Similar to the spectrum of n-butylbenzene solids, strong aromatic C-H stretch and bending signals are the most important features of the spectrum in Figure 4. The similarities between the overall appearance of the two spectral profiles are noteworthy. One readily noted difference between them is the comparatively higher intensities of the aliphatic CH stretch and bending vibrations in Figure 4, indicating that the 2,4,6-tri-t-butylphenol solids are more heavily substituted and conjugated than n-butylbenzene solids. This difference can be attributed to the presence of three alkyl groups in the starting t-butyl phenol vs only one alkyl group in n-butylbenzene. Figure 5 gives the DRIFT spectrum of the solids

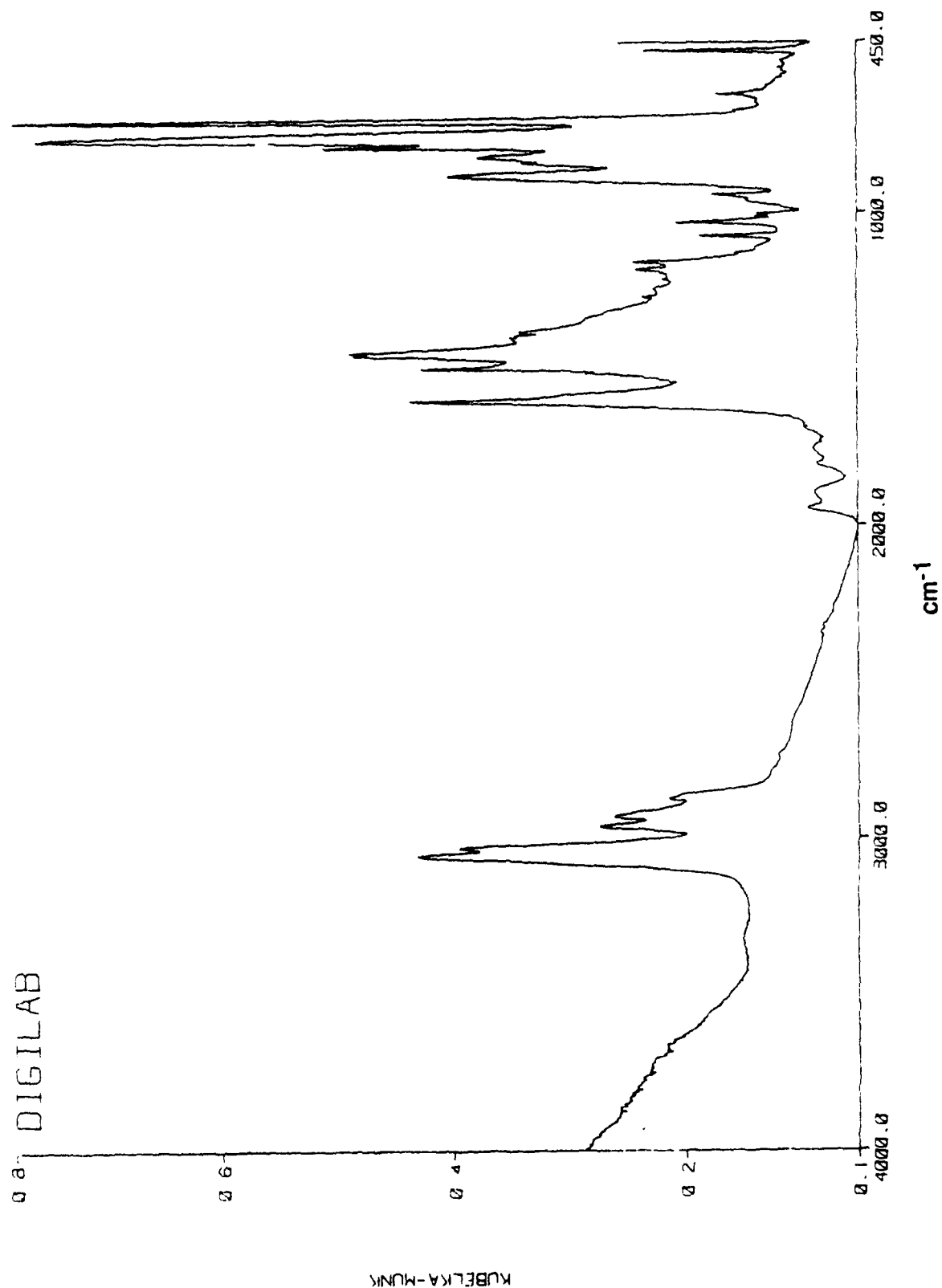


Figure 3. DRIFT spectrum of the solids produced from n-butylbenzene at 450°C for 4 h.

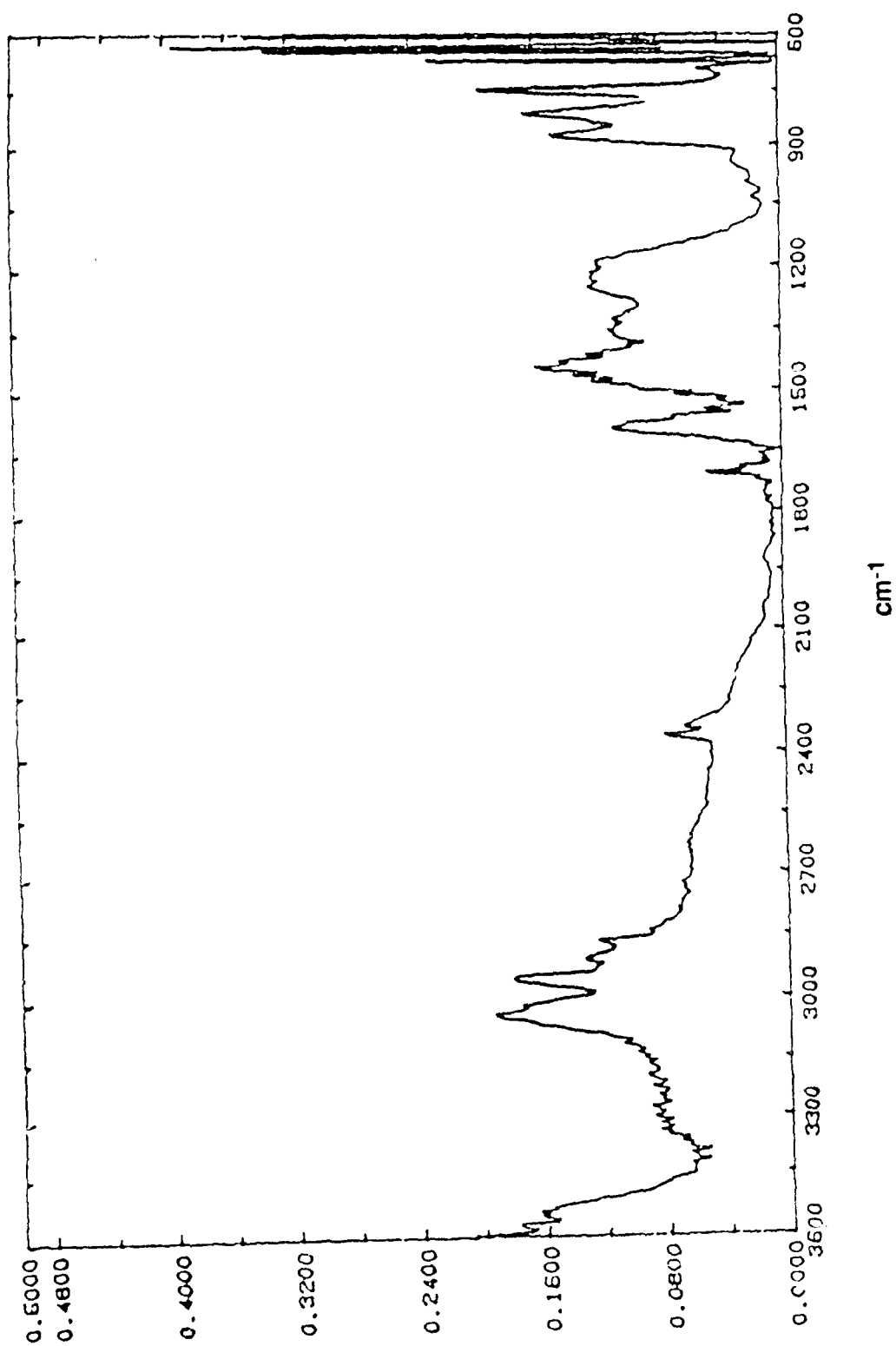


Figure 4. DRIFT spectrum of the solids produced from 2,4,6-tri-t-butylphenol at 450°C for 4 h.

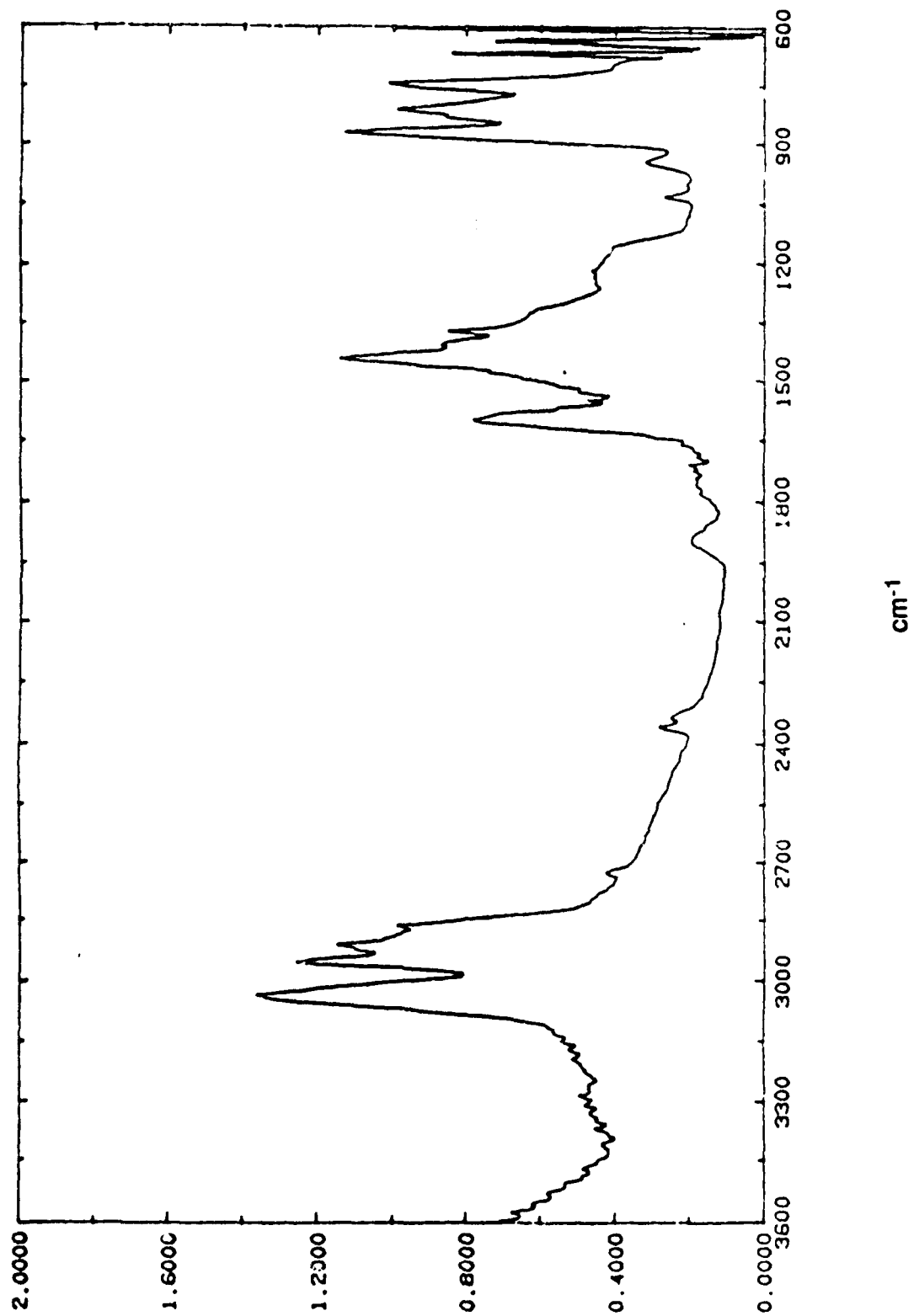


Figure 5. DRIFT spectrum of the solids produced from JP-8/JFA-5 treated at 450°C for 4 h.

produced from JP-8/JFA-5 treated at 450°C for 4 h. The qualitative similarity of this spectrum with that of Figure 3 suggests structural similarities between the solid products of n-butylbenzene and an authentic fuel, and, by extension, possibly similar mechanisms of formation.

The solid products obtained from n-butylbenzene treated at 450°C for 4 hr were also analyzed by solid state ^{13}C NMR spectroscopy. A Chemagnetics M-100 was used for this cross polarization with magic angle spinning (CPMAS) analysis, with the instrument conditions of 1 msec contact time; pulse repetition rate, 1 sec; line broadening, 40 Hz; sweep width, 14 KHz; ^{13}C frequency, 25.03 MHz; and sample spinning rate, 3.5 KHz. The spectrum, shown in Figure 6, indicates the highly aromatic nature of the n-butylbenzene solids, as was also shown by the DRIFT spectrum above. These findings strongly suggest that the formation of solid deposits is associated with the formation of highly condensed polyaromatic compounds.

n-Butylcyclohexane

The liquid products from the treatment of n-butylcyclohexane were analyzed by GC/MS. Figure 7 shows the GC/MS TIC of the liquid product obtained from n-butylcyclohexane at 450°C for 1 hour. Under these conditions n-butylcyclohexane did not produce any solids. Figure 8 shows a specific mass ($m/z = 83$, representing cyclohexyl ions) chromatogram of the same sample indicating the peaks which contain cyclohexyl ions. It can be seen that the cyclohexyl chromatogram almost exactly reproduces the TIC shown in Figure 8, indicating that almost every peak in the TIC contains cyclohexyl as a structural component. This relatively simple chemical constitution of the n-butylcyclohexane liquid compared to the complex structure of n-butylbenzene liquid is another indication of superior thermal stability of n-butylcyclohexane. Some of the molecular components of the n-butylcyclohexane liquid have been identified by mass spectroscopy of selected peaks in the TIC. The TIC showed that butylcyclohexane is the major component of the liquid product. The intense butylcyclohexane peak in the TIC was removed to amplify the intensities of the signals from the degradation products. Peak a in the TIC (Figure 7), the major component of the degradation products, is a methylbutylbicyclohexyl. Peak b in the TIC has been identified as a dimethylbutylbicyclohexyl. Peak c is 2-butyl-1,1'-bicyclohexyl. The structures of the identified molecules in the liquid product from n-butylcyclohexane indicate that initial thermal degradation of this compound involves loss or rearrangement of alkyl groups and self-coupling of completely or partially dealkylated and methylated molecules or coupling of these molecules with n-butylcyclohexane molecules. These chemical changes are similar to

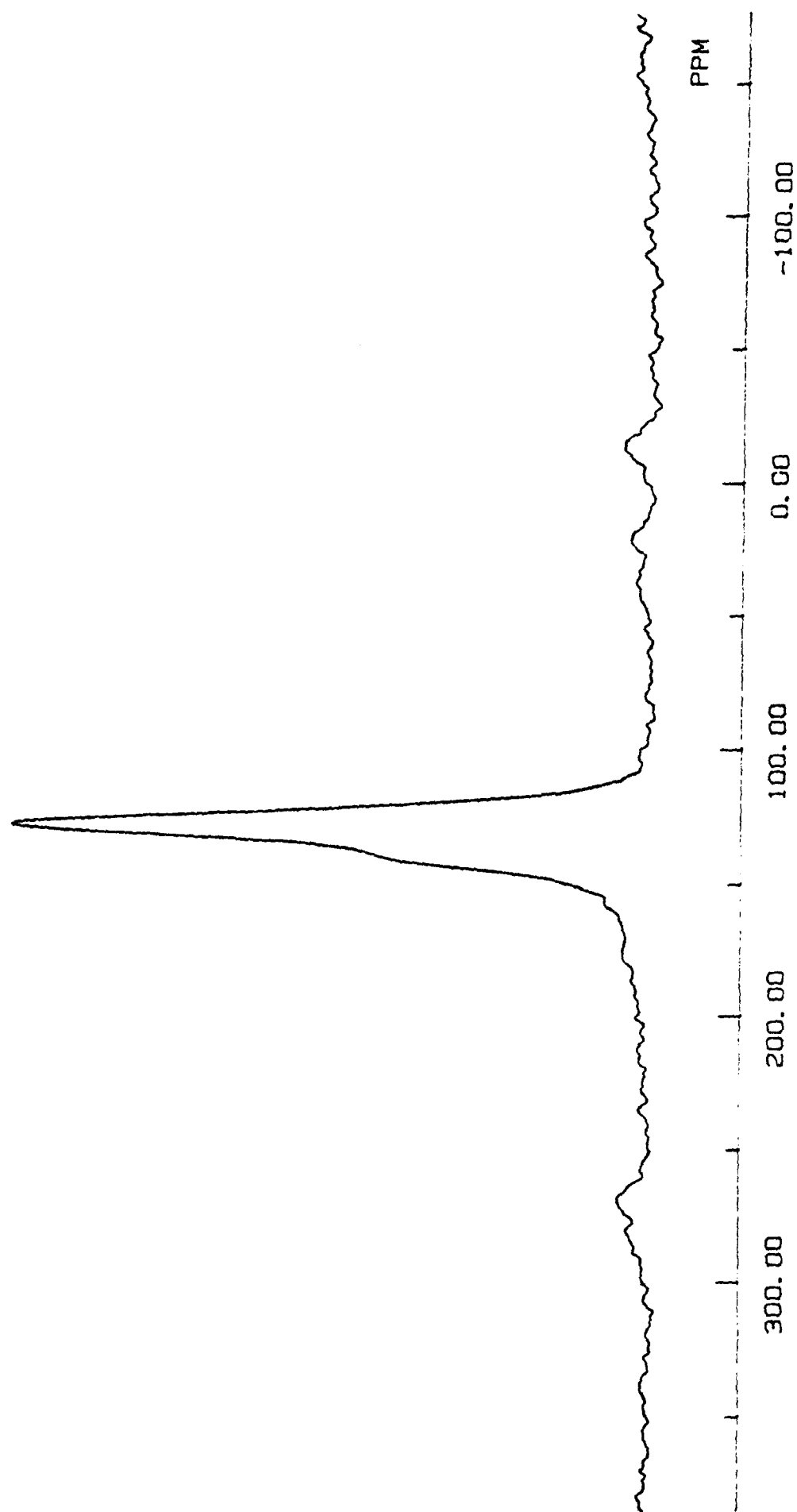


Figure 6. Solid State CPMAS ^{13}C NMR spectrum of n-butylbenzene solids produced at 450°C for 4 hours.

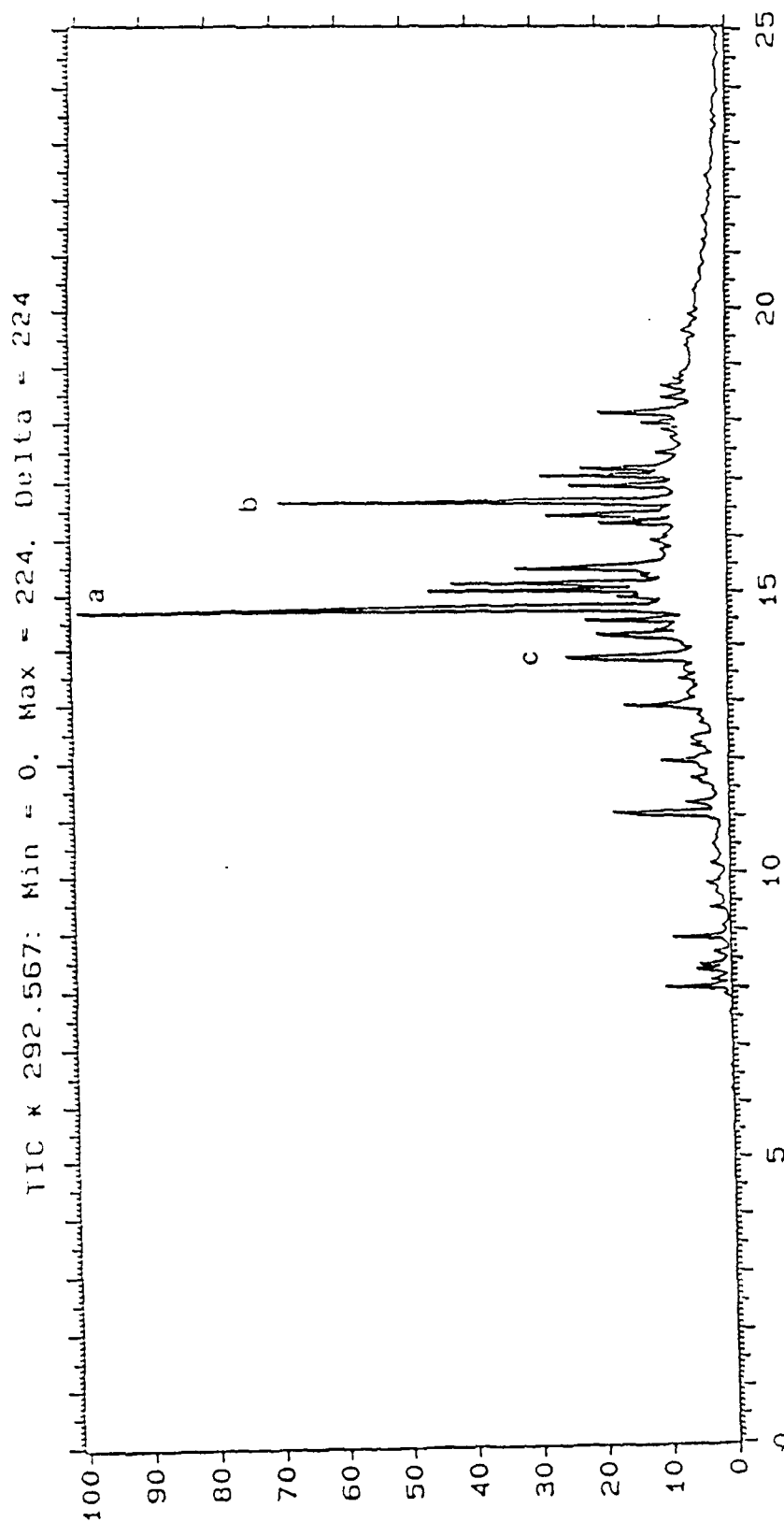


Figure 7. Total ion chromatogram of the liquid product from n-butylcyclohexane treated at 450°C for 1 h.

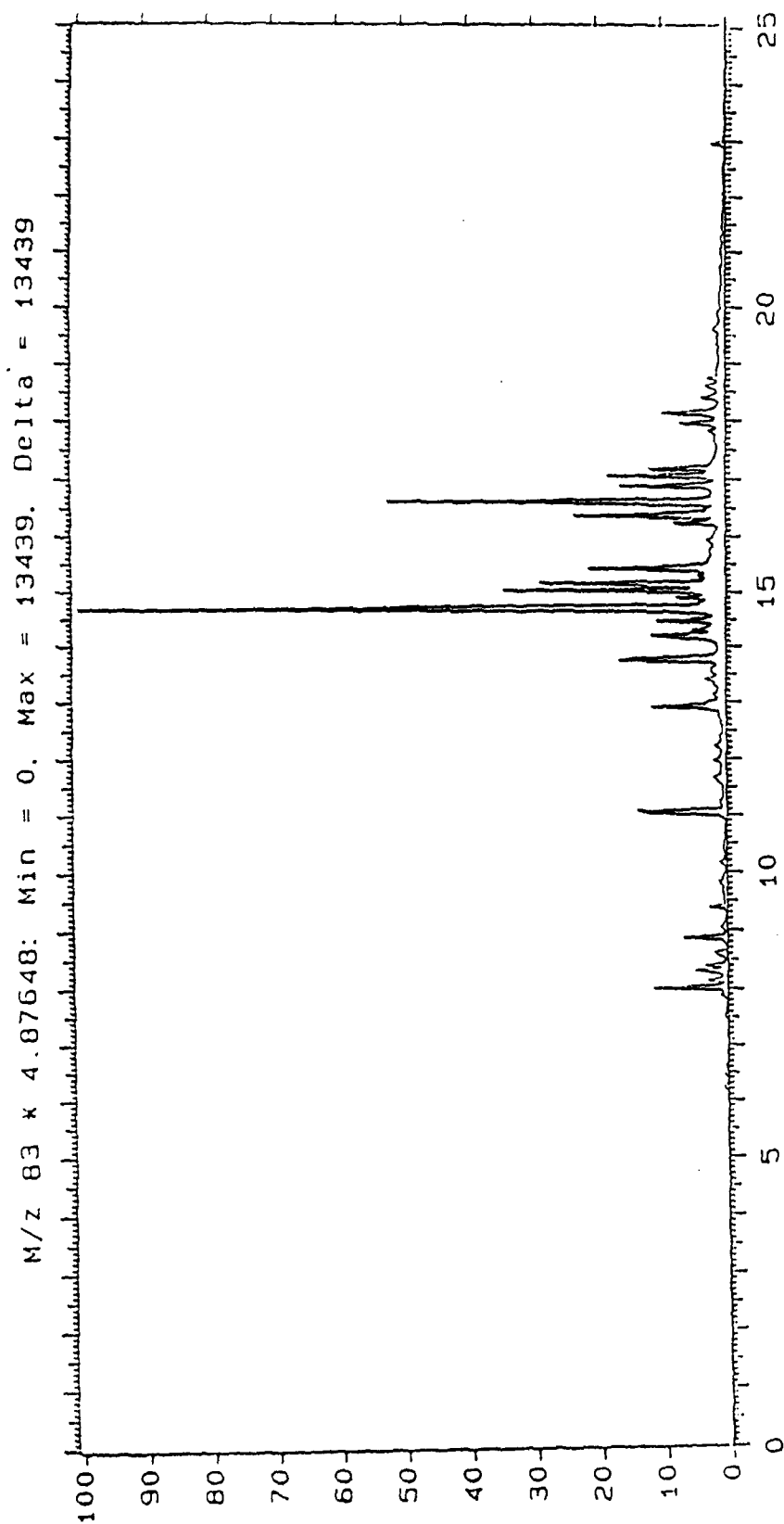


Figure 8. Specific ion ($m/z=83$) chromatogram of the liquid product from *n*-butylcyclohexane treated at 450°C for 1 h.

those observed during thermal treatment of alkylated phenols described in the cited quarterly reports for DOE project DE-AC-88PC88827.

Figure 9 shows the GC/MS TIC of the liquid produced from butylcyclohexane treated at 450°C for 4 hours. This treatment produced some solids. The major components of the liquid product include methylcyclohexene, ethylcyclohexane, C₄-cyclohexane, butylbenzene, and small concentrations of methylindan, naphthalene, and alkylnaphthalenes, as shown in Table 2 and Figure 9. Apparently, butylcyclohexane is still the predominant component of the liquid product, showing the comparatively high thermal stability of butylcyclohexane. The presence of butylbenzene as a major degradation product suggests that dehydrogenation of the saturated ring occurs more readily than the C-C bond cleavage in the butyl side chain. The formation of naphthalene and alkylnaphthalenes can be considered to result from further reactions of butylbenzene, as discussed above.

Figure 10 shows a DRIFT spectrum of the solids produced from *n*-butylcyclohexane at 450°C for 4 hours. Compared to the solids from *n*-butylbenzene produced under the same conditions, *n*-butylcyclohexane solids appear to contain higher concentrations of aliphatic CH functionalities. The comparison of the intensities of the absorptions in the aliphatic region in the range 2850-2950 cm⁻¹ implies that the *n*-butylcyclohexane solids contain higher proportions of methylene groups.

n-Decane

Treatment of decane showed extensive thermal degradation producing substantial quantities of solids in a N₂ atmosphere at 400, 425 and 450°C for the reaction times ranging from 1 hour to 72 hours. The amount of solids produced from decane at the three temperatures as a function of time is shown in Figure 11. The plots show a strong dependence of the solid formation on reaction temperature. For example, the treatment at 400°C for 72 hours produced 45 mg of solids from 10 ml of decane, while the treatment at 450°C for 10 hours produced 460 mg of solids. As was discussed above, the decreasing mass of solids in going from 24 hour treatment to 48 hour treatment at both 400° and 425°C is possibly due to higher solubility of the solids in the respective liquid products obtained in the 48 hour treatment. This behavior presents difficulties in the kinetic analysis of the experimental data as will be discussed in the section on the kinetics of solid formation.

The GC/MS TIC's of the liquids produced from decane at 450°C for 6 hours and 24 hours are shown in Figure 12a and 12b. Tables 3 and 4 give lists of the identified compounds with the respective scan numbers on the TIC's. It should be noted that the

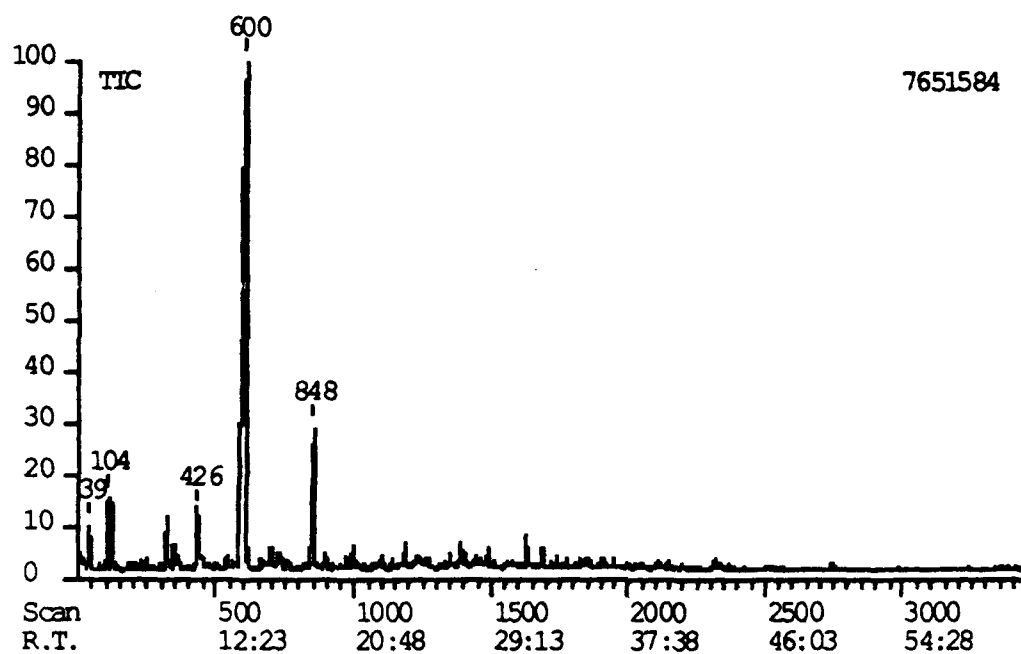


Figure 9. Total ion chromatogram of the liquid product from n-butylcyclohexane treated at 450°C for 4 h.

Table 2. Identified products in thermally treated n-butylcyclohexane at 450°C for 4 h under He atmosphere

Peak Scan No.	Molecular Ion	Base Peak	Identified Compounds
39	96	81	Methylcyclohexene
104	112	83	Ethylcyclohexane
426	140	55	C ₄ -cyclohexane
600	140	83	n-Butylcyclohexane
848	134	91	n-Butylbenzene
998	132	117	Methylindan
1187	132	117	Methylindan
1387	128	128	Naphthalene
1622	142	142	2-Methylnaphthalene
1681	142	142	1-Methylnaphthalene
1901	156	156	Dimethylnaphthalene

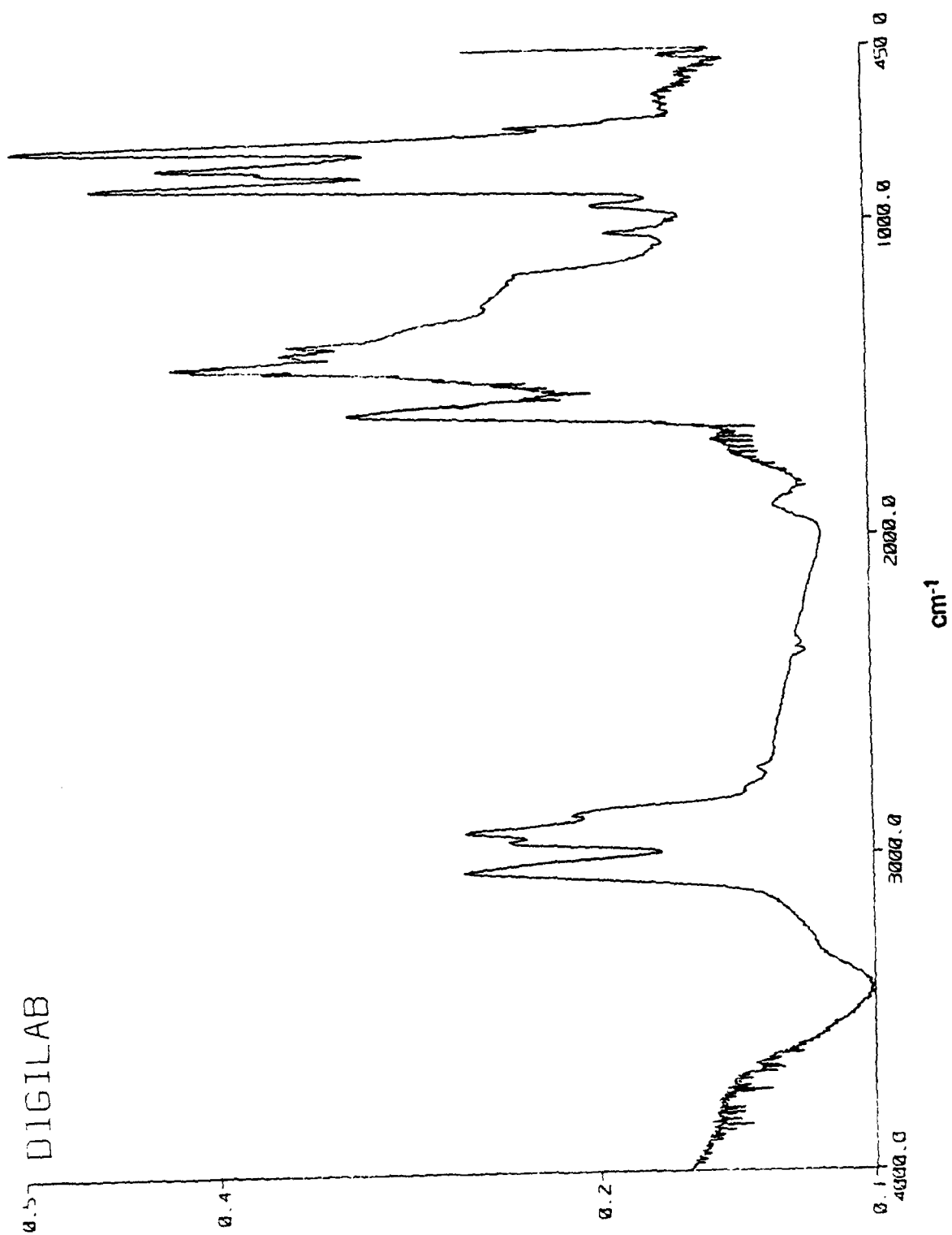


Figure 10. DRIFT spectrum of the solids produced from n-butylcyclohexane at 450°C for 4 h.

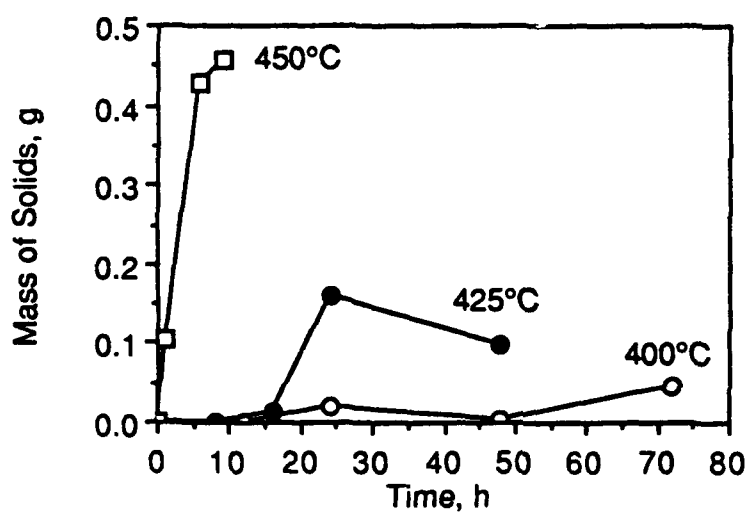
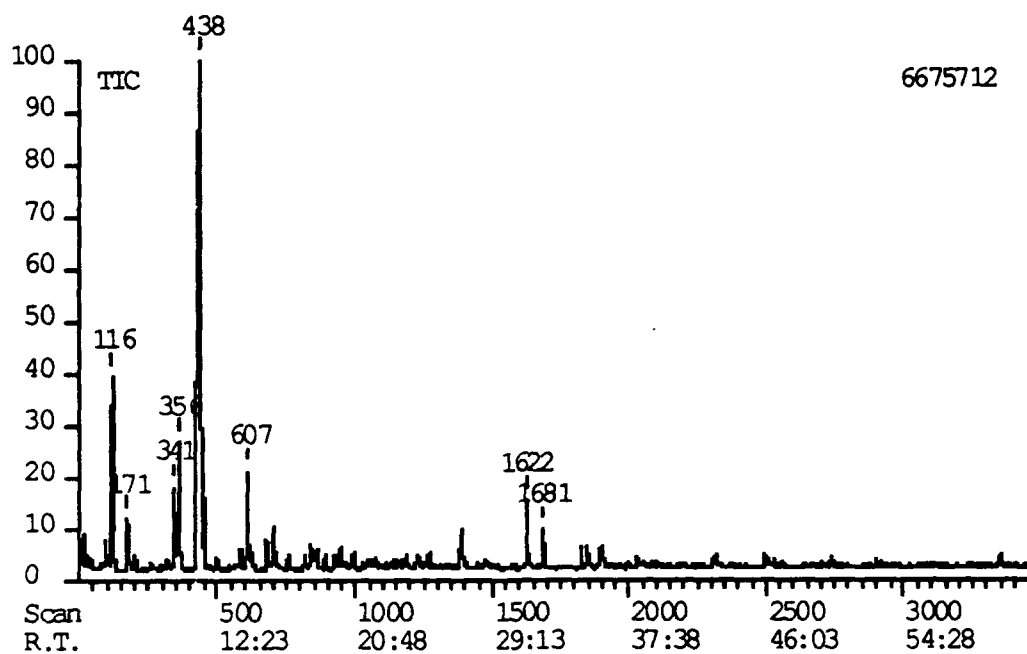
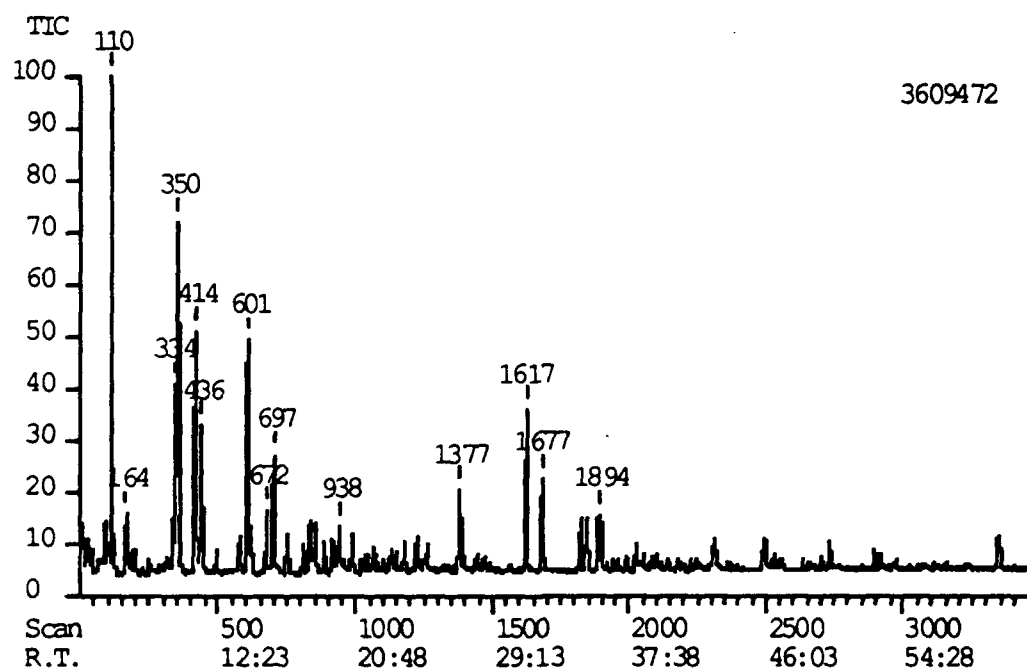


Figure 11. Formation of solids from n-decane at 400, 425, and 450°C.



a



b

Figure 12. Total ion chromatogram of the liquid product from decane treated at 450°C for 6 (a) and 24 (b) hours.

Table 3. Identified products in thermally treated decane at 450°C for 6 h under N₂ atmosphere

Peak Scan No.	Molecular Ion	Base Peak	Identified Compounds
116	92	91	Toluene
171	128	43	iso-Nonane (iso-C ₉)
341	106	91	Ethylbenzene
356	106	91	p-Xylene
438	142	43	n-Decane (n-C ₁₀)
607	120	105	Trimethylbenzene
704	120	105	Trimethylbenzene
1387	128	18	Naphthalene
1622	142	142	2-Methylnaphthalene
1681	142	142	1-Methylnaphthalene
1823	156	141	2-Ethylnaphthalene
1842	156	156	Dimethylnaphthalene
1901	156	156	Dimethylnaphthalene

Table 4. Identified products in thermally treated decane at 450°C for 24 h under N₂ atmosphere.

Peak Scan No.	Molecular Ion	Base Peak	Identified Compounds
110	92	91	Toluene
164	128	43	iso-Nonane
334	106	91	Ethylbenzene
350	106	91	p-Xylene
414	142	57	n-Decane (n-C10)
436	106	91	Xylene
601	120	105	Trimethylbenzene
672	120	105	C ₃ -benzene
697	120	105	C ₃ -benzene
938	134	119	C ₄ -benzene
1377	128	128	Naphthalene
1617	142	142	2-Methylnaphthalene
1677	142	142	1-Methylnaphthalene
1823	156	141	2-Ethylnaphthalene
1842	156	156	Dimethylnaphthalene
1894	156	156	Dimethylnaphthalene
2726	178	178	Phenanthrene
3346	202	202	Pyrene

liquids obtained in both experiments were coproduced with substantial quantities of solids. Tables 3 and 4 indicate that the 6 hour liquid product consists principally of alkylbenzenes and alkylnaphthalenes and the 24 hour product contains three- and four-ring aromatics in addition to alkylbenzenes and alkylnaphthalenes. Compared to the 6 hour liquid, the 24 hour liquid contains unreacted decane at a much lower concentration and has higher concentrations of more heavily substituted alkylbenzenes. It is clear from the GC/MS analysis that thermal degradation of decane involves extensive cyclization and dehydrogenation reactions leading to the formation of a range of aromatic compounds.

Figure 13 shows the solid state ¹³C NMR spectrum of the solids produced from decane at 450°C for 6 hours. The highly aromatic nature of the solids is clearly seen in the spectrum. The integration of the respective signal intensities gave an aliphatic carbon content of 8% for this solid product. It is interesting to note that the aliphatic carbon

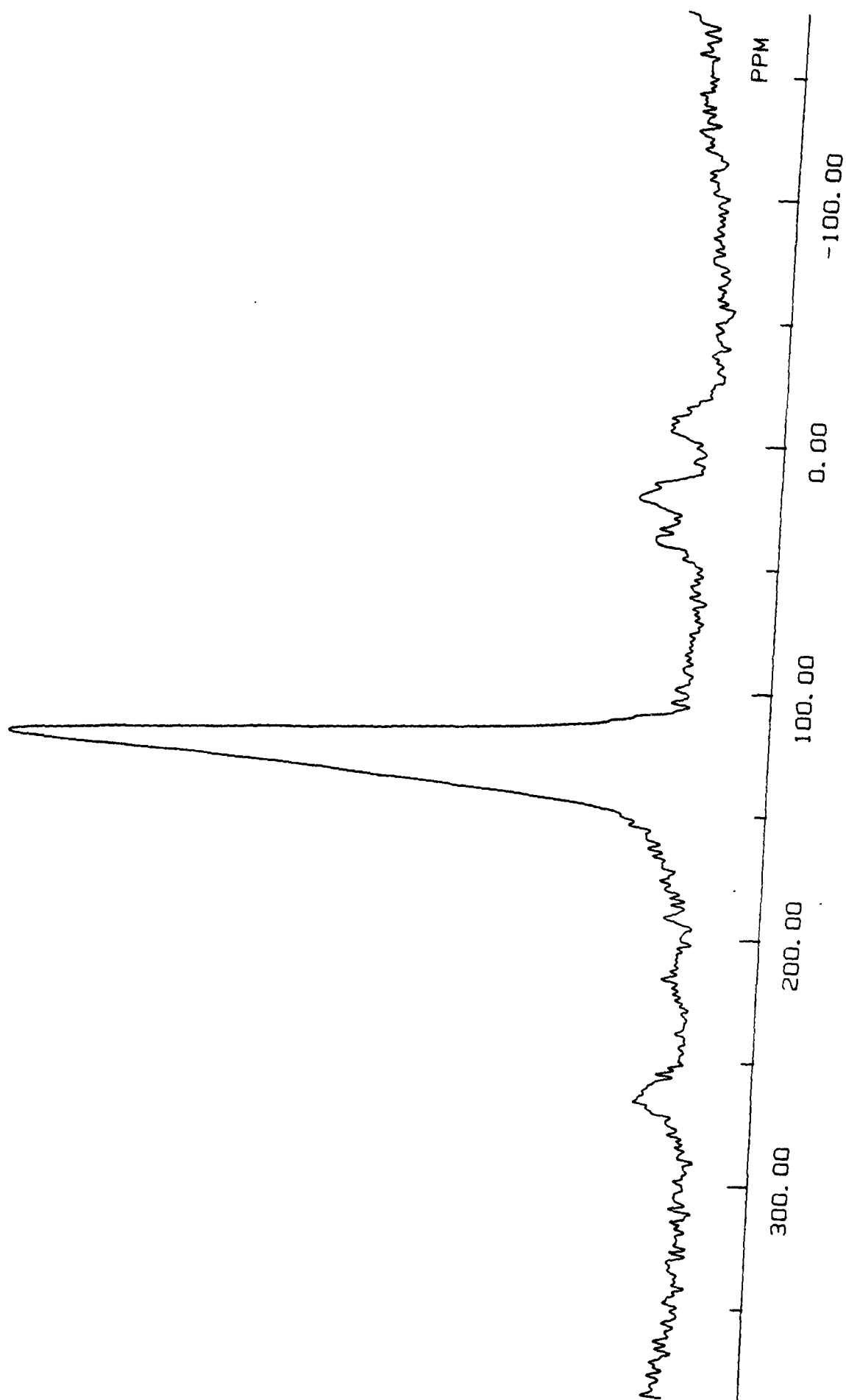


Figure 13. Solid State CPMAS ^{13}C NMR spectrum of the solids produced from decane at 450°C for 6 hours.

content of the solids was observed to increase slightly with the increasing reaction time at 450°C. The solids produced in 9 hours and 24 hours at 450°C contained 10% and 13% aliphatic carbon, respectively. This observation is significant in that it suggests a chemical interaction of the solids with the other degradation products after the precipitation of the solids. The increasing aliphatic carbon content can be explained by hydrogenation and/or alkylation of the solid deposits.

Decalin

In thermal treatment experiments decalin showed a much higher thermal stability than decane. Prolonged heating (for 24 to 48 hours) at 400 and 425°C did not produce any measurable quantities of solids from decalin. There were no solids formed in the reactor even after a 24 hour treatment at 450°C. Figure 14 compares the solid formation from decane and decalin at 425 and 450°C. The only significant amount of solids produced from decalin (93 mg) was obtained by treatment for 73 hours at 450°C, while decane produced approximately 460 mg solids from a 10 ml sample in 10 hours at 450°C.

Figure 15 shows the GC/MS TIC's of the liquid products obtained from decalin at 450°C for 6 hours (a) and for 24 hours (b). The identified compounds in these liquid products are shown in Tables 5 and 6. A notable feature of both TIC's in Figure 14 is that unreacted decalin is the major component with a substantially higher concentrations than those of the degradation products. It can be seen that the major degradation products from decalin include alkylbenzenes, naphthalene, and alkyl naphthalenes with relatively high concentrations of naphthalene and toluene compared to the concentrations of the other degradation products. It was noted that the cis-decalin to trans-decalin ratio decreases with increasing treatment severity. This behavior can be explained either by the isomerization of cis- to trans-decalin or by relatively high thermal stability of trans-decalin. As different from the liquid products obtained from decane under similar conditions (Figure 12, Tables 3 and 4), decalin liquids contain cycloalkanes and tetralin. Another contrast between the liquid products of decane and decalin is that the chemical composition of the decalin liquids does not show any significant change in going from the 6 hour to the 24 hour product, again pointing out the high thermal stability of decalin. The absence of three- or four- ring aromatics in the 24 hour product of decalin should also be noted.

Figure 16 shows the solid state ^{13}C NMR spectrum of the solids produced from decalin at 450°C for 73 hours. It can be seen from the spectrum that the decalin solids hardly contain any aliphatic carbon and they are more aromatic in nature than the decane solids (Figure 13). Based on the differences in the composition of the liquids and the

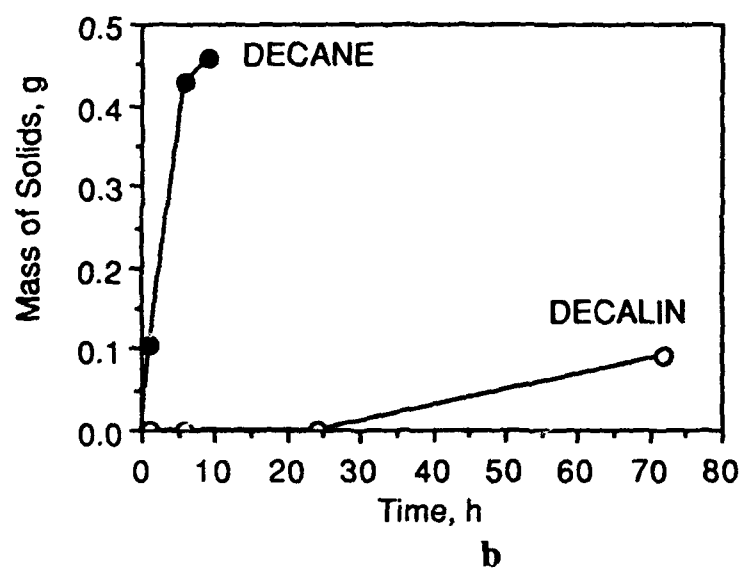
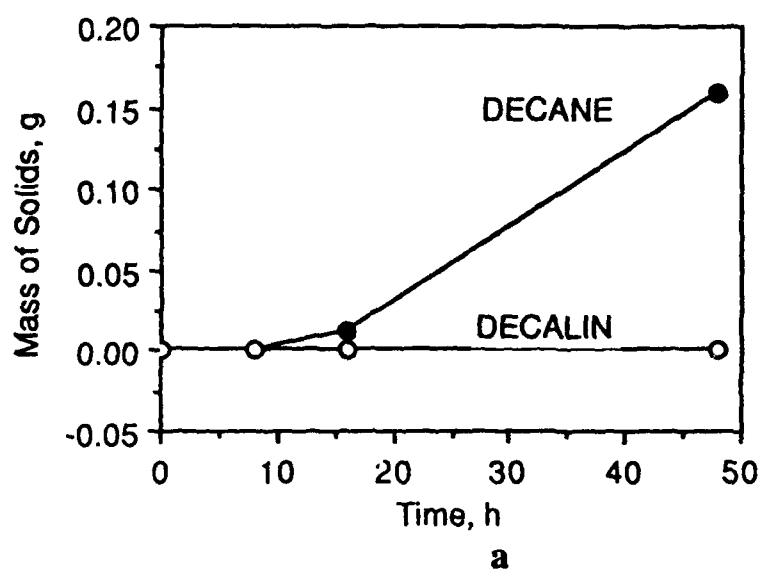
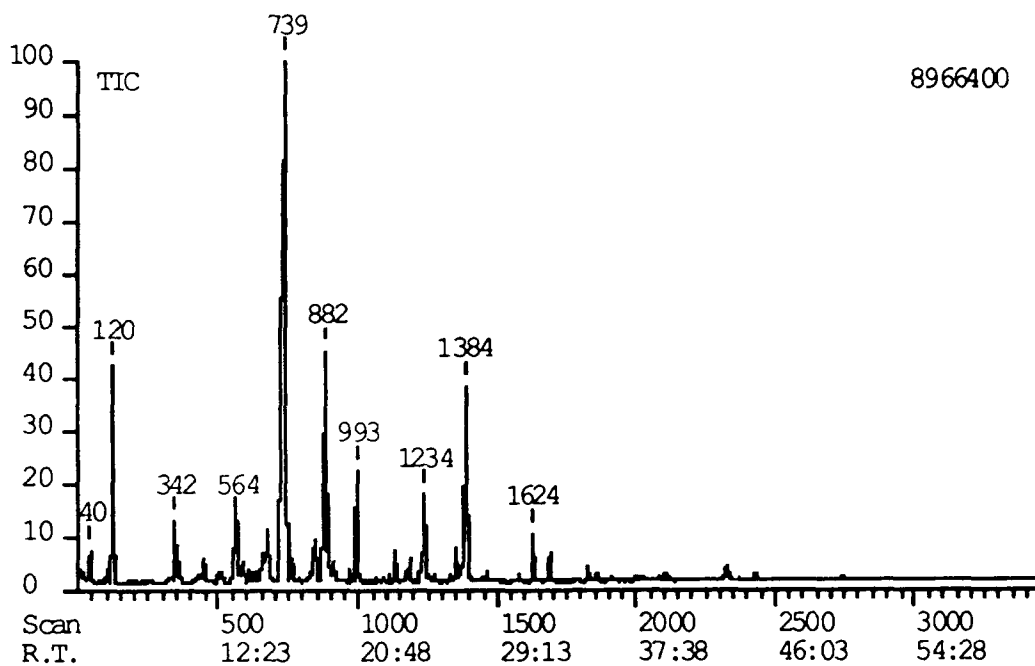
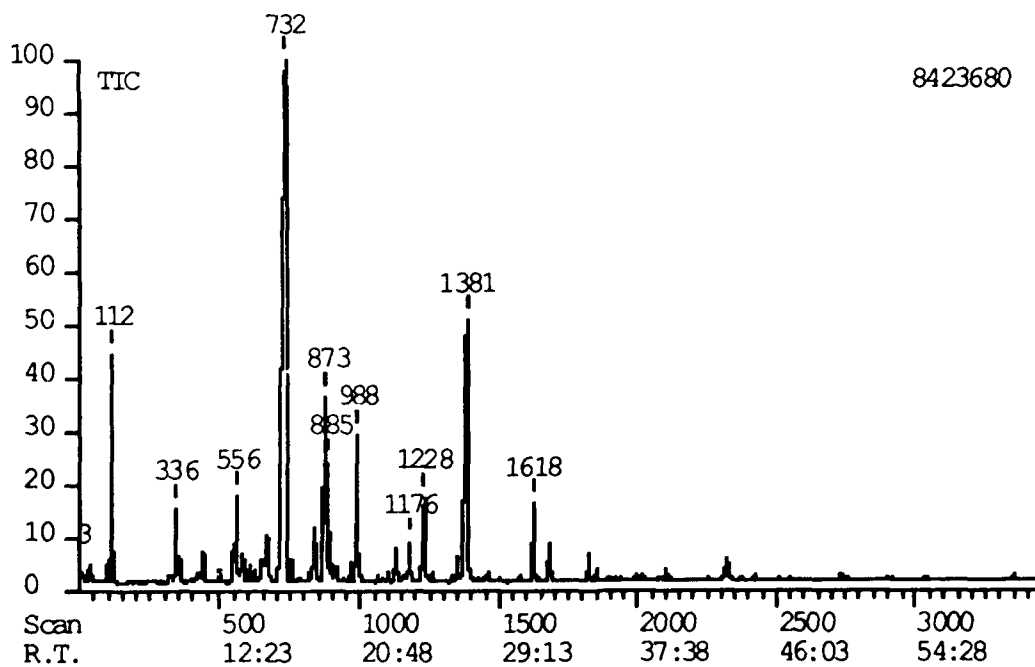


Figure 14. Solid formation from decane and decalin at 425 °C (a) and 450°C (b).



a



b

Figure 15. GC/MS total ion chromatogram of the liquid products from decalin treated at 450°C for 6 (a) and 24 (b) hours.

Table 5. Identified products in thermally treated decalin at 450°C for 6 h under N₂ atmosphere

Peak Scan No.	Molecular Ion	Base Peak	Identified Compounds
40	96	81	Methylcyclohexene
120	92	91	Toluene
342	106	91	Ethylbenzene
564	138	67	Methylhexahydroindan
672	138	96	Methylhexahydroindan
739	138	138	trans-Decalin
882	138	138	cis-Decalin
993	132	117	Methylindan
	136		Bicyclicalkene
1234	132	105	Tetralin
1384	128	128	Naphthalene
1624	142	142	2-Methylnaphthalene
1681	142	142	1-Methylnaphthalene
1823	156	141	2-Ethylnaphthalene
2329	168	168	Methylacenaphthene

Table 6. Identified products in thermally treated decalin at 450°C for 24 h under N₂ atmosphere

Peak Scan No.	Molecular Ion	Base Peak	Identified Compounds
3	112	83	Dimethylcyclohexane
112	92	91	Toluene
336	106	91	Ethylbenzene
437	106	91	Xylene
556	138	67	Methylhexahydroindan
664	138	96	Methylhexahydroindan
732	138	138	trans-Decalin
873	138	138	cis-Decalin
885	118	117	Indan
988	132	117	Methylindan
1176	132	117	Methylindan
1228	132	104	Tetralin
1381	128	128	Naphthalene
1618	142	142	2-Methylnaphthalene
1681	142	142	1-Methylnaphthalene
1823	156	141	2-Ethylnaphthalene
2317	168	168	Methylacenaphthene

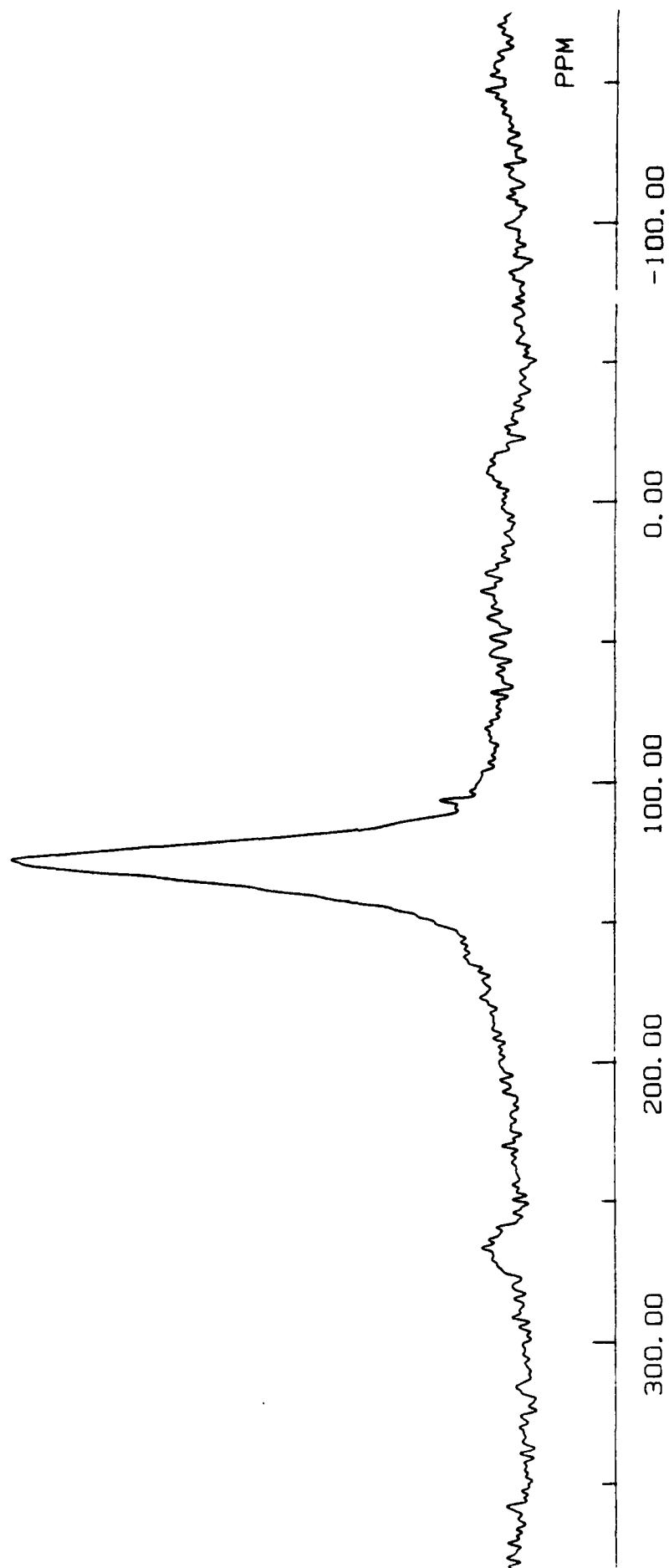


Figure 16. Solid State CPMAS ^{13}C NMR spectrum of decalin solids produced at 450°C for 73 hours.

molecular nature of the solids, it can be concluded that the principal mechanisms of solid formation from decane and decalin are different in addition to the difference in thermal stability of these compounds. It can be speculated that the principal reaction involved in initiating the thermal degradation of decalin is dehydrogenation which leads to the formation of a relatively stable aromatic molecule, naphthalene. In contrast, the initial cracking of decane appears to give rise to reactive intermediates which can rapidly form alkyl substituted polyaromatic molecules that can lead to solid deposits.

Tetralin and Naphthalene

The heat treatment of tetralin and naphthalene in a nitrogen atmosphere at 425 and 450°C for different reaction times up to 48 hours did not produce any carbonaceous solids. Naphthalene did not show any sign of degradation under these conditions, while the liquid product from tetralin showed an increased darkening in color with the increasing severity of thermal treatment. More stringent treatments at 475°C up to 4 hours and 500°C up to 3 hours did not produce any apparent solids either, while the treatment at 500°C for 6 hours produced a very viscous, black liquid from tetralin and brown crystals from naphthalene. Additional heat treatment experiments and analytical characterization of the treatment products will be carried out to elucidate the chemistry and kinetics of thermal degradation of tetralin and naphthalene. The results obtained so far indicate that, as expected, naphthalene is the most stable compound in the selected subset of hydrocarbons with ten carbon atoms.

t-Butylbenzene

t-Butylbenzene has been treated at 450°C for periods of 1, 4, 8, 12, 16, and 20 hours. The sample size was 5 ml. All reactions were performed with a 100 psi nitrogen overpressure. The deposition of solids as a function of time is shown in Figure 17. In comparison with the isomer *n*-butylbenzene, the *t*-butylbenzene is much less reactive at the same temperature and pressure. For example, in 1 hour of reaction at 450°C, *n*-butylbenzene produced 72.5 mg of deposit, whereas no deposit formed from the *t*-butyl isomer. Similarly, at eight hours, 282.5 mg of deposit was formed by decomposition of *n*-butylbenzene, but only 97.5 mg from *t*-butylbenzene. Presuming that deposit formation is a free radical process, initiation of the reactions leading to deposition probably is a result of cleavage of the α bond in the alkyl side chain, forming the benzyl radical from *n*-butylbenzene but forming the α,α -dimethylbenzyl radical from *t*-butylbenzene. The benzyl radical may be reactive and easily enters into dimerization reactions, whereas the dimethylbenzyl radical could be relatively stabilized by increased electron density supplied

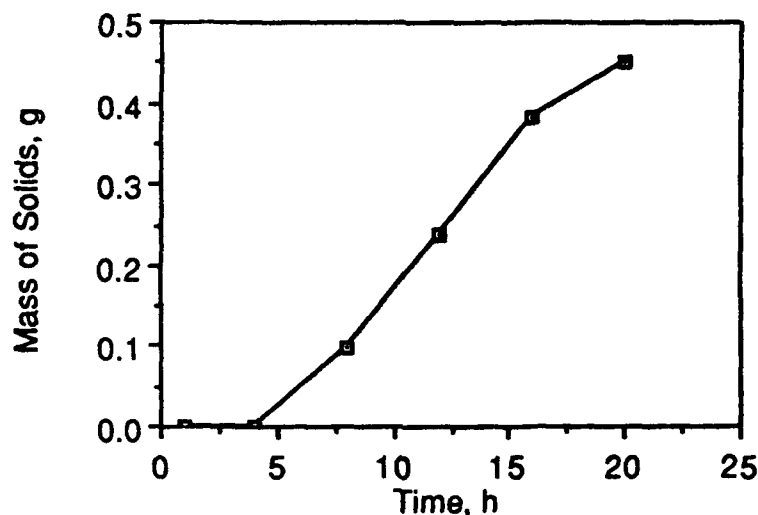


Figure 17. Solid formation from t-butylbenzene at 450°C

from the two methyl groups to the radical center. Thus n-butylbenzene would produce the benzyl radical which easily reacts with other available molecules or radicals leading to condensation, aromatization, and eventual formation of polycyclic aromatic solids. In comparison, the relatively more stable dimethylbenzyl radical may not have as great a tendency to participate in such reactions. A comparison of the reactivity of n- and t-butylbenzene is further discussed in the section on kinetics of solid formation. A more detailed explanation of the comparative reactivity of the alkylated aromatic compounds will be obtained after further kinetic studies and supporting analytical work have been completed.

A limited amount of testing of t-butylbenzene has been done at 350°C, also using 5 ml samples with 100 psi nitrogen overpressure. After 16 hours of reaction, no solid had formed.

Tetradecane

Thermal stability tests of tetradecane have been conducted at two different temperatures: 400° and 425°C. These tests were done using 10 ml of sample. The tetradecane trials at 400°C show no signs of deposit formation or deposit precursors. Some color change is observed, along with a slight decrease in liquid volume, suggestive of possible cracking reactions. In 4.5 hours at 400°C, 95% recovery (by volume) of the original liquid was obtained. The liquid had a slight yellowish color. Tests for 24 hours at

400°C showed pale to distinct yellow coloration of the liquid, with 85% recovery of the original liquid volume.

The tetradecane trials at 425°C show deposit formation for test durations of 8 hours or longer, with an increase in deposit formation with increasing reaction time. A dark brown coloration of the liquid was evident even in those tests in which no solid deposit formed. The deposit formation is shown as a function of time in Figure 18.

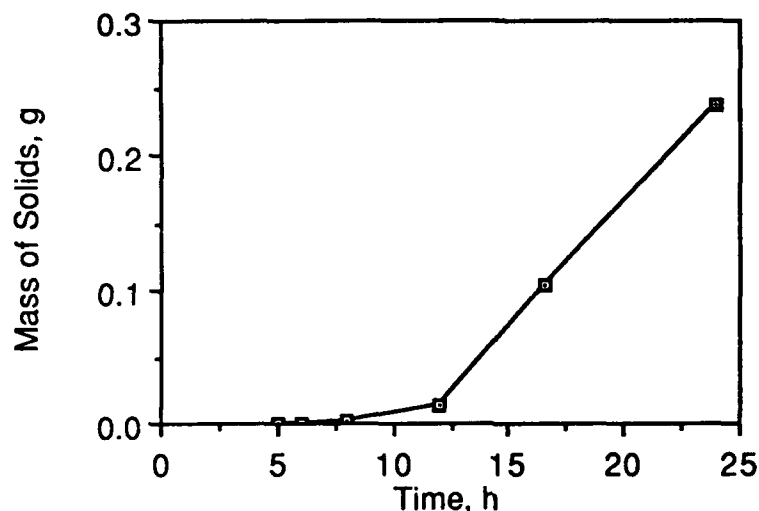


Figure 18. Solid formation from tetradecane at 425°C.

Kinetics of Solid Formation

A comparison of the amount of solids produced from model compounds by thermal stressing as a function of the treatment severity can be used for rating their thermal stability. The severity of the thermal treatment can, in turn, be considered to depend on both the treatment temperature and the time involved. Considering the wide range of model compounds used in this study and the need for studying their thermal stability within a range of temperatures and reaction times, it is not possible to select a single temperature or reaction time for a direct comparison of the amount of solids produced from the model compounds at a comparable treatment severity. Therefore, there is a need to define a severity parameter to reflect the contribution of both temperature and time so that the thermal stability of model compounds can be compared in a single plot over a range of temperatures and treatment times. Consequently, a severity index was defined to consist of an exponential term involving the temperature multiplied by time, $SI = (\exp[-25,000/T])(t)$. The exponential term mimics the exponential part of an Arrhenius relationship with an

activation energy of approximately 50 kcal/mole, which is a reasonable activation energy for thermal decomposition of hydrocarbons. It should be noted that the arbitrary selection of this activation energy is for the purpose of quantifying the severity of thermal treatment only; it does not introduce any assumptions regarding the chemistry of thermal degradation.

Figure 19 shows a plot of the mass of solids formed from 10 ml of model compounds at different temperatures and reaction times as a function of treatment severity. The treatment time used in calculating the severity index is the time period elapsed between the start and end of the experiments without any correction for the apparent induction periods for the formation of solids. The solid masses shown for butylbenzenes were calculated by doubling the amount of solids produced from 5 ml samples. It should be noted that the plot in Figure 19 is based on a limited set of data; the completion of the temperature-time matrix for all of the selected model compounds will present a more complete picture in a similar plot. There are, however, some general trends that can be pointed out in Figure 19. In the range of treatment severity given in Figure 19 one can see, especially in the case of decane, that the maximum amount of solids produced from a compound can be a strong function of temperature. It is shown more clearly in Figure 20 that the amounts of solids produced from decane at 450°C are much higher than those produced at 425°C with comparable treatment severity. The same trend, to a lesser extent, is also observed for n-butylbenzene for which the kinetic data are displayed for two different temperatures. This temperature dependency of the solid mass can lead to differences in the maximum amount of solids obtained at different temperatures and cause difficulties in a kinetic analysis of solid formation, as will be discussed later.

It is interesting to note in Figure 19 that decane has a similar propensity for solid formation to that of n-butylbenzene at low treatment severities. The comparison of the data points for n-butylbenzene and t-butylbenzene show, as was indicated before, that n-butylbenzene is generally more reactive than its isomer. At a high treatment severity, however, both isomers appear to have the same reactivity. This trend can be explained by the differences in the chemical mechanisms (including the differences in induction periods) during thermal decomposition of the two isomers, as was discussed above.

A comparison of the data points in Figure 20 shows the substantially higher thermal stability of decalin compared to decane. Figure 20 also shows a higher propensity of tetradecane than that of decane for solid formation at least at 425°C. The use of a severity index in the plots shown in Figures 19 and 20 enables a direct comparison of the experimental data without involving any assumptions required to set up kinetic expressions. It also displays the trends in solid formation as a function of both temperature and time in a practical fashion.

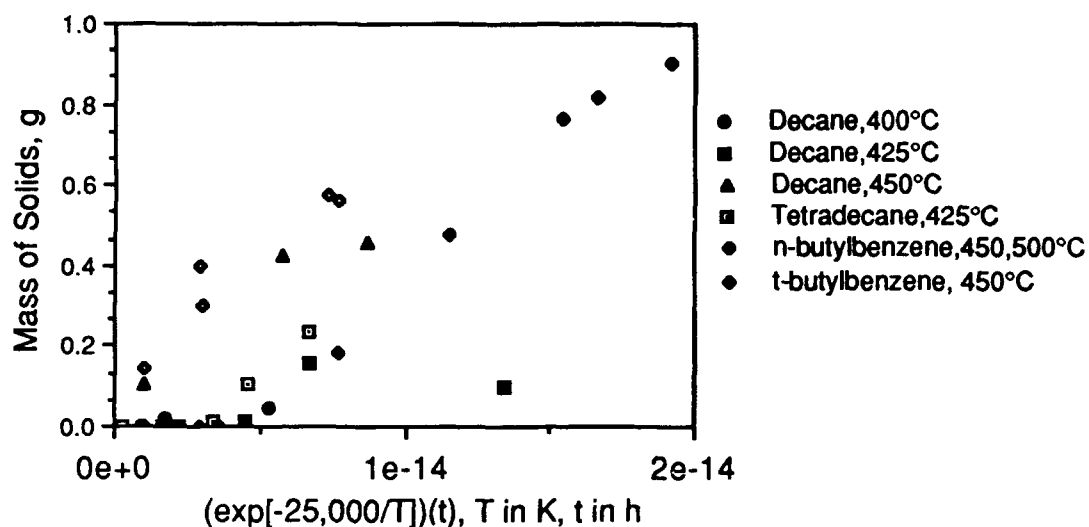


Figure 19. Formation of solids from model compounds as a function of treatment severity.

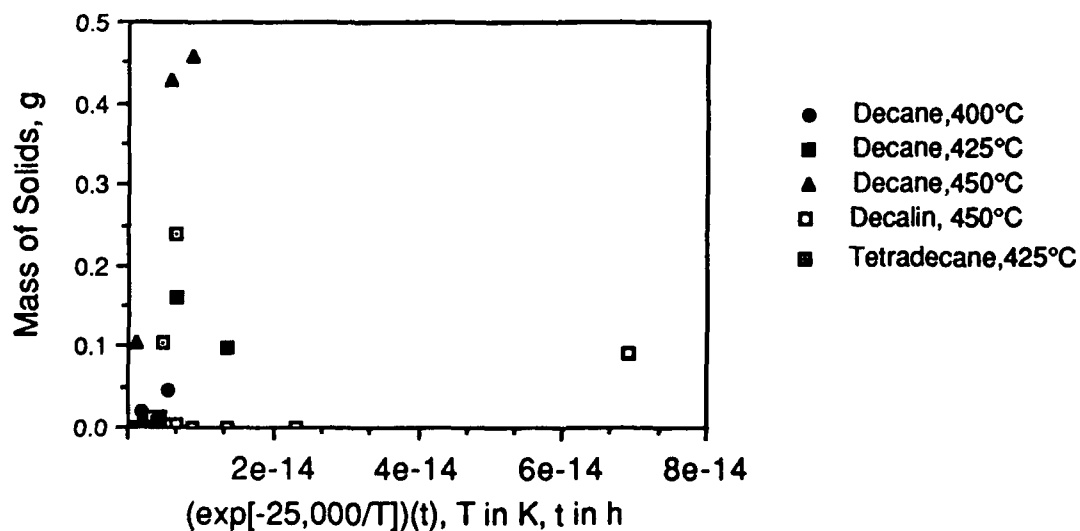


Figure 20. Formation of solids from decane, tetradecane and decalin as a function of treatment severity.

A calculation of global kinetic parameters for the formation of solids from model compounds provides a more quantitative comparison of the thermal stability of different compounds. The use of the mass of solids produced in the experiments as a kinetic parameter has, however, presented some difficulties in the kinetic analysis. First of all in some cases, the mass of solids went through a minimum with the increasing reaction time at a constant temperature. As was discussed above (Figure 11), this is most probably due to a physical interaction between the solid and the liquid products in the reactor, namely the change in the solubility of the solids as a function of compositional changes in the liquid. In such cases, the observed minima were not included in the kinetic analysis. Secondly, the method of solid recovery (scrapping the solids off the surfaces of the reactors) may introduce a significant error when small quantities of solids are produced. Therefore, in some cases, it was necessary to use excessively high temperatures and long reaction times to get significantly large quantities of solids for more accurate measurements. Thirdly, a rigorous kinetic analysis requires the maximum conversion be independent of temperature. In the thermal treatment of decane, as was discussed above, the maximum conversion (amount of solids) was found to be a function of temperature. Therefore, the kinetic expression was modified to include the variation of maximum yield of solids as a function of temperature.

In thermal treatment experiments, the volume of the liquid product was observed to decrease consistently with the increasing degree of thermal degradation. Figure 21 shows the decreasing volume of the liquid product from decane and decalin as a function of time

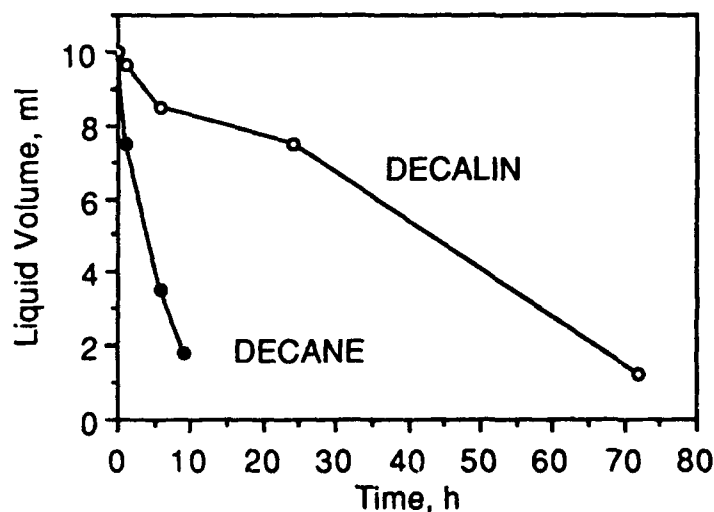


Figure 21. Depletion of liquid products as a function of time in thermal treatment of decane and decalin.

at 450°C. This consistent decrease with the increasing conversion suggested that the volume of the liquid product can be used as a kinetic parameter to describe the thermal decomposition process.

For a kinetic analysis of solid formation, an apparent first-order behavior was assumed to calculate the kinetic parameters. The rate expression used is as follows:

$$dm/dt = k (1 - m/m_{\max})$$

where m is the mass of solids produced, m_{\max} is the maximum mass of solids that can be produced at a given temperature, and t is the reaction time. The plot of $\ln(1 - m/m_{\max})$ vs time at given temperature should give straight lines with a slope equal to the reaction rate constant at the respective temperature. For practical purposes, the maximum amount of solids produced at each temperature was determined experimentally as the amount of solids produced by either a treatment for 72 hours at the given temperature or by a treatment that produces a 4000 psi pressure in the reactors.

In order to determine the kinetics of liquid depletion the following kinetic expression was used:

$$dl/dt = k (l - l_{\min}/10 - l_{\min})$$

where l is the volume of the liquid product, l_{\min} is the minimum volume of the liquid product obtained at a given temperature, and t is the reaction time. The l_{\min} was experimentally determined using the same method as that used to determine m_{\max} . The plot of $\ln(l - l_{\min}/10 - l_{\min})$ versus time should give straight lines with slopes equal to the rate constants at the given temperatures. The apparent first-order plots for the formation of solids and the depletion of liquids gave reasonable straight lines from which the respective rate constants were calculated. The Arrhenius plots for the formation of solids and the depletion of solids from decane are shown in Figure 22. The linear regression equations with the respective correlation coefficients are also shown in Figure 22. It can be seen that the formation of solids and the depletion of liquids give similar kinetic parameters, suggesting that the chemical processes that lead to the production of solids are similar to those involved in the depletion of liquids. The apparent activation energy and the preexponential factor calculated for the formation of solids from decane are 47 kcal/mole and $5.42 \times 10^{13} \text{ h}^{-1}$, respectively.

The Arrhenius plots for the depletion of the liquids in the thermal treatments of decane and decalin are compared in Figure 23. The apparent activation energy and the preexponential factor for decane reactions are 49 kcal/mole and $2.06 \times 10^{14} \text{ h}^{-1}$ and for

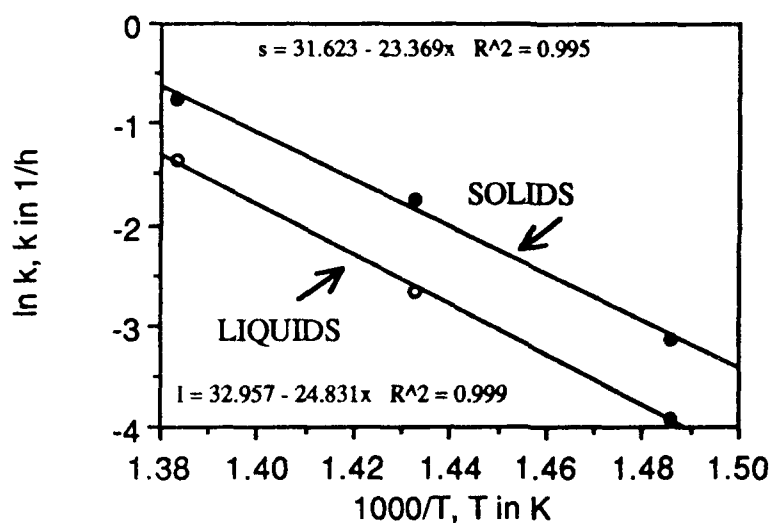


Figure 22. Arrhenius plots for the formation of solids and depletion of liquids during thermal treatment of decane.

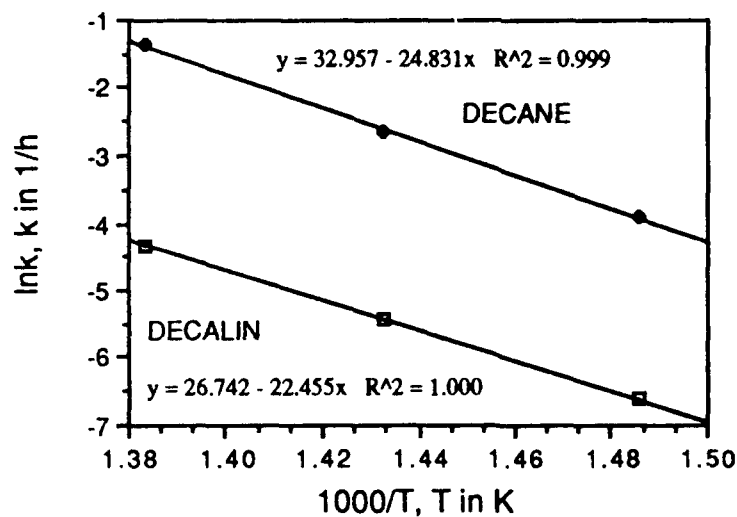


Figure 23. Arrhenius plots for the depletion of liquids during thermal treatment of decane and decalin.

decalin reactions 45 kcal/mole and $4.11 \times 10^{11} \text{ h}^{-1}$, respectively. It should be noted that the kinetic parameters for liquid depletion are very different for decane and decalin implying that different chemical processes are involved in the two systems. Although the calculated apparent activation energy for the decalin reactions are lower than that for decane reactions, the rate constants for the depletion of liquids from decalin are substantially smaller than those for decane due to the small preexponential factor in the decalin rate constants.

Figure 24 shows an Arrhenius plot for the progressive darkening of the liquid product from decalin as a function of increasing severity of thermal treatment. The rate constants used in the Arrhenius plots were calculated from the transmittance data taken on the samples of the liquids produced from decalin. This method is described in detail in the section on Task 2 Activity 3. The Arrhenius plot in Figure 24 yields an apparent activation energy of 52 kcal/mole and an apparent preexponential factor of $1.33 \times 10^{15} \text{ h}^{-1}$. A significantly higher activation energy calculated for the darkening of the liquids than that for the depletion of liquids suggests that the reactions involved in producing larger molecules in the liquid phase are different from those leading to the depletion of the liquid product.

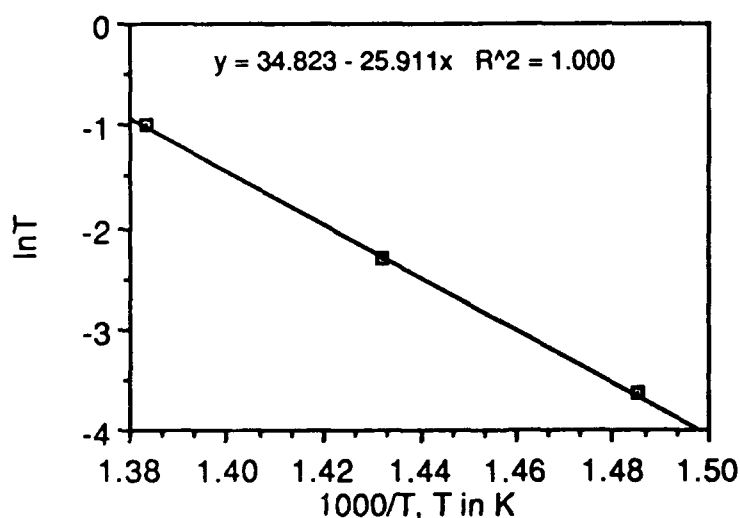


Figure 24. Arrhenius plots for the darkening of liquids during thermal treatment of decalin.

It can be concluded from the kinetic data and calculations presented in this section that the different sets of kinetic data and the different methods used to analyze the kinetic data provide complementary information. The usefulness of each data set and each method of analysis or presentation depends upon the specific application ranging from a qualitative mapping of the relative thermal stabilities of model compounds or fuels to elucidation of chemical mechanisms involved in thermal degradation of hydrocarbons.

Optical Microscopic Characterization of Solid Deposits

The solids produced from decane, decalin, n-butylbenzene, and a petroleum-derived JP-8 jet fuel sample were analyzed by optical microscopy using reflected plane-polarized light. The polished sections of all the solid specimens displayed extinction contours of varying sizes, indicating anisotropic microstructures. The presence of these structures suggest that the solids were formed via a mesophase -a pseudo liquid crystal-stage [21]. It is known that the formation of mesophase takes place in a liquid phase and involves the formation of large, planar, aromatic molecules that are aligned parallel to each other [22]. This microstructural feature of the solid products is consistent with the information derived from the FTIR and ^{13}C NMR spectra of the solids. It is interesting to note that the aligned regions of anisotropic structures in the wall deposits were generally found to be perpendicular the reactor surface.

The colored micrographs of the solid samples are in file in the Fuel Science Program for reference. They were not included in this report because of their poor reproduction upon copying.

Activity 3. Thermal Stability Ratings

This activity will be carried out after collecting more data on thermal stability of model compounds and fuel fractions.

TASK 2

The objective of Task 2 is to extend the work of Task 1 to mixtures of hydrocarbon compounds obtained from distillate fractions typical of jet fuels.

Activity 1. Fractionation of Fuel Samples.

Background

Both coal-derived and petroleum-derived jet fuels are complex mixtures with several hundred components. There are several reasons for using a chromatographic separation technique to fractionate the samples for thermal stability testing. First of all,

fractionation of jet fuels by liquid chromatography allows detailed characterization of each fraction, which simplifies the characterization relative to trying to characterize the fuel without fractionation. Information on the composition and structure of different jet fuels at the molecular level is still limited. The analysis of the chromatographic fractions by GC/MS provides important information on major and minor components of jet fuels. Moreover, preparative-scale separation allows collection of individual fractions containing chemically similar compounds. Thermal treating of these fractions from authentic jet fuels will help us to identify compound classes that are thermally stable. Combination of these results with those for "whole" jet fuels would reveal the possible causes of thermal degradation. For example, whether it occurs via intramolecular or intermolecular reactions, or both, and the contribution from major and minor fuel components to degradation. Further model compound tests using the compounds typical of the components of a particular fraction can be used to evaluate and clarify the reaction mechanism.

Separation Method

Complex hydrocarbon mixtures can be separated into different compound classes by liquid chromatography using appropriate sorbent and elution solvents. Numerous chromatographic methods have been employed in many investigations to separate coal-derived liquids and oil sand bitumen [23-27]. Based on previous methods using silica-alumina and alumina sorbents, and a series of elution solvents for separating heavy liquids, a method for separation of jet fuel was developed in this laboratory. Adaptability, simplicity and availability for future scale-up were considered when choosing the sorbent and solvents.

The preliminary procedure for analytical-scale separation uses neutral alumina gel and a series of solvent systems including pentane, benzene-pentane, benzene, ethanol-chloroform, and ethanol-tetrahydrofuran (THF). This procedure will be further modified as necessary to improve the resolution. Concepts for the chromatographic and spectroscopic approach are summarized in Scheme 1.

Scheme 1. Chromatographic Separation of Jet Fuels

I: Analytical-scale Separation

- 1) Separation of jet fuels of different origin into chemically similar compounds: Saturates, Aromatics with sub-fractions, Polar with sub-fractions
- 2) Characterization of chromatographic fractions by GC/MS
- 3) Information feed-back from step 2 to step 1 to improve the separation method

- 4) Determination of neutral/polar fractions and major/minor components

II: Large-scale Separation

- 5) Preparative-scale separation of different jet fuels using the established method
- 6) Thermal treatment of the chromatographic fractions in microreactors
- 7) Work-up of products from step 6 and chromatographic/spectroscopic analyses
- 8) Data interpretation and information feed-back to step 6.

Experimental

Activity Super I neutral alumina (from ICN, formerly Woelm) gel was chosen, because its capacity is approximately double that of activity I alumina in a non-polar environment. This Super I alumina gel is considered to be more suitable for separating jet fuel sample, although Activity I is widely used for heavy liquids. The specific surface area and particle size of ICN Super I are 200 m²/g and 50-200 μ m, respectively. The solvents used for elution are HPLC grade n-pentane, benzene, chloroform, and THF and technical grade ethanol.

A 22 mm i.d. x 500 mm glass column with removable Teflon stopcock was used. Small pieces of glass wool and 3 mm glass beads were used to retain the packing. The column was wet-packed using alumina and n-pentane. The neutral Al₂O₃ was added to the pentane-filled column slowly with continuous tapping to avoid trapping air and to insure a homogeneous sorbent bed. The jet fuel sample was placed directly on top of the Al₂O₃ column and was allowed to pre-adsorb on the Al₂O₃ gel at the top of the column. The procedure for the analytical-scale separation is shown in Figure 25. The solvents and their volume are as follows: n-pentane, 350 ml; 5% benzene-pentane, 200 ml; benzene, 250 ml; 1% ethanol-chloroform, 300 ml; 10 % ethanol-THF, 200 ml.

The chromatographic fractions were analyzed by gas chromatography-mass spectrometry (GC/MS) on a Kratos MS-80 RFA high resolution apparatus. A Hewlett-Packard fused silica capillary column (HP-17, 0.25 mm i.d. x 30 m) was used for GC. The column temperature was programmed from 40°C to 280°C at a heating rate of 4°C/min after a 5 minute isothermal period. The ionization mode on the mass spectrometer was electron impact (EI, 70 eV). This GC/MS apparatus is equipped with a data processing DS90 system.

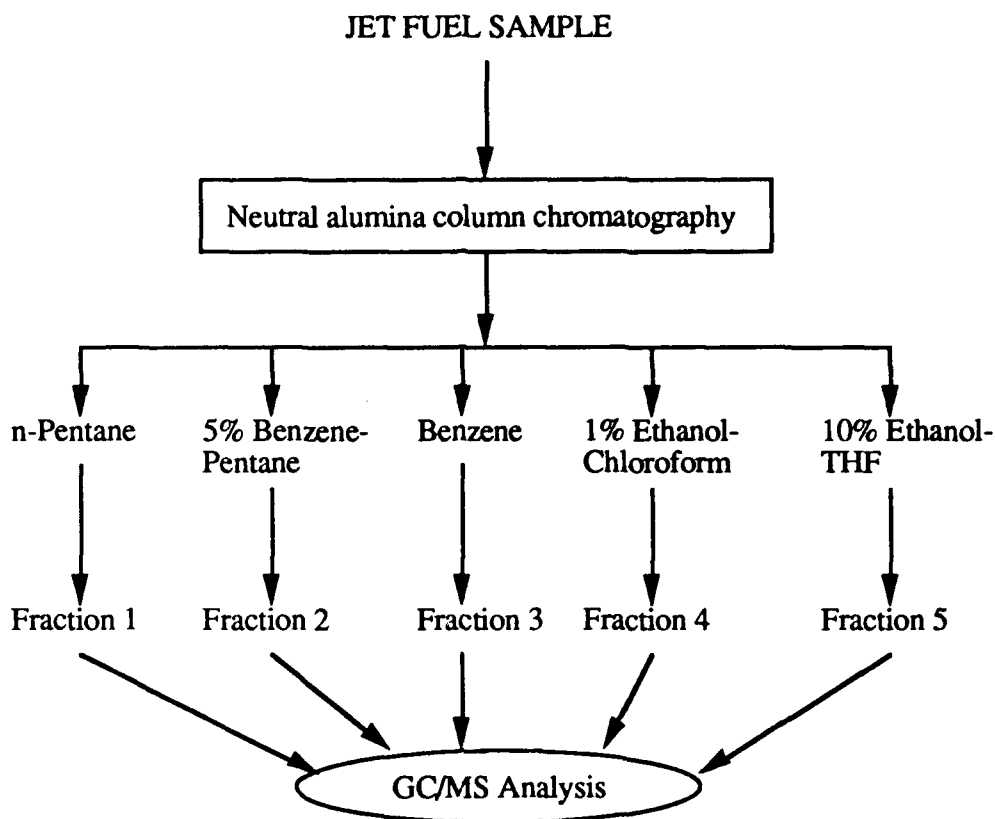


Figure 25. Preliminary procedure for chromatographic separation of jet fuel

Results

Fractionation of jet fuel

The analytical-scale chromatographic separation was carried out using 4 g of jet fuel sample. The preliminary results for separation of coal- and petroleum-derived JP-8 jet fuels are shown in Table 7 and Table 8, respectively. To examine the reproducibility of the method, separation of each sample was repeated. As shown in Tables 7 and 8, yields of the first three fractions from two runs of each sample were similar to each other. These three fractions are the major fractions of either coal- or petroleum-derived jet fuel. The yields of fraction 4 and 5 were very low. Since the recovery for the chromatographic separation on neutral alumina column was as high as 94-97%, the uneluted materials, if any, were very limited.

Table 7. Chromatographic separation of coal-derived jet fuel JP8-C on neutral alumina column

Fraction No.	Elution System Solvent	Vol (ml)	Yields (wt%)			Appearance (color)	Compounds ^b Class
			JP8-C	JP8-C	Ave.		
1	n-Pentane	350	65.9	68.9	67.4	Colorless	Saturates
2	5% Benzene-Pentane	200	11.7	11.2	11.5	Colorless	Monoaromatics
3	Benzene	250	12.1	13.8	13.0	Yellowish	Aromatics+Polar
4	1% EtOH-Chloroform	350	1.1	0.2	0.7	Colorless	Polar-1
5	10% EtOH-THF	200	0.8	1.7	1.3	Yellow	Polar-2

a) 4 g of jet fuel was separated on 130 g of Al₂O₃ gel.

b) As revealed by GC/MS analysis

Table 8. Chromatographic separation of petroleum-derived jet fuel JP8-P on neutral alumina column

Fraction No.	Elution System Solvent	Vol (ml)	Yields (wt%)			Appearance (Color)	Compounds Class
			JP8-P	JP8-P	Ave.		
1	n-Pentane	350	82.7	82.6	82.7	Colorless	Saturates
2	5% Benzene-Pentane	200	5.7	6.5	6.1	Colorless	Monoaromatic
3	Benzene	250	6.2	7.1	6.7	Yellowish	Aromatic+Polar
4	1% EtOH-Chloroform	350	0.7	0.8	0.8	Colorless	Polar-1
5	10% EtOH-THF	200	0.6	1.0	0.8	Yellow	Polar-2

GC/MS analysis of jet fuel fractions

Each chromatographic fraction from coal-derived jet fuel was analyzed by GC/MS. The n-pentane elute (Fraction 1) and 5% benzene-pentane elute (Fraction 2) are composed of saturate and monoaromatic compounds, respectively. The Fraction 3 (benzene elute) contains a wide range of aromatic compounds including some nitrogen-containing heterocyclic compounds. The polar solvent, 1% EtOH-chloroform elute, (Fraction 4) is mainly composed of nitrogen-containing compounds, as reflected by many odd-number molecular ions. The fraction 5 (10% EtOH-THF elute) contains hydroxy compounds. The n-pentane elute (Fraction 1) of coal-derived jet fuel JP8-C is aliphatic in molecular nature and is almost free of aromatic compounds. Table 9 shows the composition of this fraction. The scan numbers in Table 9 correspond to those on the peaks in Figure 26. As can be seen from Table 9 and Figure 26, most components in this fraction are cyclic hydrocarbons ranging from 1-ring to 3-ring with alkyl groups.

Table 9. Identified compounds in n-pentane eluted saturated Fraction (Fr.1) of coal-derived jet fuel JP8-C

Peak Scan No.	Molecular Ion	Base Peak	Identified Compounds
22	112	97	Dimethylchclohexane
68	128	43	iso-Nonane (iso-C ₉)
80	112	83	Ethylcyclohexane
154	128	43	iso-Nonane (iso-C ₉)
182	126	97	Methylethylcyclohexane
241	126	97	Methylethylcyclohexane
304	126	83	n-Propylcyclohexane
421	140	97	Methylpropylcyclohexane
467	140	69	C ₄ -cyclohexane
555	138	81	Methylhexahydroindan
577	140	83	n-Butylchclohexane
681	156	57	iso-Undecane (iso-C ₁₁)
723	138	138	trans-Decalin
750	154	69	C ₅ -cyclohexane
842	152	152	C ₂ -hexahydroindan
874	138	96	cis-Decalin
896	152	152	Methyldecalin
918	152	152	Methyldecalin
930	170	57	n-Dodecane (n-C ₁₂)
949	166	55	C ₃ -hexahydroindan
	168	97	C ₆ -cyclohexane
956	166	55	C ₃ -hexahydroindan
968	152	95	Methyldecalin
988	168	83	Heptylcyclohexane
1004	166	81	Dimethyldecalin
1028	166	81	Dimethyldecalin
1048	166	95	C ₂ -Decalin
1097	168	83	Heptylcyclohexane
1130	166	137	Ethyldecalin
1163	184	57	n-Tridecane (n-C ₁₃)
1236	180	95	C ₃ -Decalin
1255	180	83	C ₃ -Decalin

Table 9. Identified compounds in n-pentane eluted saturated Fraction (Fr.1) of coal-derived jet fuel JP8-C (continued)

Peak Scan No.	Molecular Ion	Base Peak	Identified Compounds
1332	180	83	C ₃ -Decalin
1351	166	82	Bicyclohexyl
1382	198	57	n-Tetradecane (n-C ₁₄)
1437	180	55	C ₃ -Decalin
1471	226	57	iso-Hexadecane (iso-C ₁₆)
1502	178	178	Perhydrobenzoindan
1533	194	97	C ₄ -Decalin
	178		Perhydrobenzoindan
1578	194	137	Butyldecalin
1586	212	57	n-Pentadecane (n-C ₁₅)
1740	192	192	Perhydroanthracene or Perhydrophenanthrene
1760	210	83	C ₉ -cyclohexane
1777	192	192	Perhydroanthracene or Perhydrophenanthrene
	226	57	n-Hexadecane (n-C ₁₆)
1840	192	135	Perhydroanthracene or Perhydrophenanthrene
1846	192	192	Perhydrophenanthrene
	206		C ₁ -Perhydroanthracene or C ₁ - Perhydrophenanthrene
1903	192	192	Perhydrophenanthrene
1922	268	57	Pristane (iso-C ₁₉)
1960	240	57	n-Heptadecane (n-C ₁₇)
2134	254	57	n-Octadecane (n-C ₁₈)

DS90 Chromatogram report Run: SONG20011, 20-Mar-90 13:59
 SONG S01-A1 JP8-C PENTANE ELUTE 40-5 TO 280-5 AT 4 HP-17 IU

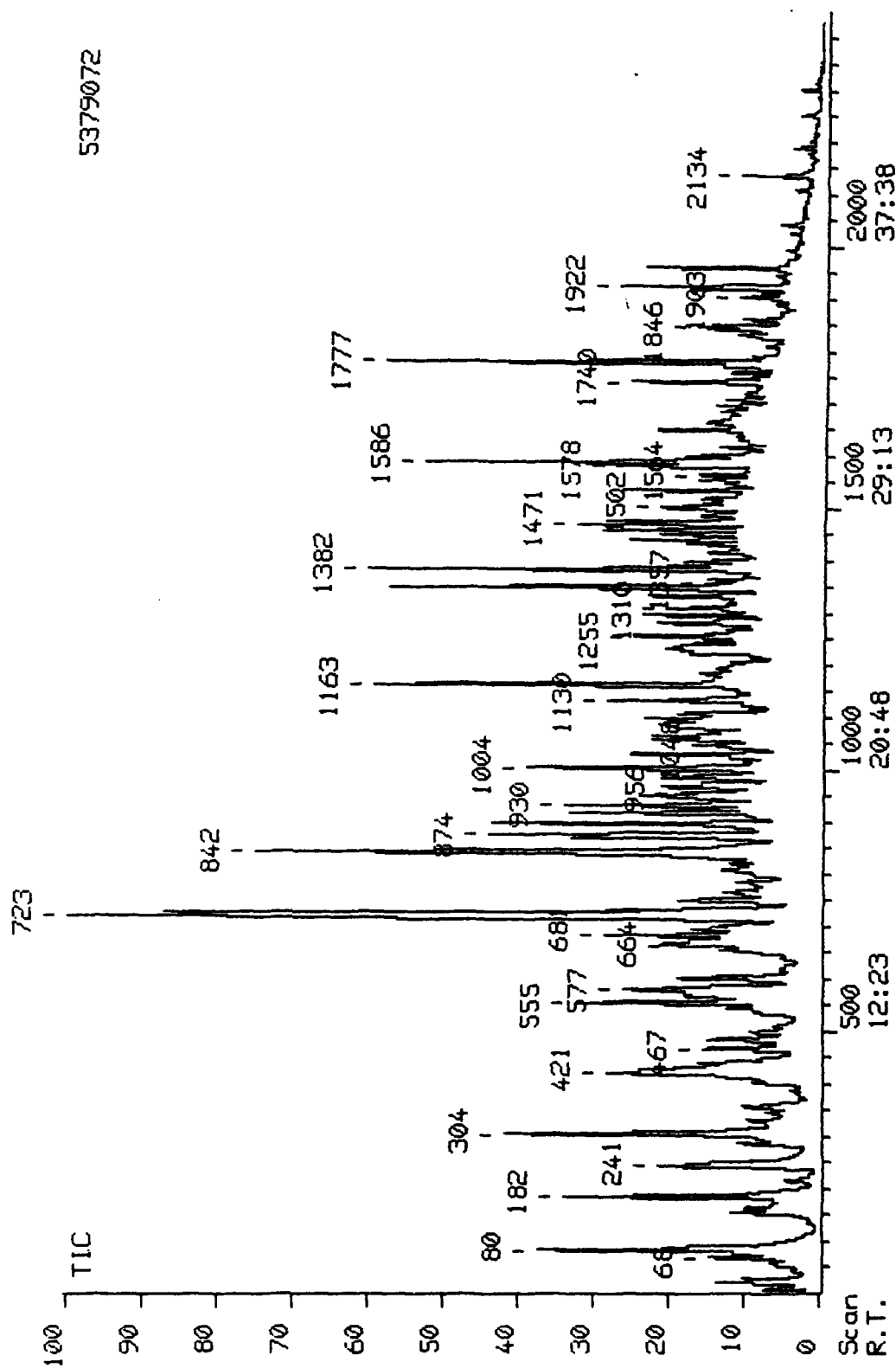


Figure 26. GC/MS total ion chromatogram of n-pentane eluted saturated Fraction (Fr.1) of coal-derived jet fuel JP8-C.

They are C₂- to C₉- substituted cyclohexane, decalin and C₁- to C₄- substituted decalins, and some perhydro-phenanthrene homologues. Some long-chain paraffinic compounds ranging from C₁₂ to C₁₉ are also present in this fraction. In the mass spectra, the relative intensities of the peaks for the ions with m/z 138 and m/z 96 were compared to distinguish between cis- and trans-decalin. Under the analysis conditions used in this study, the molecular ion (m/z 138) is clearly the base peak for trans-decalin, whereas for cis-decalin, the intensities of the m/z 138 and m/z 96 are very close to each other (both nearly 100%). In some cases, m/z 96 ion rather than the molecular ion is the base peak for cis-decalin (Tables 5 and 9).

Figure 27 presents the total ion chromatogram, and Table 10 shows the GC/MS results of 5% benzene-pentane elute (Fraction 2) of JP8-C. This fraction is composed of monoaromatics and was well-resolved from both saturate and diaromatic hydrocarbons. The components of this fraction include C₃- to C₇ benzenes, C₁-C₅ tetralins and indanes, and some octahydrophenanthrenes.

The total ion chromatogram and identification results of the peaks of fraction 3 (benzene elute) of JP8-C are shown in Figure 28 and Table 11, respectively. It was intended to concentrate diaromatic and polyaromatic (if any) compounds in this fraction. This was achieved, as naphthalene and methyl naphthalenes were found only in this fraction. However, monoaromatic compounds such as tetralins are also present in this fraction at high concentrations. A modification of the solvent system and/or the elution volume may improve the resolution.

The column chromatographic fractions of petroleum-derived JP-8 jet fuel were also analyzed by GC/MS. Figure 29 and Table 12 show the GC/MS results on the n-pentane elute (Fraction 1). It can be seen that this fraction is composed mainly of long-chain paraffins ranging from C₈ to C₁₆. The major components of this fraction are straight-chain C₁₀ to C₁₅ paraffins. The cycloalkanes are present only in trace amounts. This is in contrast to the corresponding fraction of the coal-derived jet fuel.

Figure 30 and Table 13 present the GC/MS analysis of the 5% benzene-pentane elute. This fraction is a monoaromatic fraction consisting principally of alkylbenzenes. It appeared that multi-substituted benzene rather than long-chain alkylbenzenes are the major components. Some methylindans are also present in this fraction, but their concentrations are much lower than those found in coal-derived jet fuel.

Figure 31 and Table 14 show the GC/MS analysis of the benzene elute fraction of JP8-P. This fraction is a diaromatic fraction. The major components include naphthalene

DS90 Chromatogram report Run: SONG20012, 20-Mar-90 15:26
 SONG S01-A2 JP8-C 5%BENZENE-PENTANE ELU 40-5 TO 280-5 AT 4

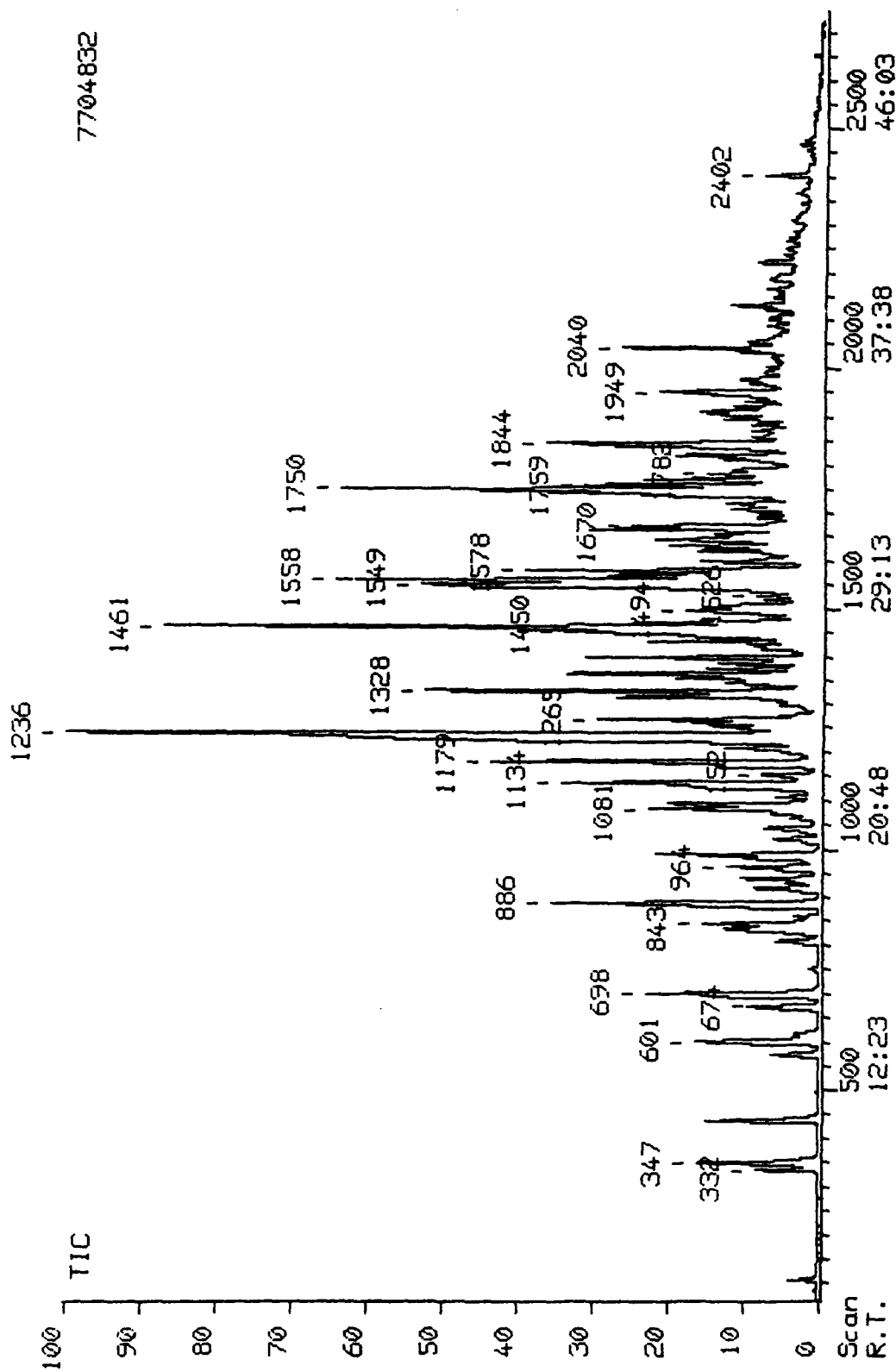


Figure 27. GC/MS total ion chromatogram of 5% benzene-n-pentane eluted
 Fraction (Fr.2) of coal-derived jet fuel JP8-C.

Table 10. Identified compounds in 5% benzene-pentane elute fraction (Fr.2) of coal-derived jet fuel JP8-C

Peak Scan No.	Molecular Ion	Base Peak	Identified Compounds
332	106	91	Ethylbenzene
347	106	91	p-Xylene
434	106	91	Xylene
601	120	105	Ethylmethylbenzene
674	120	105	Ethylmethylbenzene
698	120	105	Trimethylbenzene
829	134	105	Methylpropylbenzene
843	134	91	n-Butylbenzene
886	118	117	Indan
	134	105	Methylpropylbenzene
922	134	119	C ₄ -benzene
940	134	119	C ₄ -benzene
964	132	117	Methylindan
989	132	117	Methylindan
1044	134	119	C ₄ -benzene
1081	148	105	Methylbutylbenzene
1092	148	91	n-Pentylbenzene
1134	132	117	Methylindan
1152	148	119	C ₅ -benzene
1170	132	117	Methylindan
1179	132	117	Methylindan
1206	146	131	C ₂ -indan
1236	132	104	Tetralin
	146		C ₂ -indan
1265	146	131	C ₂ -indan
1328	146	104	2-Methyltetralin
1363	146	131	1-Methyltetralin
1374	146	117	C ₂ -indan
1384	162	119	C ₆ -benzene
1398	146	131	C ₂ -indan
1415	160	131	C ₂ -tetralin
1430	176	106	C ₇ -benzene

Table 10. Identified compounds in 5% benzene-pentane elute fraction (Fr.2) of coal-derived jet fuel JP8-C (continued)

Peak Scan No.	Molecular Ion	Base Peak	Identified Compounds
1461	146	131	5- or 6-Methyltetralin
1404	160	131	C ₂ -tetralin
	176		C ₇ -benzene
1526	176	106	C ₈ -benzene
1549	160	118	Dimethyltetralin
1558	160	104	Cyclohexylbenzene
1566	160	145	C ₂ -tetralin
1578	160	145	C ₂ -tetralin
1597	176	119	C ₈ -benzene
1619	174	145	C ₃ -tetralin
1620	160	118	Dimethyltetralin
1641	174	174	C ₃ -tetralin
1654	174	131	C ₃ -tetralin
	190		C ₈ -benzene
1663	160	131	C ₂ -tetralin
1670	174	145	C ₃ -tetralin
1718	174	91	C ₃ -tetralin
1737	174	159	C ₃ -tetralin
1750	190	119	C ₈ -benzene
1759	174	174	C ₃ -tetralin
1770	174	131	C ₃ -tetralin
1782	174	145	C ₃ -tetralin
1819	174	159	C ₃ -tetralin
1844	188	129	C ₄ -tetralin
	172		Tetrahydrobenzoindan
1904	188	145	C ₄ -tetralin
1912	188	145	C ₄ -tetralin
	172	157	Tetrahydrobenzoindan
1949	186	159	Octahydroanthracene isomer
	188		C ₄ -tetralin
2040	188	145	Butyltetralin
2402	186	158	Octahydroanthracene

DS90 Chromatogram report Run: SONG20021, 11-Apr-90 19:30
 SONG S01-A3 JP8-C BENZENE ELUTE 40-5 TO 280-5 AT 4 1UL

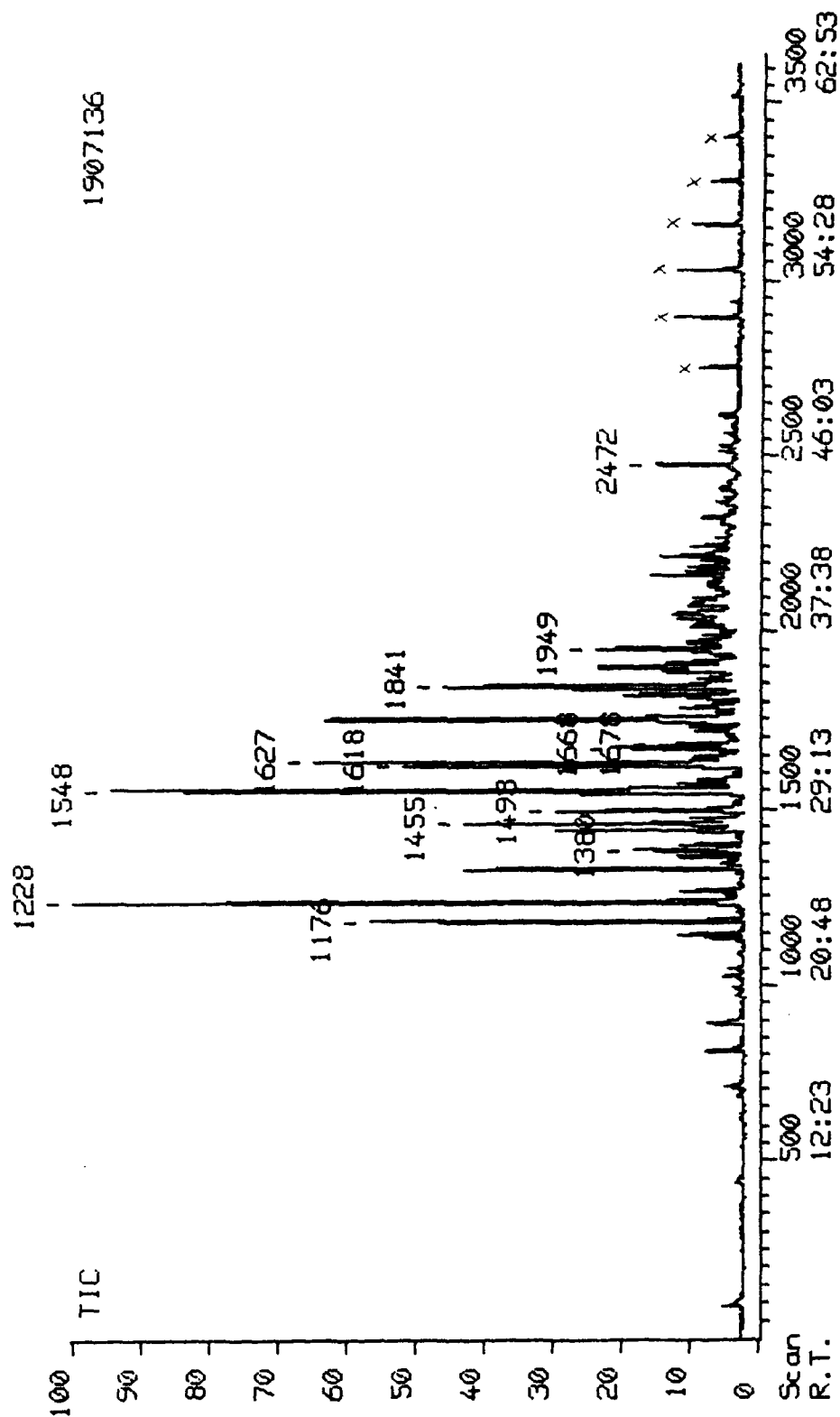


Figure 28. GC/MS total ion chromatogram of benzene eluted fraction (Fr.3) of coal-derived jet fuel JP8-C.

Table 11. Identified compounds in benzene elute fraction (Fr.3) of coal-derived jet fuel JP8-C

Peak Scan No.	Molecular Ion	Base Peak	Identified Compounds
1134	132	117	Methylindan
1145	134	119	C ₄ -benzene
1176	132	117	Methylindan
1228	132	104	Tetralin
1264	146	131	C ₂ -Indan
1325	146	104	2-Methyltetralin
1362	146	131	1-Methyltetralin
1380	128	128	Naphthalene
1436	146	131	C ₂ -indan
1455	146	131	5- or 6-methyltetralin
1493	146	131	C ₂ -indan
1548	146	131	5- or 6-methyltetralin
1618	142	142	2-Methylnaphthalene
1627	160	118	Dimethyltetralin
1668	160	145	C ₂ -tetralin
1678	142	142	1-methylnaphthalene
1745	190	119	C ₈ -benzene
1817	174	1159	C ₃ -tetralin
	156	141	2-Ethylnaphthalene
1841	156	156	Dimethylnaphthalene
	172		Tetrahydrobenzoindan
1896	156	156	Dimethylnaphthalene
1949	186	159	Octahydroanthracene isomer
2036	188	145	C ₄ -tetralin
	168	168	Methylbiphenyl
2051	186	186	Octahydroanthracene
2163	200	172	Methyltetrahydrobenzoindan
2174	186	186	Octahydroanthracene or Octahydrophenanthrene
2188	184	141	C ₄ -naphthalene

Table 11. Identified compounds in benzene elute (Fr.3) of coal-derived jet fuel JP8-C (continued)

Peak Scan No.	Molecular Ion	Base Peak	Identified Compounds
2218	186	186	Octahydrophenanthrene or Octahydroanthracene
2303	166	166	Fluorene
2321	168	168	Methylbiphenyl or Methylacenaphthene
2365	186	186	Octahydroanthracene
2472	186	186	Octahydrophenanthrene
2615	182	182	Tetrahydroanthracene or Tetrahydrophenanthrene

DS90 Chromatogram report Run: SONG200002, 6-Mar-90 12:39
 SONG 503-A1 JP8-P N-PENTANE ELUTE 35-S TO 280 AT 5 1 UL

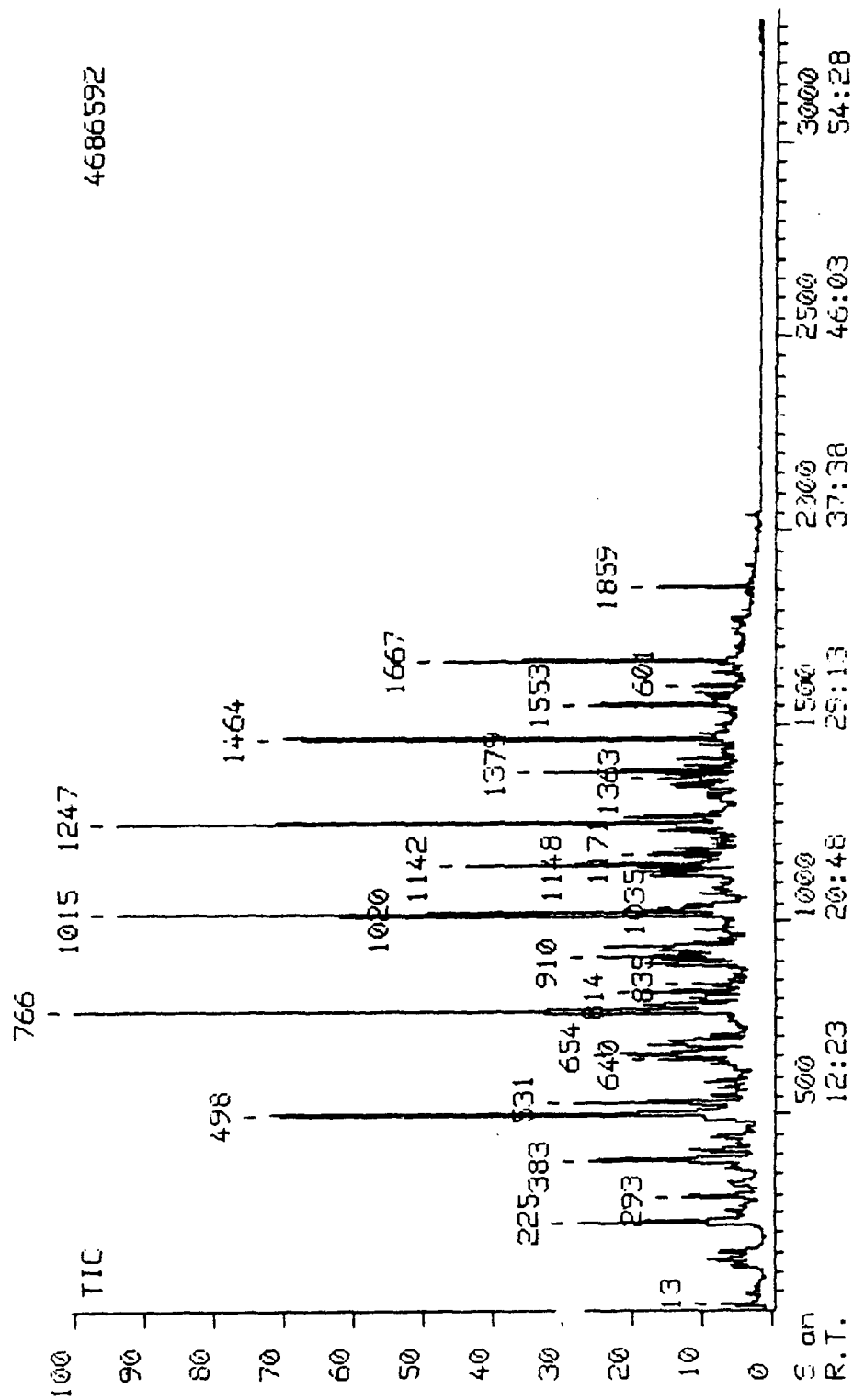


Figure 29. GC/MS total ion chromatogram of n-pentane eluted saturated Fraction (Fr.1) of petroleum-derived jet fuel JP8-P.

Table 12. Identified compounds in n-Pentane eluted saturate fraction (Fr. 1)
of petroleum-derived jet fuel JP8-P.

Peak Scan No.	Molecular Ion	Base Peak	Identified Compounds
13	114	43	iso-Octane (iso-C ₈)
225	128	43	iso-Nonane (iso-C ₉)
293	142	57	iso-Decane (iso-C ₁₀)
383	142	57	iso-Decane (iso-C ₁₀)
498	142	57	n-Decane (n-C ₁₀)
531	156	71	iso-Undecane (iso-C ₁₁)
640	156	57	iso-Undecane (iso-C ₁₁)
654	156	57	iso-Undecane (iso-C ₁₁)
680	156	57	iso-Undecane (iso-C ₁₁)
766	156	57	n-Undecane (n-C ₁₁)
814	170	57	iso-Dodecane (iso-C ₁₂)
	154		C ₅ -Cyclohexane
889	170	57	iso-Dodecane (iso-C ₁₂)
910	170	57	iso-Dodecane (iso-C ₁₂)
933	170	57	iso-Dodecane (iso-C ₁₂)
980	152	152	Methyldecalin
1015	170	57	n-Dodecane (n-C ₁₂)
1020	184	57	iso-Tridecane (iso-C ₁₃)
1027	184	57	iso-Tridecane (iso-C ₁₃)
1035	168	119	C ₆ -Cyclohexane
1120	184	57	iso-Tridecane (iso-C ₁₃)
1142	198	57	iso-Tetradecane (iso-C ₁₄)
1181	168	83	C ₆ -Cyclohexane
1231	196	69	C ₈ -Cyclohexane
1247	184	57	n-Tridecane (n-C ₁₃)
1265	198	57	iso-Tetradecane (iso-C ₁₄)
1363	198	71	iso-Tetradecane (iso-C ₁₄)
1379	212	57	iso-Pentadecane (iso-C ₁₅)
1464	198	57	n-Tetradecane (n-C ₁₄)
1533	226	57	iso-Hexadecane (iso-C ₁₆)

Table 12. Identified compounds in n-Pentane eluted saturate fraction (Fr. 1)
of petroleum-derived jet fuel JP8-P (continued)

Peak Scan No.	Molecular Ion	Base Peak	Identified Compounds
1601	212	57	iso-Pentadecane (iso-C ₁₅)
1667	212	57	n-Pentadecane (n-C ₁₅)
1859	226	57	n-Hexadecane (n-C ₁₆)

DS90 Chromatogram report Run: SONG200003, 6-Mar-90 14:03
 SONG 503-A2 JP8-P 5%BENZENE-PENTANE ELUTE 35-5 TO 280 AT 4

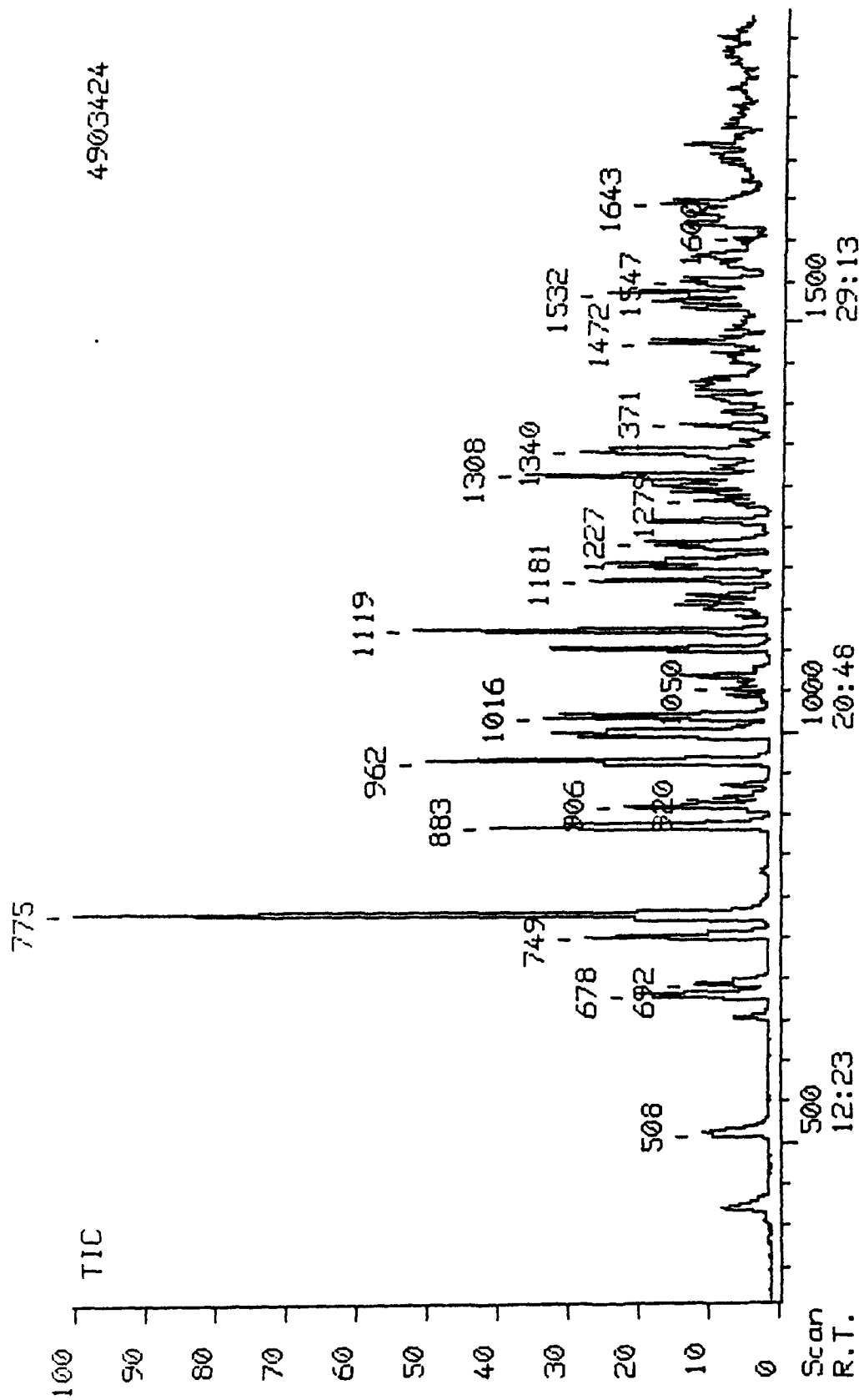


Figure 30. GC/MS total ion chromatogram of 5% benzene-n-pentane eluted Fraction (Fr.2) of petroleum-derived jet fuel JP8-P.

Table 13. Identified compounds in 5% benzene-pentane elute (Fr.2) of petroleum-derived jet fuel JP8-P

Peak Scan No.	Molecular Ion	Base Peak	Identified Compounds
508	106	91	Xylene
678	120	105	Ethylmethylbenzene
692	120	105	Trimethylbenzene
749	120	105	Ethylmethylbenzene
775	120	105	Trimethylbenzene
883	120	105	C ₃ -benzene
906	134	105	Methylpropylbenzene
920	134	91	n-Butylbenzene
962	134	105	Methylpropylbenzene
992	134	119	C ₄ -benzene
1016	134	119	C ₄ -benzene
1050	134	119	C ₄ -benzene
1065	132	117	Methylindan
1098	134	119	C ₄ -benzene
1119	134	119	C ₄ -benzene
1150	148	119	C ₄ -benzene
1181	148	119	C ₅ -benzene
1197	148	119	C ₅ -benzene
1204	148	119	C ₅ -benzene
1227	148	119	C ₅ -benzene
1253	132	117	Methylindan
1308	146	131	Dimethylindan
1340	146	131	Dimethylindan
1371	162	119	C ₆ -benzene
1398	162	91	Heptylbenzene
1424	162	119	C ₆ -benzene
1472	162	133	C ₆ -benzene
1532	146	131	Methyltetralin
1547	160	145	C ₂ -tetralin
1600	176	106	C ₇ -benzene
1616	176	145	C ₇ -benzene
1643	176	105	C ₇ -benzene

Table 13. Identified compounds in 5% benzene-pentane elute (Fr.2) of petroleum-derived jet fuel JP8-P (continued)

Peak Scan No.	Molecular Ion	Base Peak	Identified Compounds
1715	174	159	C ₄ -Indan
	190		C ₈ -benzene

DS90 Chromatogram report Run: SONG20005, 6-Mar-90 17:46
 SONG S03-A3 JP8-P BENZENE ELUTE 35-5 TO 280 AT 5.1 UL

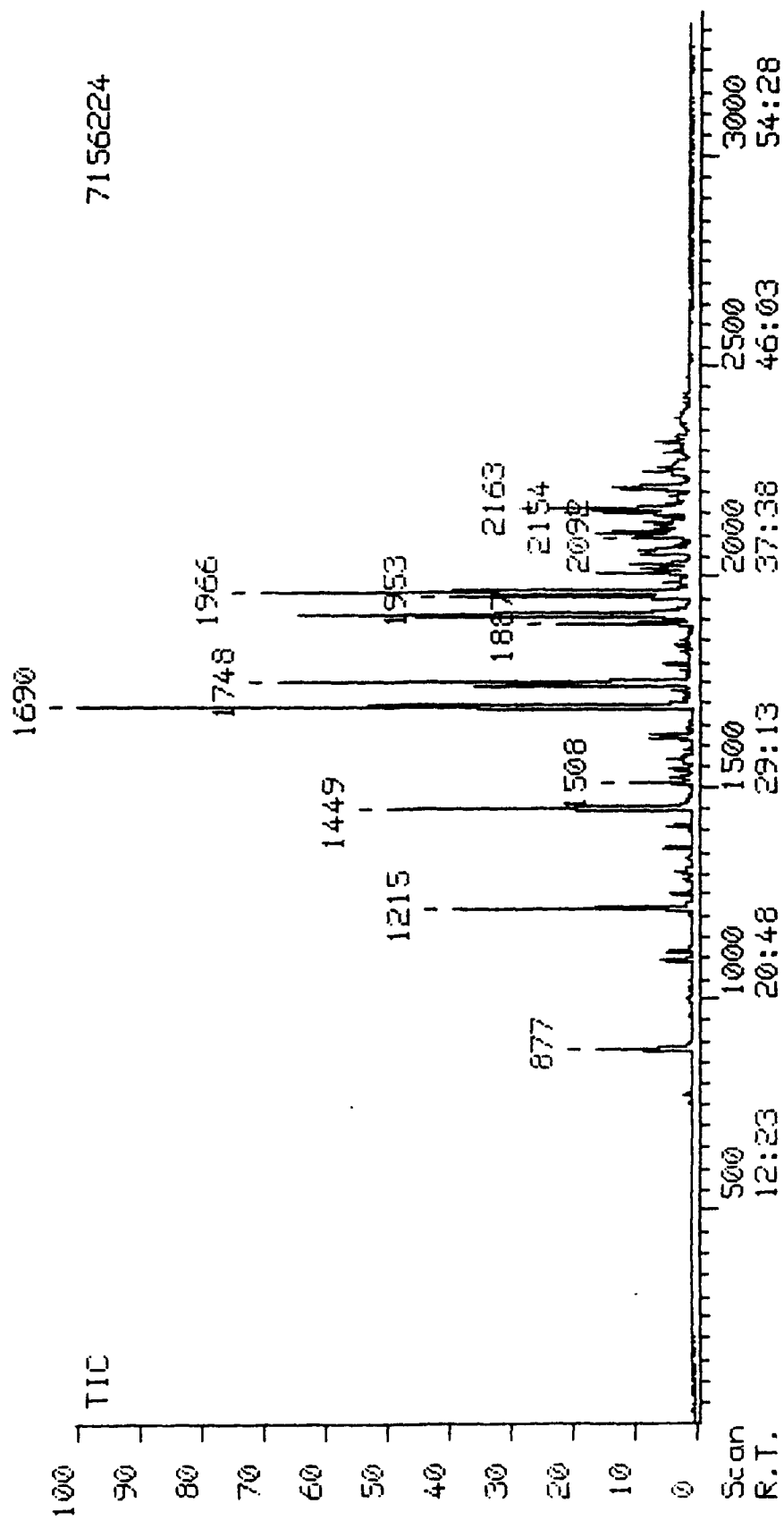


Figure 31. GC/MS total ion chromatogram of benzene eluted Fraction (Fr.3) of petroleum-derived jet fuel JP8-P.

Table 14. Identified compounds in benzene elute (Fr.3) of petroleum-derived jet fuel JP8-P

Peak Scan No.	Molecular Ion	Base Peak	Identified Compounds
877	120	105	Trimethylbenzene
1215	134	119	Tetramethylbenzene
1449	128	128	Naphthalene
1690	142	142	2-Methylnaphthalene
1748	142	142	1-Methylnaphthalene
1887	156	141	2-Ethylnaphthalene
1911	156	156	Dimethylnaphthalene
1953	156	156	Dimethylnaphthalene
1966	156	156	Dimethylnaphthalene
2007	156	156	Dimethylnaphthalene
2018	156	156	Dimethylnaphthalene
2030	156	156	Dimethylnaphthalene
2058	156	156	Dimethylnaphthalene
2092	170	155	Methylethylnaphthalene
2154	170	170	Trimethylnaphthalene
2163	170	170	Trimethylnaphthalene
2205	170	170	Trimethylnaphthalene
2213	170	170	Trimethylnaphthalene
2247	170	170	Trimethylnaphthalene

DS90 Chromatogram report Run: SONG20019, 11-Apr-90 15:56
 SONG JP8-P ORIG P-JET FUEL 40-5 TO 280-5 AT 4 1/1000 1 UL

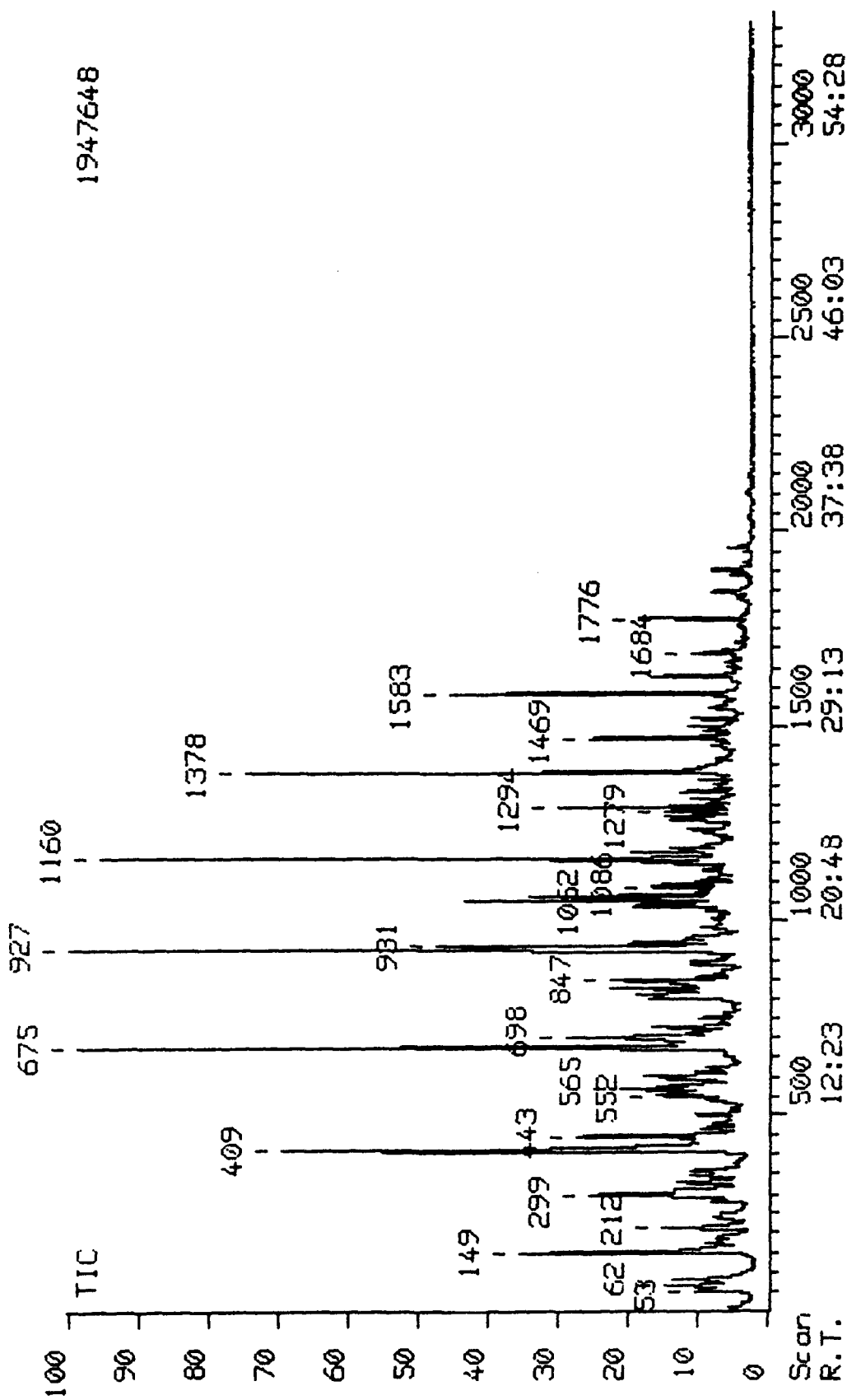


Figure 32. GC/MS total ion chromatogram of petroleum-derived jet fuel JP8-P.

Table 15. Identified compounds in petroleum-derived jet fuel JP8-P

Peak Scan No.	Molecular Ion	Base Peak	Identified Compounds
62	128	57	iso-Nonane (iso-C ₉)
149	128	57	iso-Nonane (iso-C ₉)
212	142	57	iso-Decane (iso-C ₁₀)
299	142	57	iso-Decane (iso-C ₁₀)
324	142	57	iso-Decane (iso-C ₁₀)
409	142	57	n-Decane (n-C ₁₀)
443	156	57	iso-Undecane (iso-C ₁₁)
565	156	57	iso-Undecane (iso-C ₁₁)
602	120	105	Methylethylbenzene
675	156	57	n-Undecane (n-C ₁₁)
698	120	105	Trimethylbenzene
727	170	57	iso-Dodecane (iso-C ₁₂)
927	170	57	n-Dodecane (n-C ₁₂)
1055	198	57	iso-Tetradecane (iso-C ₁₄)
1160	184	57	n-Tridecane (n-C ₁₃)
1294	212	57	iso-pentadecane (iso-C ₁₅)
1378	198	57	n-Tetradecane (n-C ₁₄)
1469	226	57	iso-Hexadecane (iso-C ₁₆)
1583	212	57	n-Pentadecane (n-C ₁₅)
1625	142	142	2-Methylnaphthalene
1684	142	142	1-Methylnaphthalene
1776	226	57	n-Hexadecane (n-C ₁₆)

D590 Chromatogram report Run: SONG20018, 11-Apr-90 14:23
 SONG JP8-C ORIG C-JET FUEL 40-5 TO 280-5 AT 4 1/1000 1 UL

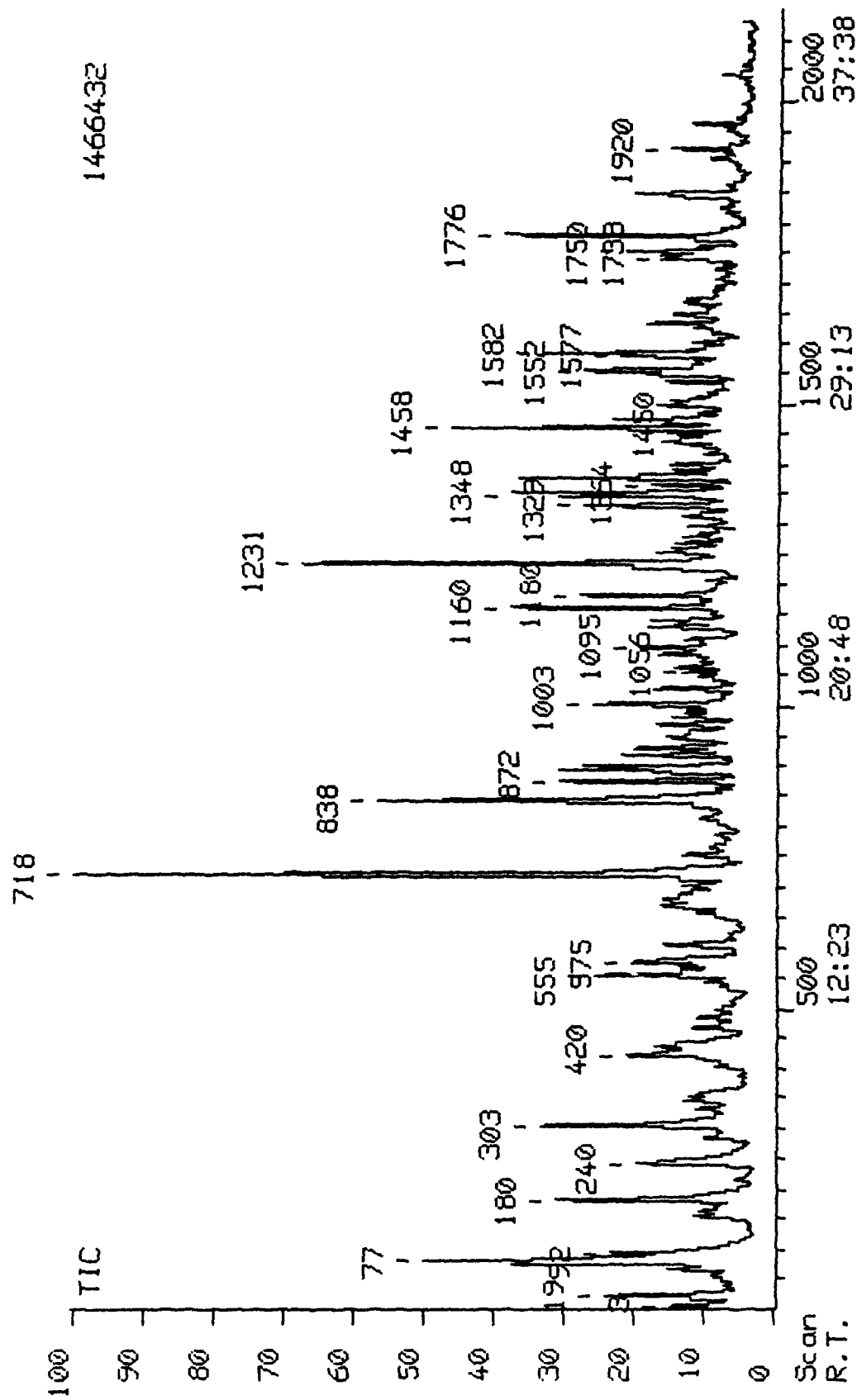


Figure 33. GC/MS total ion chromatogram of coal-derived jet fuel JP8-C.

Table 16. Identified compounds in coal-derived jet fuel JP8-C

Peak Scan No.	Molecular Ion	Base Peak	Identified Compounds
19	112	97	Dimethylcyclohexane
77	112	83	Ethylcyclohexane
80	126	97	Ethylmethylcyclohexane
240	126	97	Methylethylcyclohexane
303	126	83	n-Propylcyclohexane
420	140	97	Methylpropylcyclohexane
555	138	96	Methylhexahydroindan
575	140	83	n-Butylcyclohexane
604	120	105	Methylethylbenzene
718	138	138	trans-Decalin
838	152	81	C ₂ -Hexahydroindan
872	138	96	cis-Decalin
895	152	152	Methyldecalin
917	152	81	Methyldecalin
968	152	95	Methyldecalin
1003	166	81	Dimethyldecalin
1027	166	81	Dimethyldecalin
1095	168	93	Heptylcyclohexane
	148	91	C ₅ -benzene
1160	184	57	n-Tridecane (n-C ₁₃)
1180	132	117	Methylindan
1231	132	104	Tetralin
1329	146	104	2-Methyltetralin
1348	166	82	Bicyclohexyl
1378	198	57	n-Tetradecane (n-C ₁₄)
1458	146	131	Methyltetralin
1552	160	131	Ethyltetralin
1582	212	57	n-Pentadecane (n-C ₁₅)
1631	160	118	C ₂ -tetralin
1664	160	131	C ₂ -tetralin

Table 16. Identified compounds in coal-derived jet fuel JP8-C (continued)

Peak Scan No.	Molecular Ion	Base Peak	Identified Compounds
1738	192	192	Perhydroanthracene or Perhydrophenanthrene
1750	190	119	C ₈ -benzene
1776	192	192	Perhydroanthracene or Perhydrophenanthrene
1846	226	57	n-Hexadecane (n-C ₁₆)
	192	129	Perhydrophenanthrene
	206		C ₁ -Perhydroanthracene or C ₁ -Perhydrophenanthrene
1960	240	57	n-Heptadecane(n-C ₁₇)

and a number of alkylnaphthalenes. The corresponding fraction of the coal-derived JP-8 appeared to be much more complex in chemical composition.

For the purpose of comparison, the "whole" jet fuels, both the coal-derived and the petroleum derived JP-8's were analyzed by GC/MS. The results are summarized in Figure 32 and Table 15 for JP8-P and in Figure 33 and Table 16 for JP8-C. Evidently, the major components identified in the saturate fractions were also found to be the major components in the "whole" fuels. However, numerous components identified in the monoaromatic and aromatic fractions could not be detected in the "whole" fuels because of their low concentrations. Consequently, the column chromatographic separation of the jet fuels and GC/MS analysis of the fractions provided important information on the chemical composition of the jet fuels. Previously, jet fuel distillate fractions were also analyzed in this laboratory using GC/MS. For comparison with the chromatographically separated fractions, Figures 34 and 35 and Figures 36 and 37 show the total ion chromatograms of the 185-215°C and 215-240°C distillates from coal-derived and petroleum-derived JP-8 jet fuels, respectively. These two fractions constitute 39% of JP8-C, and 56% of JP8-P. The corresponding GC/MS results are given in Tables 17 and 18 for JP8-C and Tables 19 and 20 for JP8-P, respectively

It should be noted that the low-boiling and high-boiling distillate fractions of the petroleum derived jet fuel contain the same type of compound classes (i.e., paraffins) with different carbon numbers. In contrast, different distillate fractions of the coal-derived jet

DS90 Chromatogram report Run: SONG0010, 18-Jan-90 16:19
 JP8-C 185-215 UNTREATED 40 FOR 5 TO 280 AT 4 I UL

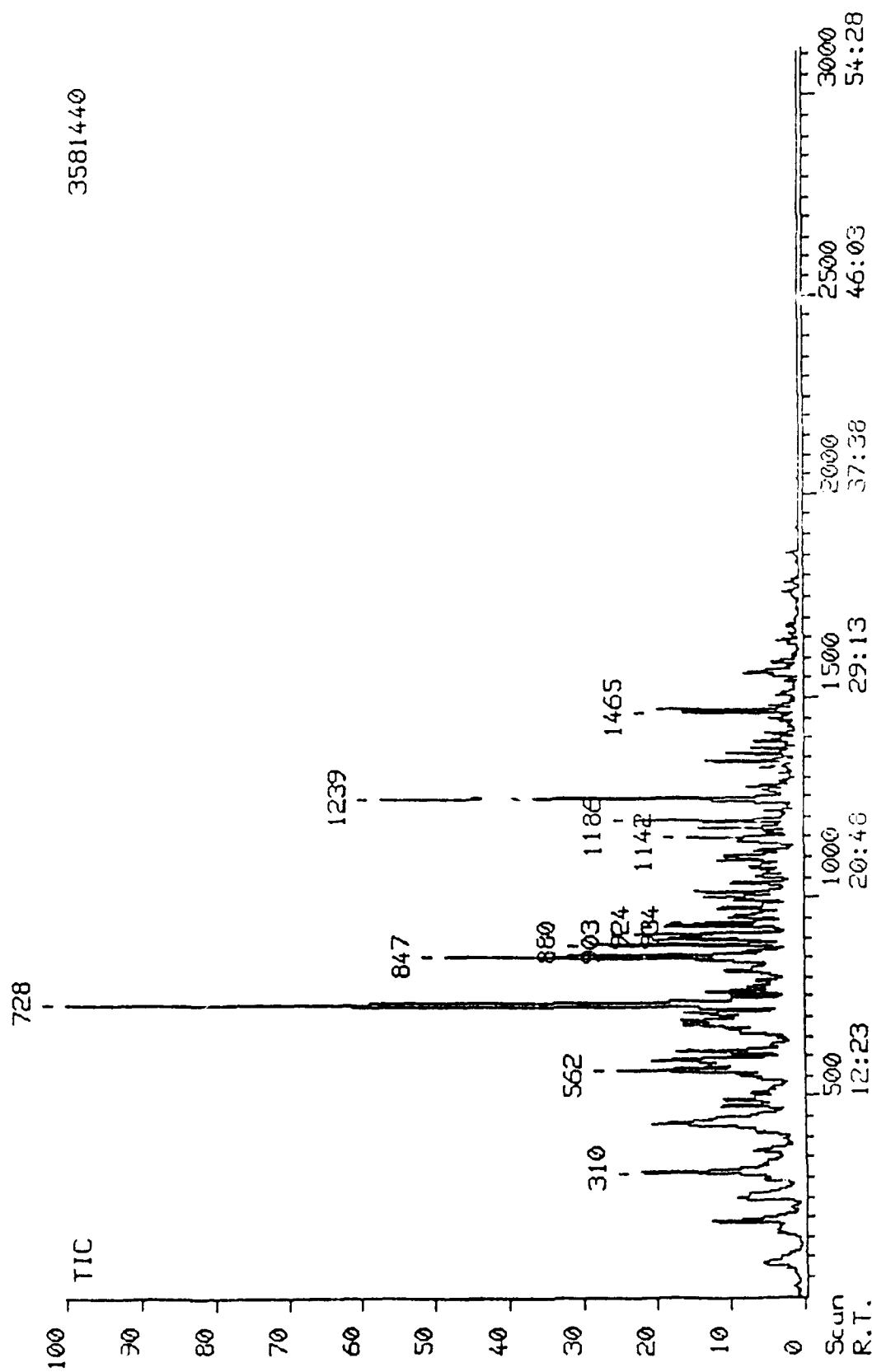


Figure 34. GC/MS total ion chromatogram of 185-215°C fraction of the coal-derived jet fuel JP8-C.

DS90 Chromatogram report Run: SONG0002, 16-Jan-90 10:42
 JP8-C 215-240 C UNTREATED HP-17 40-FOR 5 TO 280 AT 4.1 UL

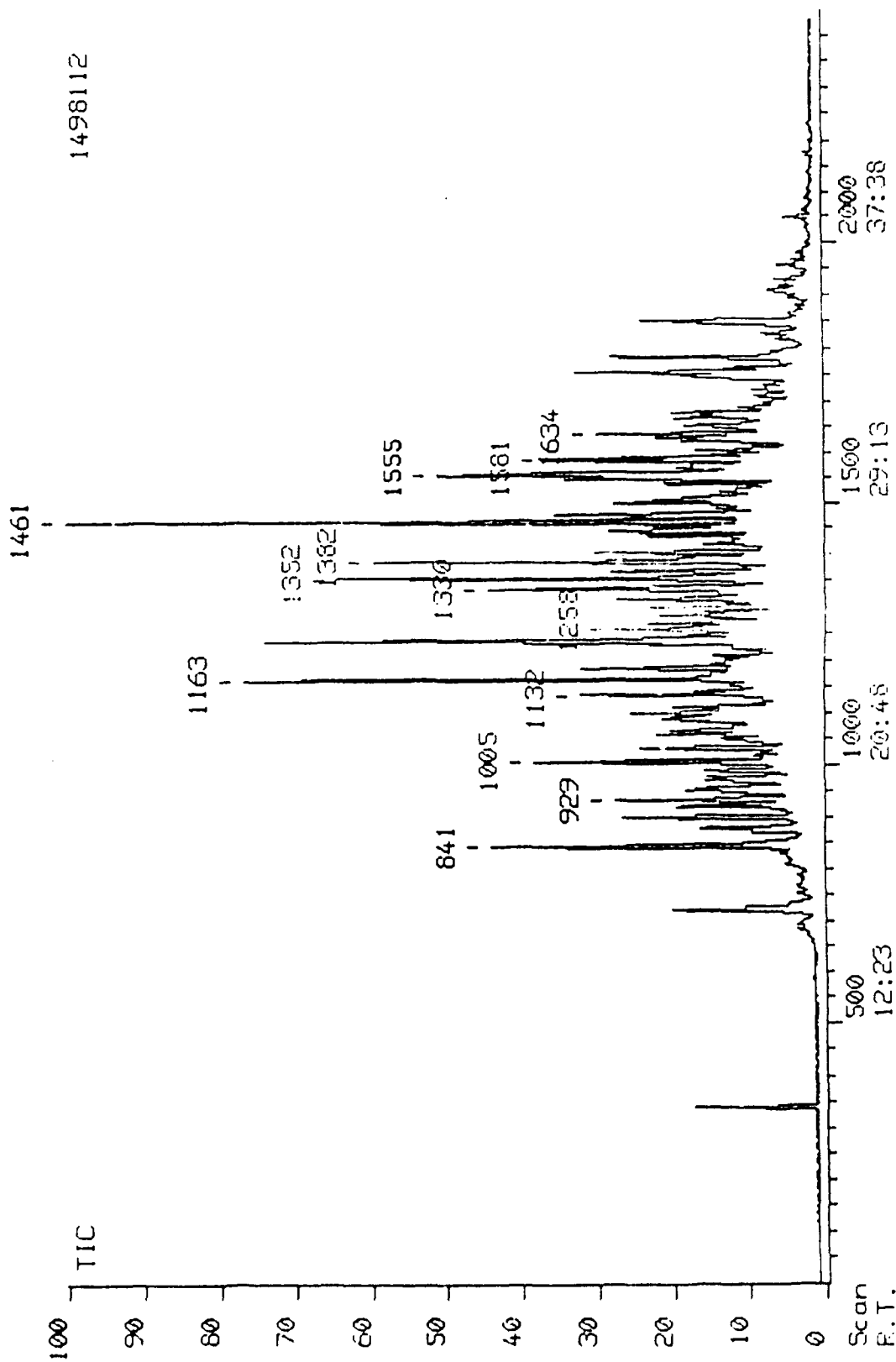


Figure 35. GC/MS total ion chromatogram of 215-240°C fraction of the coal-derived jet fuel JP8-C.

DS90 Chromatogram report Run: SONG0009, 18-Jan-90 14:25
 JP8-P 185-215 UNTREATED 40 FOR 5 TO 280 AT 4 1 (L)

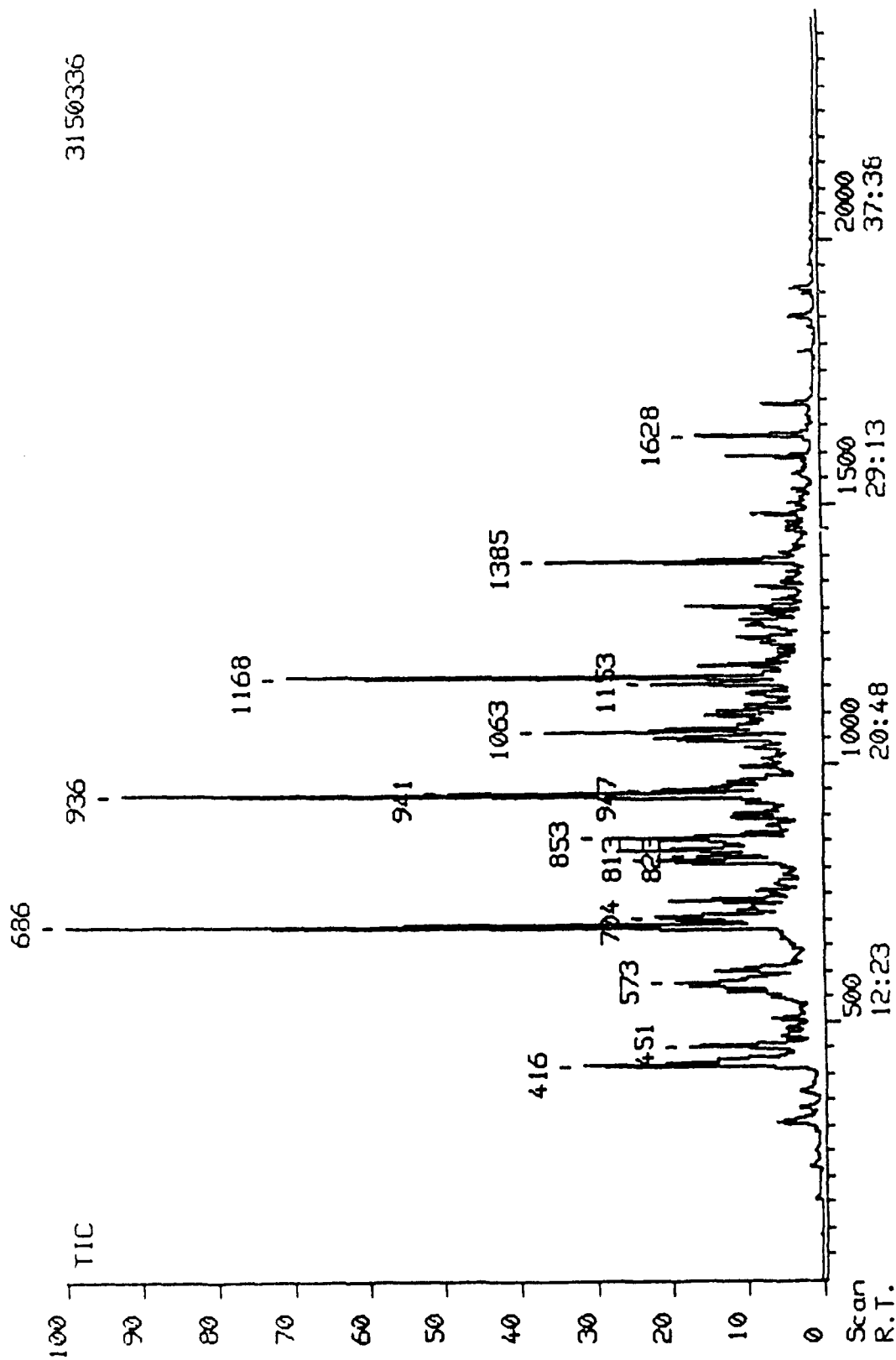


Figure 36. GC/MS total ion chromatogram of 185-215°C fraction of the coal-derived jet fuels JP8-P.

DS90 Chromatogram report Run: PGH20010, 14-Jan-90 16:47
 JP8-P UNTREATED 4005 TO 28004 HOLD 5 HP-17 IUL DILUTED1/500 215-240 C UNTREATED

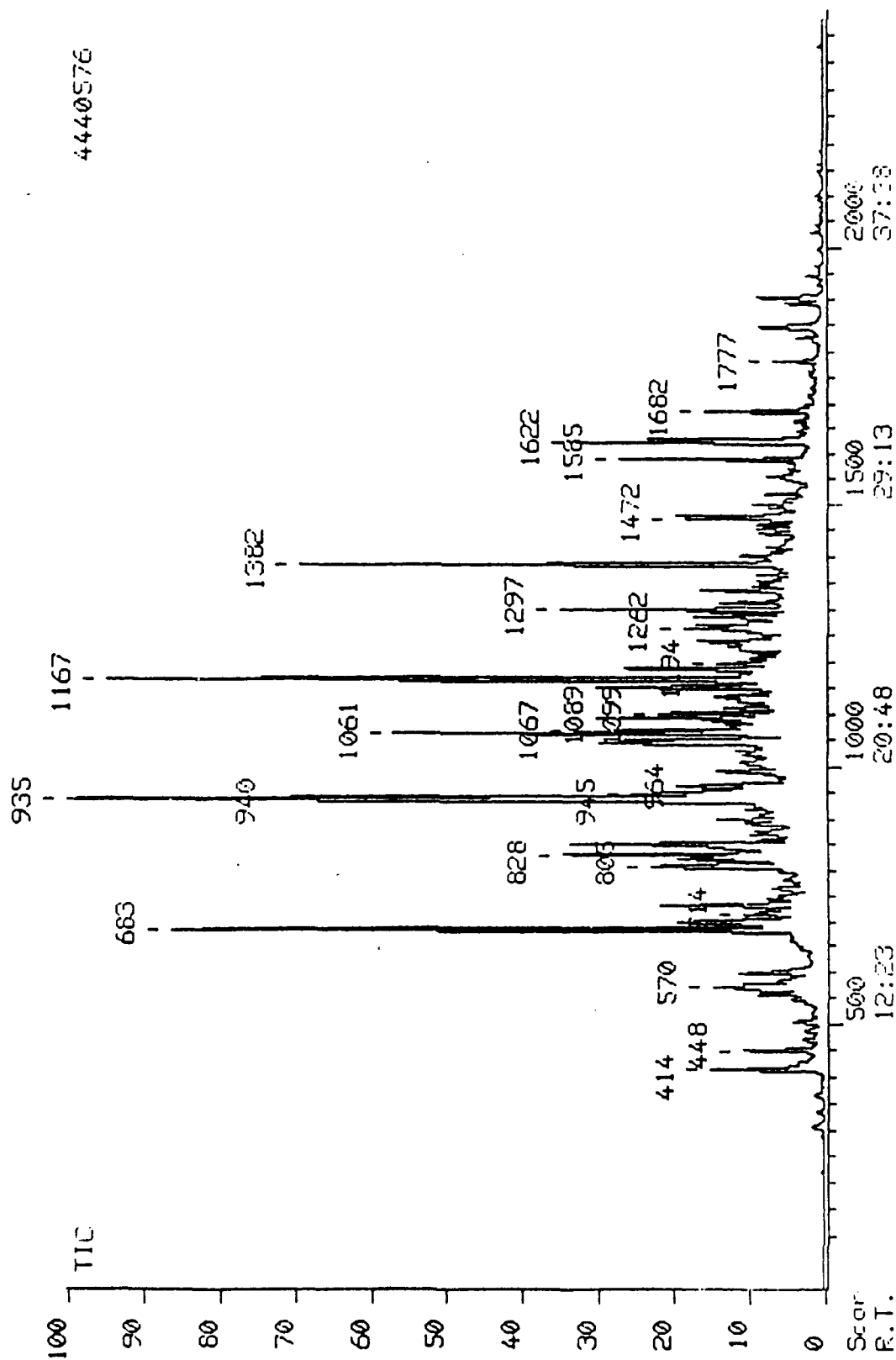


Figure 37. GC/MS total ion chromatogram of 215-240°C fraction of the coal-derived jet fuels JP8-P.

Table 17. Components of the 185-215°C fraction of the coal-derived jet fuels JP8-C

Peak Scan No.	Molecular Ion Mass	Compounds Identified
310	126	C ₃ -cyclohexane
426	140	C ₄ -cyclohexane
562	138	Decalin isomer
728	138	Decalin
847	152	C ₁ -decalin
880	138	Decalin
903	152	C ₁ -decalin
924	152	C ₁ -decalin
934	170	C ₁₂ H ₂₆ paraffin
1142	132	C ₁ -indane
1186	132	C ₁ -indane
1239	132	Tetralin
1465	146	C ₁ -tetralin

Table 18. Components of the 215-240°C fraction of the coal-derived jet fuels JP8-C

Peak Scan No.	Molecular Ion Mass	Compounds Identified
720	138	Decalin
841	152	C ₁ -decalin
897	152	C ₁ -decalin
919	152	C ₁ -decalin
929	170	C ₁₂ H ₂₆ paraffine
1005	166	C ₂ -decalin
1029	166	C ₂ -decalin
1132	166	C ₂ -decalin
1163	166	C ₂ -decalin
	184	C ₁₂ H ₂₈ paraffin
1181	132	C ₁ -indane
1234	132	Tetralin
1258	180	C ₃ -decalin
1328	146	C ₁ -tetralin
1352	180	C ₃ -decalin
	166	Bicyclohexyl
1382	198	C ₁₃ H ₃₀ paraffin
1461	146	C ₁ -tetralin
1555	146	C ₁ -tetralin
1581	194	C ₄ -decalin
1634	174	C ₃ -tetralin

Table 19. Components of the 185-215°C fraction of the petroleum-derived jet fuels JP8-P

Peak Scan No.	Molecular Ion Mass	Compounds Identified
416	142	n-C ₁₀ H ₂₂
573	156	C ₁₁ H ₂₄
686	156	n-C ₁₁ H ₂₄
823	168	C ₆ -cyclohexane
	170	C ₁₂ -H ₂₆
853	168	C ₆ -cyclohexane
936	170	n-C ₁₂ H ₂₆
941	184	C ₁₃ H ₂₈
947	184	C ₁₃ H ₂₈
1063	198	C ₁₄ H ₃₀
1168	184	n-C ₁₃ H ₂₈
1385	198	n-C ₁₄ -H ₃₀
1628	142	C ₁ -naphthalene

Table 20. Components of the 215-240°C fraction of the petroleum-derived jet fuels JP8-P

Peak Scan No.	Molecular Ion Mass	Compounds Identified
414	142	n-C ₁₀ H ₂₂
448	156	C ₁₁ H ₂₄
570	156	C ₁₁ H ₂₄
683	156	n-C ₁₁ H ₂₄
714	170	C ₁₂ H ₂₆
730	170	C ₁₂ H ₂₆
805	168	C ₆ -cyclohexane
828	170	C ₁₂ H ₂₆
935	170	n-C ₁₂ H ₂₆
940	184	C ₁₃ H ₂₈
964	184	C ₁₃ H ₂₈
1061	198	C ₁₄ H ₃₀
1067	184	C ₁₃ H ₂₈
1089	184	C ₁₃ H ₂₈
1099	168	C ₆ -cyclohexane
1167	184	n-C ₁₃ H ₂₈
1281	198	C- ₁₄ H ₃₀
1297	212	C ₁₅ H ₃₂
1382	198	n-C ₁₄ H ₃₀
1472	212	C ₁₅ H ₃₂
1585	212	n-C ₁₅ H ₃₂
1622	142	C ₁ -naphthalene
1682	142	C ₁ -naphthalene
1777	226	C ₁₆ H ₃₄

fuel showed a segregation of main compound classes. For example, the high-boiling fraction of the coal-derived jet fuel appeared to have a higher concentration of aromatics, principally alkylated tetralins and indans, than the low-boiling fraction.

Fractionation by distillation is very simple and can separate jet fuel with respect to differences in boiling points of individual components. A distillate fraction contains chemically different compound classes, and there is also overlapping of specific components in different fractions because of the co-boiling phenomena. These trends are also evident from Tables 17 through 20. Nevertheless, the GC/MS analysis of the distillate fractions provided important information on the compositional difference between coal- and petroleum-derived jet fuels.

Based on the results presented in this section, it can be concluded that, high resolution GC/MS analysis of the column chromatographic and distillate fractions has revealed significant differences in the chemical composition of jet fuels with different origins. The coal-derived jet fuel consists mainly of monocyclic and bicyclic alkanes and some hydroaromatic compounds as the major components. However, the petroleum-derived jet fuel is composed mainly of long-chain paraffins mixed with low concentrations of alkylbenzenes and alkylnaphthalenes.

Activity 2. Thermal Stability Testing of Fuel Fractions.

Thermal stability testing of the selected distillate fractions of the petroleum- and coal-derived JP-8 jet fuel has been reported in the interim report AFWAL-TR-87-2042. Column chromatographic fractions of the petroleum- and coal-derived JP-8 jet fuel have been prepared for thermal stressing.

Activity 3. Thermal Stability Testing of Unseparated Fuels.

Two jet fuel samples, identified as JP-8-Neat and JP-8/JFA-5, were provided by Lt. Jeffrey Moler of Wright-Patterson Air Force Base for thermal stress tests. The JP-8/JFA-5 sample is reported to contain a thermal stability additive. These fuels were heat treated at different temperatures following two different procedures for removing the air over the fuel sample in the microautoclave reactors and/or removing air (oxygen) dissolved in the fuel samples. One procedure employed to remove air from the microautoclaves involved repetitive pressurization to 1000 psi with UHP He and purging after the sample is loaded. Typically, this cycle is repeated five times before the microautoclave is pressurized to the operating pressure of 100 psi. The second procedure involves bubbling UHP He through the fuel sample for which a new set of microautoclaves were designed and made. As different from the conventional microautoclave, the new reactor has an extended stem

Table 21. Comparative thermal testing of JP-8 Neat and JP-8/JFA-5

FUEL TREATMENT		DEOXYGENATION	COLOR*	SOLIDS	SEDIMENT UPON STORAGE
Neat	300°C-24 h	Helium flush	1	no	no
JFA-5	"	"	1	no	no
Neat	"	Helium overpressure	1	no	no
JFA-5	"	"	1	no	yes
Neat	350°C-4 h	Helium flush	1	no	no
JFA-5	"	"	1	no	no
Neat	"	Helium overpressure	1	no	no
JFA-5	"	"	1.5	no	yes
JFA-5	350°C-5h	Helium flush	1	no	no
JFA-5	"	Helium flush	1.5	no	yes
		air overpressure			
Neat	380°C-24 h	Helium flush	2	yes	no
JFA-5	"	"	2	no	no
Neat	"	Helium overpressure	2	yes	no
JFA-5	"	"	2	yes	no
Neat	400°C-1 h	Helium flush	1	no	no
JFA-5	"	"	1	no	no
Neat	400°C-6 h	Helium flush	1	no	no
JFA-5	"	"	1	no	no

Table 21. Comparative thermal testing of JP-8 Neat and JP-8/JFA-5 (continued).

FUEL	TREATMENT	DEOXYGENATION	COLOR*	SOLIDS	SEDIMENT UPON STORAGE
Neat	425°C-3h	Helium flush	3	no	no
JFA-5	"	"	3	no	no
Neat	"	Helium overpressure	3	yes	no
JFA-5	"	"	3	yes	no
Neat	425°C-3h	Helium flush	3	yes	no
		air overpressure			
JFA-5	"	"	3	yes	no
Neat	450°C-4 h	Helium overpressure	4	yes	no
JFA-5	"	"	4	yes	no

* Qualitative darkening 1= Clear, 4= Black

which reaches the bottom of the reactor and an additional side arm connected to the body with a valve at the end. The He gas at approximately 15 psi flows through the stem at a rate of 60 ml/min and comes out of the holes at the bottom end of the stem to bubble through the fuel before it is vented to the atmosphere via the side arm. After 15 minutes of flushing with He the valve on the side arm is closed and the reactor is pressurized to 100 psi.

The two jet fuel samples showed different extents of discoloration depending on the temperature-time conditions of the heat treatment and the procedure used for deoxygenation of the fuel and reactor. In some cases, sediments formed upon storing the stressed samples in closed vials under air atmosphere and in light. More stringent stress conditions produced solids during the thermal treatment. Table 21 summarizes the results obtained from the thermal stress tests. Among the thermal treatments, only 450°C-4 h treatment produced solids in measurable quantities. The 10 ml of JP-8/JFA-5 produced 660 mg of solids upon treatment at 450°C for 4 h.

The observed differences between the thermal stability of JP-8 neat and JP-8/JFA-5 appeared to depend on the procedure used for deoxygenation of the reactor contents prior to thermal treatments. When He was bubbled through the fuel samples before the treatment, JP-8/JFA-5 appeared to be more stable (lighter color in the liquid product, no solids) than JP-8 neat under the same heat treatment conditions. In contrast, JP-8/JFA-5 appeared to be more reactive (sediment formation during storage, darker color in the liquid product) than JP-8 neat when the repetitive pressurization with He and venting was used to remove air from the reactor contents, as can be seen in Table 21. This consistent reversal in stability with the change of deoxygenation procedure was considered to be due to a high-temperature retrogressive interaction of JP-8/JFA-5 with dissolved oxygen and to the relatively higher concentrations of dissolved oxygen remaining in the fuel after cyclic pressurization and venting compared to flushing with He. In order to test this notion, before treatment at 350°C and 425°C, JP-8/JFA-5 samples were flushed with He in the reactors which were then pressurized with air (instead of helium) to 100 psi. The results obtained from the treatment in the presence of 100 psi air after helium flush were seen to be parallel to those obtained in the experiments where cyclic pressurization with He was used as a means of removing the air from the reactors, Table 21. These observations suggest that concentration of residual oxygen in the fuel is higher following cyclic pressurization and depressurization and support the preliminary observation that JP-8/JFA-5 is more prone to thermal degradation in the presence of dissolved oxygen in fuel than is JP-8 neat.

The different extents of discoloration displayed by the thermal treatment products from the two fuels were quantified by spectrophotometry. In addition, a set of thermal treatment experiments was performed on JP-8 Neat to determine the kinetics of the color change observed in the products.

In view of the distinct color changes produced by the thermal treatment of the fuels, it was considered that the extent of color change could be related to the extent of thermal degradation reactions. It was evident from a large number of experiments that the degree of discoloration of the fuels as a result of thermal treatment depends upon the starting fuel and the severity of the thermal treatment. In simple terms, the darkening of the fuels can be attributed to the increasing absorption of the visible light by large, essentially aromatic molecules produced by thermal degradation reactions.

The differences in the extent of discoloration of JP-8-Neat and JP8/ JFA-5 were quantified by using a spectrophotometer (Milton Roy Spectronic 20 D). In spectrophotometric measurements, transmittance of a 520 nm wavelength light through the samples was determined based on 100% transmittance through distilled water. It is

considered that transmittance will be inversely related to the extent of thermal degradation, since high-molecular-weight thermal degradation products are considered to be responsible for the absorption of the visible light. Duplicate measurements showed that the reproducibility of transmittance measurements was within 1%.

Figure 38 compares the transmittance of the products obtained from JP-8-Neat and JP-8/JFA-5 at 300°C-24 h and 350°C-4 h with and without flushing the fuels with helium prior to the thermal treatments. All the experiments were carried out in a helium atmosphere (100 psi cold). In the experiments which did not involve deoxygenation by flushing with helium, the loaded microautoclaves were pressurized to 1000 psi with UHP He and purged five times before final pressurization to 100 psi. It can be seen in Figure 38 that in both cases (at 300°C-24 h and 350°C-4h) the products obtained from JP-8/JFA-5 without deoxygenation had a lower transmittance than those obtained from JP-8-Neat. Further, it has been observed that the products obtained from JP-8/JFA-5 without deoxygenation by helium flush produced sediments upon storage, while the corresponding products obtained from JP-8-Neat did not. The lower stability of JP-8/JFA-5 with dissolved oxygen is, thus, shown more quantitatively in Figure 38, indicating also that the decreasing thermal stability due to the presence of oxygen is more pronounced at 350°C than that at 300°C.

In order to verify that the difference in thermal stability of JP-8/JFA-5 observed in the experiments with and without helium flush is due to the difference in dissolved oxygen

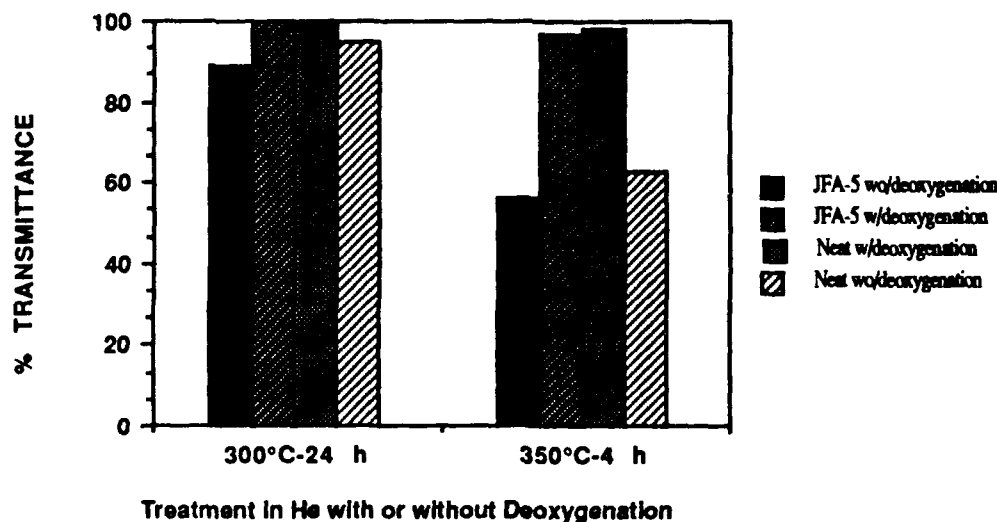


Figure 38. Transmittance of 520 nm light through the liquid products obtained

from JP-8-Neat and JP-8/JFA-5 at 300°C-24 h and 350°C-4 h with or without deoxygenation before thermal treatment.

concentration, a number of experiments were carried out using a 100 psi air overpressure after flushing the fuel with helium. Figure 39 compares percent transmittance of the products obtained from JP-8/JFA-5 at 350°C-5 h in an air and helium atmosphere following deoxygenation by helium flush. Clearly, the transmittance of the product obtained in an air atmosphere is substantially lower than that obtained in a helium atmosphere. It should, however, be noted that transmittance of the 350°C-5 h product obtained in an air atmosphere after a helium flush is higher than that of the 350°C-4 h product obtained in a helium atmosphere without a helium flush. Considering that the concentration of oxygen was higher and the reaction time was longer in the experiment performed under an air overpressure, one should expect a lower transmittance in the product obtained in this experiment. This discrepancy can be due to the longer storage time of the 350°C-4 h product and the different reactor configuration used in the experiments involving a helium flush.

Additional thermal treatment experiments were carried out using JP-8-Neat to determine the kinetics of discoloration of this fuel. In these experiments, care was taken to use the same set of reactors for all the experiments, and not to have different storage times involved with different products because of the darkening of the products upon storage in air. Figure 40 shows transmittance of the products obtained from JP-8-Neat under different conditions in a helium atmosphere after deoxygenation by flushing with helium.

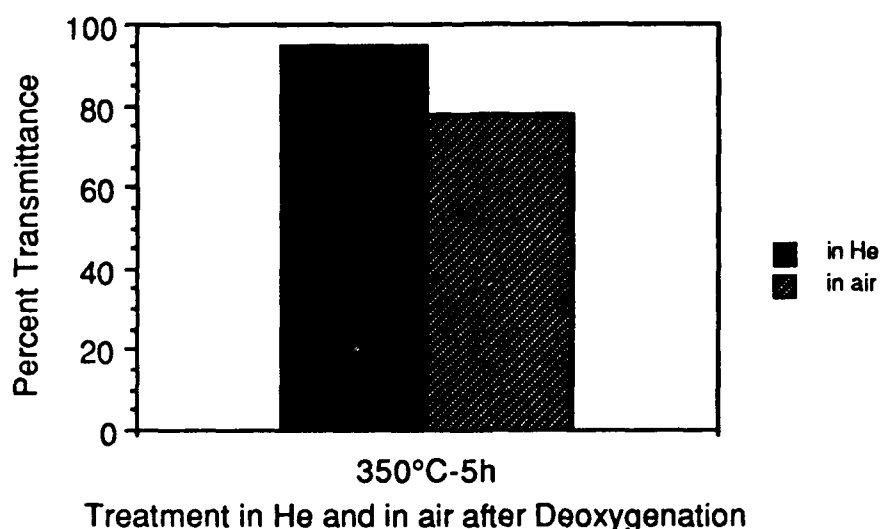


Figure 39. Transmittance of the products obtained from JP-8/JFA-5 at 350°C-5 h in air and in helium after deoxygenation by a helium

flush.

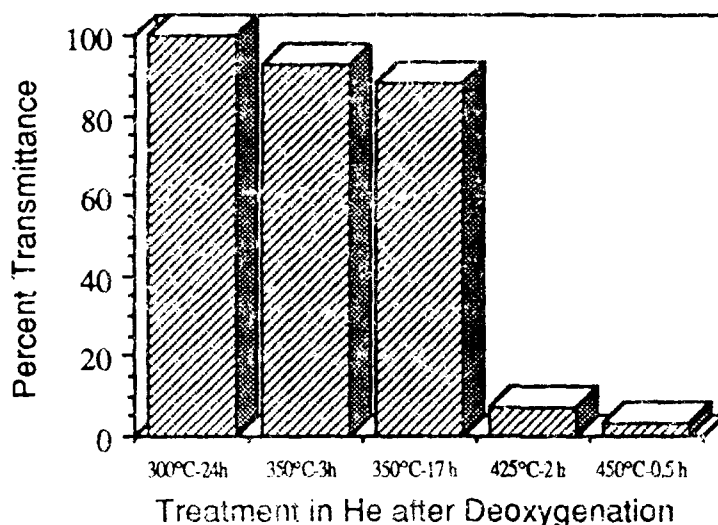


Figure 40. Transmittance of the products obtained from JP-8-Neat under different conditions in a helium atmosphere after deoxygenation by helium flush.

It is apparent that the fuel is very stable at 300°C and that transmittance decreases with the increasing severity (temperature) of the thermal treatment in the temperature range between 350 and 450°C. Assuming that the change in the light transmittance can be related to the thermal degradation reactions one can formulate a pseudo first-order rate expression as follows:

$$-d/Tdt = kT$$

where T is the fractional transmittance, t is reaction time at constant temperature and k is the pseudo first-order rate constant at the given temperature. If the change in transmittance follows a first-order kinetics, the plot of $\ln T$ versus time at different temperatures should produce straight lines.

Figure 41 shows the plots of $\ln T$ versus time at four different temperatures used to treat JP-8-Neat. It should be noted that the number of data points in Figure 41 are too few to allow a rigorous kinetic analysis, but provide reasonably sufficient information for a preliminary evaluation of the experimental data. The straight lines drawn through the data

points show a meaningful trend as a function of temperature. Figure 42 shows an Arrhenius plot for the rate constants calculated from the first-order plots in Figure 41.

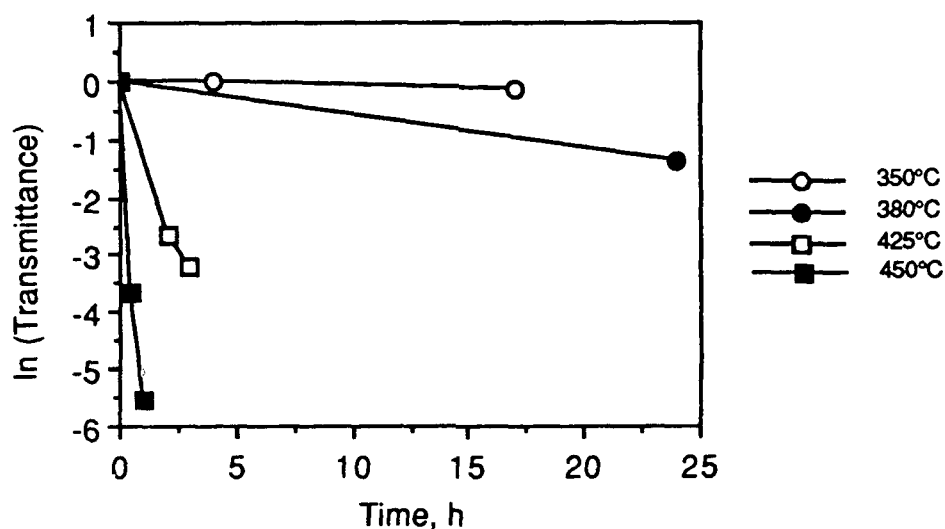


Figure 41. First-order plots for the thermal treatment of JP-8-Neat at four different temperatures.

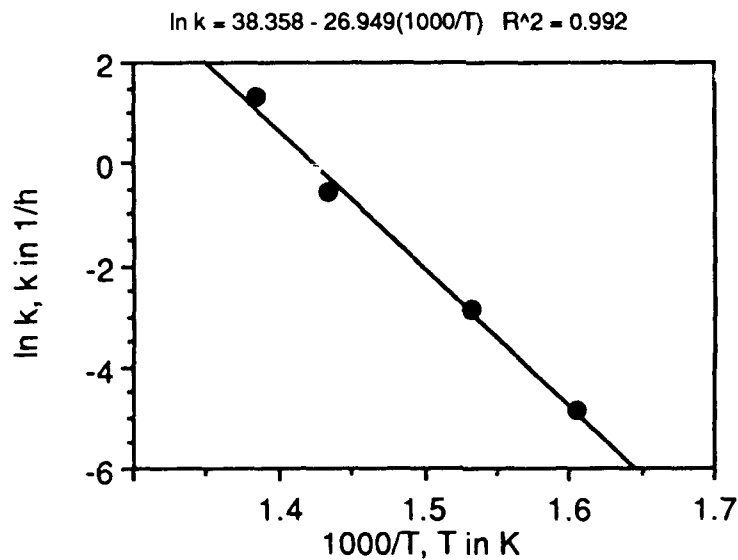


Figure 42. The Arrhenius plot for the rate constants calculated from the transmittance data shown in Figure 41.

Figure 42 also includes a linear regression equation, indicating a good fit of the rate constant data by an Arrhenius relationship. The Arrhenius plot yields an activation energy of 53 kcal/mole and a preexponential factor of $4.56 \times 10^{16} \text{ h}^{-1}$ for the change in transmittance of the reaction products. These kinetic parameters represent acceptable values for chemically controlled thermal decomposition reactions of hydrocarbons. The good fit of the rate constant data by an Arrhenius relationship and the reasonable values obtained for the activation energy and the preexponential factors do suggest that the color change during thermal treatment can be related to the chemical processes. In other words, the preliminary analysis reported here suggests that the light transmittance measurements can be used to study the kinetics of thermal degradation reactions provided that the necessary precautions are taken.

REFERENCES

1. CRC Literature Survey on the Thermal Oxidation Stability of Jet Fuel, CRC Report No. 509, Coordinating Research Council, Inc., Atlanta, Georgia, 1979.
2. G. F. Bolshakov, "The Physico-Chemical Principles of the Formation of Deposits in Jet Fuels," English Translation, Foreign Technology Division, Wright-Patterson Air Force Base, Ohio, 1974.
3. A. C. Nixon, in "Autoxidation and Antioxidants," Vol. II, W. O. Lundberg, Ed., Interscience, New York, N.Y. 1962.
4. W. F. Taylor, "Jet Fuel Thermal Stability," A conference-Workshop, NASA, Lewis Research Center, Cleveland, Ohio, 1-2 November, 1978.
5. "Combustion Problems in Turbine Engines," 62nd Propulsion and Energetics Panel Symposium, Çesme, Turkey, 3-6 October, 1983.
6. Symposium on Structure of Jet Fuels, American Chemical Society, Div. Pet. Chem., Denver, Colorado, April 5-10, 1987.
7. Symposium on Structure of Jet Fuels II, American Chemical Society, Div. Pet. Chem., Miami, Florida, September 10-15, 1989.
8. R. P. Bradley and C.R. Martel, "Thermal Oxidative Stability Test Methods for JPTS Jet Fuel," Technical Report AFAPL-TR-79-2079, Wright-Patterson Air Force Base, Ohio, 1979
9. L. L. Stavinoha, J. G. Barbee, and D. M. Yost, "Thermal Oxidative Stability of Diesel Fuels," BFLRF Report No. 205, Southwest Research Institute, San Antonio, Texas, 1986.
10. S. D. Darrah, T. Raw, R. Steendal, and T. G. DiGiuseppe, "Performance and Safety Characteristics of Improved and Alternate Fuels," Report No. GC-TR-86-1601, Geo-Centers, Inc., Suitland, Maryland, 1986.
11. R. E. Morris and R. N. Hazlett, *Energy Fuels*, **3**, 262, 1989.
12. F. R. Mayo, *Acc. Chem. Res.*, **1**, 193, 1968.
13. B. D. Boss and R. N. Hazlett, *Can. J. Chem.*, **47**, 4175, 1969.
14. W. F. Taylor, *Ind. Eng. Chem. Prod. Res. Dev.*, **8**, 379, 1969.
15. W. F. Taylor, *Ind. Eng. Chem. Prod. Res. Dev.*, **13**, 133, 1974.
16. W. F. Taylor, *Ind. Eng. Chem. Prod. Res. Dev.*, **15**, 64, 1976.
17. W. F. Taylor and J. W. Frankenfeld, *Ind. Eng. Chem. Prod. Res. Dev.*, **17**, 86, 1978.
18. J. W. Frankenfeld and W. F. Taylor, *Ind. Eng. Chem. Prod. Res. Dev.*, **19**, 65, 1980.

19. J. L. Krazinski and S. P. Vanka, "Development of a Mathematical Model for the Thermal Decomposition of aviation Fuels," Final Report, WRDC-TR-89-2139, Wright-Patterson Air Force Base, Ohio, 1989
20. G. V. Deshpande, M. A. Serio, P. R. Solomon, and R. Malhotra, "Modelling of the Thermal Stability of Aviation Fuels," Preprints, ACS Div. Fuel Chem., **34**, 955, 1989.
21. J. D. Brooks and G. H. Taylor, in "Chemistry and Physics of Carbon," Marcel Dekker Inc., NY, Volume 4, 243, 1968.
22. J. L. White, in "Progress in Solid State Chemistry," J. O. McCaldin and G. Somorjai, Eds., Pergamon Press, Oxford, U.K., **9**, 59, 1974.
23. H. Sawatzky, A. E. George, G. T. Smiley, and D. S. Montgomery, Fuel, **55**, 16, 1976.
24. M. Farcasiu, Fuel, **56**, 9, 1977.
25. J. E. Schiller and D. R. Mathiason, Anal. Chem., **49**, 1225, 1977.
26. D. Wallace, D. Henry. K. Ponger, and D. Zimmerman, Fuel, **66**, 44, 1987.
27. S. Lamey, P. Hesbach, and E. Childers, Energy Fuels, **3**, 636, 1989.